THESIS FOR THE DEGREE OF DOCTOR OF PHILOSOPHY (PHD)

Investigation of novel functions of myosin phosphatase and smoothelin-like 1 protein

by Adrienn Sipos

Supervisor: Beáta Lontay, PhD

UNIVERSITY OF DEBRECEN
DOCTORAL SCHOOL OF MOLECULAR MEDICINE

DEBRECEN, 2017

TABLE OF CONTENTS

ABBREVIATIONS

ADMA	asymmetric dimethylarginine
AMC	aminomethylcoumarin
ATP	adenosine-5'- triphosphate
BCA	bicinchoninic acid
BSA	bovine serum albumin
CaM	calmodulin
CBD1	Ca^{2+}-CaM-binding domain
CBD2	apo-CaM-binding domain
CH	calponin homology domain
CID	collision-induced dissociation
DARPP-32	cAMP-regulated phosphoprotein of 32 kDa
DMEM	Dulbecco's Modified Eagle Medium
DMSO	dimethyl sulfoxide
DTT	dithiothreitol
DUSPs	dual-specificity phosphatases
ECL	enhanced chemiluminescence
EDTA	ethylene-diamine tetraacetic acid
EF2	elongation factor 2
EGTA	ethylene glycol tetraacetic acid
FBS	fetal bovine serum
FT	flag-tagged
GLM	general linear model
H2A	histone 2A
H2AR3	histone 2A arginine 3
H4	histone 4
H4R3	histone 4 arginine 3
HCC	hepatocellular carcinoma
HDAC7	histone deacetylase 7
HepG2	human hepatocyte carcinoma
His	hexahistidine
HRP	horseradish-peroxidase
I-1	inhibitor-1
I-2	inhibitor-2
IHC	immunohistochemistry
IL	interleukin
ILK	integrin-linked kinase
IP	immunoprecipitation
JBP1	Janus-kinase-binding protein-1
KEPI	kinase-enhanced protein phosphatase type 1 inhibitor
KO	knockout
LC-MS	liquid chromatography–mass spectrometry
LMW-PTP	low-molecular-weight phosphatases

LZ	leucine zipper
M20	20 kDa small subunit of myosin phosphatase
MAPK	mitogen-activated protein kinase
MBS85	protein phosphatase 1 myosin binding 85 kDa subunit
MCF-7	human breast adenocarcinoma
MCY-LR	microcystin-LR
MDPK	myotonic dystrophy protein kinase
MEM	minimum Essential Medium
MEP50	methylosome protein 50
MHC	myosin heavy chain
MLC20	20 kDa light chain of myosin
MLCK	myosin light chain kinase
MP	myosin phosphatase
MRCKα	myotonic dystrophy kinase-related Cdc42 binding kinase-α
MTT	methyl-thiazol-tetrazolium
MyPhoNE	myosin phosphatase N-terminal element
MYPT	myosin phosphatase targeting protein
MYPT1	myosin phosphatase targeting protein 1
NEAA	non essential amino acids
NF2	neurofibromatosis type 2
NLS	nuclear localization signals
NP	non-pregnant
OD	optical density
PAK	p21-activated kinase
Par-4	prostate apoptosis response-4 protein
PAS	periodic acid-Schiff staining
PAS	Protein-A Sepharose
PBS	phosphate-buffered saline
PCC	Pearson's correlation coefficient
PEI	polyethyleneimine
pICln	chloride ion current inducer protein
PIP	phosphoinositide
PKA	cAMP-dependent protein kinase
PKG	cGMP-dependent protein kinase
PMSF	phenylmethylsulfonyl fluoride
PP1	protein phosphatase type 1
PP1c	PP1 catalytic subunit
PP2	protein phosphatase type 2
PP2B	calcineurin
PPM	metal ion-dependent phosphatases
PPP	phosphoprotein phosphatases
PR	progesterone receptor
pRb	retinoblastoma protein
PRE	pregnant

PRMT5	protein arginine methyltransferase 5
PSPRE	pseudopregnant
PTP	protein tyrosine phosphatases
RA	rectus abdominalis
Rap1	Ras-related protein 1
ROK	RhoA-associated protein kinase
RT	room temperature
RU	response unit
SAM	S-adenosyl-L-methionine
SDMA	symmetric dimethylarginine
SDS	sodium dodecyl sulfate
SDS-PAGE	sodium dodecyl sulfate-polyacrylamide gel electrophoresis
SE	standard error
SEM	standard error of the mean
Ser	serine
siRNA	small interfering RNA
SKM	skeletal muscle
SMTN-A	smoothelin A
SMTN-B	smoothelin B
SMTNL1	smoothelin-like 1 protein
SMTNL2	smoothelin-like 2 protein
SNARE	soluble N-ethylmaleimide sensitive factor attachment protein receptor
SPR	surface plasmon resonance
STAT5	signal transducer and activator of transcription 5
TBS	tris-buffered saline
TCA	trichloroacetic acid
Thr	threonine
TIMAP	TGF-β1-inhibited membrane-associated protein
tsA201	human embryonal kidney
Tyr	tyrosine
WT	wild type
ZIPK	zipper-interacting protein kinase
γ-^{32}P-ATP	radioactive-labeled adenosine-5'- triphosphate
γ-^{32}P-MLC20	radioactive-labeled 20 kDa light chain of myosin

INTRODUCTION

Protein phosphorylation and dephosphorylation is one of the essential regulatory mechanisms in the biological functions of eukaryotes and it is involved nearly in all of the signal transduction pathways in the living organisms. Cell cycle, cell development, differentiation or apoptosis are all phosphorylation-dependent processes (Cohen 1997; Shi 2009). Reversible phosphorylation of proteins is driven by protein kinase and phosphatase enzymes and the phosphorylation level of proteins depends upon the balance between the activities of these enzymes. Protein dysfunctions may be formed when the balance shifts in the direction of phosphorylation or dephosphorylation causing under- or over-phosphorylation of proteins. According to estimations about one-third of proteins contains covalently bound phosphate and is controlled by reversible phosphorylation of serine (Ser), threonine (Thr) and/or tyrosine (Tyr) side chains (Hunter 1995).

Myosin phosphatase (MP) holoenzyme is a Ser/Thr specific enzyme, which is the member of protein phosphatase type 1 (PP1) family and composed of a PP1 catalytic subunit (PP1c), a myosin phosphatase targeting subunit (MYPT1) and a small subunit (M20) with unknown function (Hartshorne et al. 1998). While PP1c is required for the catalytic activity of the holoenzyme, MYPT1 regulates MP through targeting the holoenzyme to its substrates and supplying the surface for protein-protein interactions. MP has been identified as a major regulator of smooth muscle contractility through the dephosphorylation of phosphorylated 20 kDa myosin light chain of filamentous myosin II (Somlyo et al. 2003). Cellular motility and other non-muscle cell functions such as cytokinesis or cell adhesion are also regulated by MP since the phosphorylation of myosin II light chains is required to initiate these non-muscle events (Hirano et al. 2004). MP is dominant in smooth muscle but it is expressed ubiquitously in mammalian tissues. Although numerous cytoskeletal substrates of MP have been identified, MP shows not exclusively cytoskeletal/cytosolic localization. MP plays a role in nucleus-related cellular processes such as cell division or apoptosis and it modulates tumor suppressor proteins including merlin and retinoblastoma protein as well. MYPT1 was also found in the nuclear and microsomal fractions of hepatocellular carcinoma cells (Lontay et al. 2005) and in the nucleus of neuronal cells (Lontay et al. 2004) but its exact nuclear function is still unknown.

Smoothelin-like 1 protein (SMTNL1) belongs to the smoothelin family of muscle proteins and is expressed both in smooth and skeletal muscles. SMTNL1 is a regulator of vascular smooth muscle contractility (Borman et al. 2004) and modulates cardiovascular and

skeletal muscle adaptations to exercise, development and pregnancy (Wooldridge et al. 2008; Lontay et al. 2010; Bodoor et al. 2011). During pregnancy, increased expression of SMTNL1 was detected in uterine and vascular smooth muscle and sex-hormone related tissues. Besides this, sex and hormone-dependent regulation of SMTNL1 expression was observed. Pregnancy also induced the expression of MYPT1 and SMTNL1 deletion further elevated MP activity causing a more relaxed uterine and vasculature phenotype (Wooldridge et al. 2008; Lontay et al. 2010). Although SMTNL1 has an inhibitory effect on MP activity towards phosphorylated myosin light chain (Borman et al. 2009), direct interaction between the two proteins is still uncharacterized.

In this study, first we intended to obtain more information about the possible nuclear interacting partners and roles of myosin phosphatase, a classical cytoskeletal regulator. Second, our aim was to describe the relation between SMTNL1 and MP as well as to indentify further linkage about SMTNL1-related skeletal muscle adaptation during pregnancy.

REVIEW OF THE LITERATURE

Reversible protein phosphorylation

Protein phosphorylation is one of the major post-translational modifications conserved in all observed eukaryotic organisms. Reversible phosphorylation regulates the activity and subcellular localization of proteins and is responsible for dynamic rearrangement of protein complexes (Hunter 1995). Protein kinases catalyze protein phosphorylation through the transfer of terminal γ-phosphate group of nucleoside triphosphates (mostly adenosine triphosphate) to amino acid side chains containing hydroxyl group: serine (Ser), threonine (Thr) and tyrosine (Tyr) (Cohen 1990). Reversibility is ensured by protein phosphatases hydrolyzing phospho-Ser, -Thr or -Tyr phosphoesters (Shi 2009). 518 protein kinases are encoded in human genome (Johnson et al. 2005) and Ser/Thr-, Tyr-specific or dual-specificity protein kinases can be distinguished. Surprisingly, less than 150 protein phosphatase catalytic subunits are known in human genome and approximately only 40 is specific for phospho-Ser/Thr dephosphorylation (Pennisi 2002). The number of phospho-Tyr phosphatases is 107 (Alonso et al. 2004). Besides the small number of Ser/Thr-specific catalytic subunits that are responsible for the enzyme activity of holoenzymes, multiplicity of regulatory subunits provides the wide range of holoenzyme compositions (Ingebritsen et al. 1983; Bollen et al. 2010). Regulatory subunits by binding to the catalytic subunit target the holoenzyme to its substrates and define the specific subcellular locations, as well as the interacting partners and also control the activity of the holoenzyme.

Classification of protein phosphatases

Based on biochemical qualities, Ser/Thr-specific phosphatases were first classified into PP1 (protein phosphatase type 1) and PP2 (protein phosphatase type 2) families. According to the research of Ingebritsen and Cohen, type 1 phosphatases were sensitive to small heat-stable phosphatase inhibitors (inhibitor-1 or I-1, inhibitor-2 or I-2) and to heparin while PP2 activity was not inhibited by these effectors (Ingebritsen et al. 1983). Further classification of type 2 phosphatases differentiated three subclasses depending on their metal ion necessity. PP2A was found to require no metal ions. PP2B or calcineurin was known as a Ca^{2+}/calmodulin-dependent phosphatase. Mg^{2+}-dependent PP2C was later separated as a metal ion-dependent protein phosphatase superfamily (PPM) (Cohen 1997). According to a new classification based on the amino acid sequences of protein phosphatase catalytic subunits, Ser/Thr protein phosphatases are subdivided into three families (Fig. 1).

Phosphoprotein phosphatases (PPP) contain Fe^{2+}-Zn^{2+} ions, metal ion-dependent phosphatases (PPM) can be activated by Mn^{2+}/Mg^{2+} ions and aspartate phosphatases possess a DxDxT/V motif in the active site (Ceulemans et al. 2004; Brautigan 2013). PPP family falls into PP1, PP2A, calcineurin (PP2B), and novel-type phosphatases PP4, PP5, PP6 and PP7 subgroups (Barton 1994; Cohen 1997). More than 90% of phospho-Ser/Thr dephosphorylation events are related to PP1 or PP2A enzymes.

Protein tyrosine phosphatases (PTP) can be classified into several major families according to their sequence, structure and functional properties (Fig. 1). Protein tyrosine phosphatases or "classical" PTPs hydrolyze phospho-Tyr phosphoesters. Dual-specificity phosphatases (DUSPs) dephosphorylate both of Tyr or Ser/Thr side chains (Pot et al. 1992; Barford et al. 1995). Tyr-specific phosphatases with phospholipid phosphatase activities are called phosphoinositide (PIP) phosphatases. Phosphatase and tensin homologue PTEN, which is a tumor suppressor (Steck et al. 1997) and possesses phospholipid phosphatase activity, is often classified as a DUSP. Low-molecular-weight phosphatases (LMW-PTP) can also be discriminated.

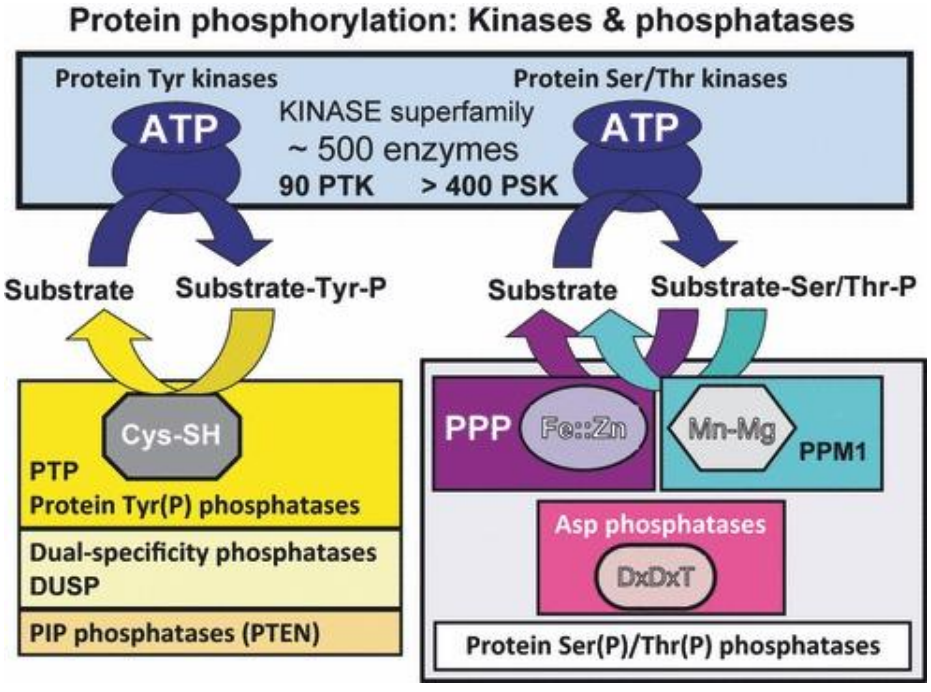

Figure 1. Families of protein phosphorylation enzymes.
Classification of proteins with kinase (upper box) and phosphatase (lower boxes) activity specified for tyrosine (Tyr) and serine/threonine (Ser/Thr) types. Tyr-specific phosphatases (PTP family, lower left) are partitioned to PTP, DUSP and PIP groups. Subdivision of Ser/Thr phosphatases (lower right) contains three different families, PPP, PPM and Asp phosphatases. (Brautigan 2013)

Protein phosphatase 1

PP1 enzymes are the major Ser/Thr-specific phosphatases and are expressed in a wide range of eukaryotic cells. PP1s play a role in many cellular processes including cytoskeletal reorganization, apoptosis, protein synthesis, cell cycle regulation or metabolism (Ceulemans et al. 2004). PP1 holoenzymes are composed of a 35-38 kDa catalytic subunit (PP1c) and a regulatory subunit (Fig. 2). The five mammalian splice variants of PP1c, namely PP1cα_1, PP1cα_2, PP1cδ (also known as PP1β), PP1cγ_1 and PP1cγ_2 are encoded by three genes (Zhang et al. 1993). PP1c isoforms are highly conserved and they show sequence homology greater than 90%. Since PP1 catalytic subunits cannot be found freely in the cell but they associate with a wide range of the regulatory subunits, PP1c subunits create a large variety of holoenzymes with different regulators resulting in distinct substrate specificities and activities.

Approximately 200 putative regulatory subunits of PP1c have been identified (Bollen et al. 2010; Choy et al. 2012) and they modulate the activity and substrate specificity of PP1c and target the catalytic subunit to different subcellular locations. In addition to the various structural features, a short PP1c binding motif, a consensus RVxF (K/R-x1-V/I-x2-F/W) sequence can be found in almost each of regulatory subunits (Endo et al. 1996; Egloff et al. 1997). Secondary binding sites of the regulatory subunits are described with lower binding affinity, but they have an effect on activity and substrate specificity of PP1 holoenzyme (Bollen 2001; Wakula et al. 2003). Substrate-binding sites can also be found in the sequence of targeting subunits next to PP1c binding motif. Regulators/interactors of PP1c subunits can be classified based on a number of different aspects. Regulatory subunits can be classified

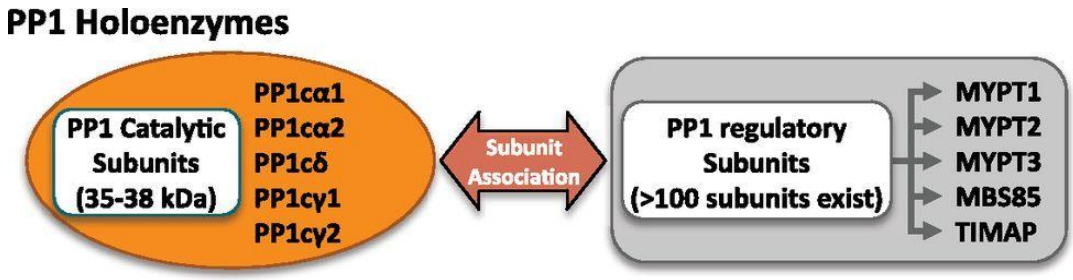

Figure 2. Composition of protein phosphatase 1 holoenzymes.
PP1 holoenzymes consist of a catalytic subunit and one or more targeting subunit/s. PP1 catalytic subunits have five different isoforms, which can interact with almost 200 regulatory subunits. Targeting subunits indicating on the figure are the members of myosin phosphatase targeting (MYPT) family.(Butler et al. 2013)

into two groups depending on their action: activating/targeting and inhibitory proteins. For example, small, heat-stable inhibitors (I-1, I-2, CPI17) decrease the PP1 enzyme activity after bound to PP1c (Connor et al. 1999). However, *e.g.* inhibitor-1, -2, dopamine or DARPP-32 (cAMP-regulated phosphoprotein of 32 kDa) can be designated as substrate-independent activity regulators. In addition, there are substrate specifiers (generally called targeting subunits) such as G subunits and MYPTs, and substrates notably Aurora kinases or Nek2. Some regulatory subunits bind to PP1c in an isoform-dependent manner (MYPTs, Neurabins).

Myosin phosphatase targeting (MYPT) protein family

Myosin phosphatase is one of the most prominent PP1 holoenzymes consisting of a PP1 catalytic subunit and a MYPT protein family regulatory subunit. Myosin phosphatase targeting (MYPT) protein family members are the MYPT1 (Shimizu et al. 1994), MYPT2 (Fujioka et al. 1998), MYPT3 (Skinner et al. 2001), protein phosphatase 1 myosin binding 85 kDa subunit (MBS85) (Tan et al. 2001) and TGF-β1-inhibited membrane-associated protein (TIMAP) (Cao et al. 2002). Mammalian MYPT family members are the products of five genes and they target protein phosphatase type 1δ catalytic subunit (PP1cδ) to its substrates. According to the latest nomenclature of protein phosphatases MYPT1, MYPT2, MYPT3, MBS85 and TIMAP received the PPP1R12A, PPP1R12B, PPP1R116A, PPP1R12C and PPP1R16B denominations, respectively. MYPT1 is expressed in most of the tissues especially in smooth muscle and nowadays it is considered as a housekeeping protein. 110 kDa MYPT2 was found mainly in striated (cardiac, skeletal) muscles and in brain or some other tissues (Fujioka et al. 1998; Arimura et al. 2001). MBS85 was explored as a substrate of myotonic dystrophy kinase-related Cdc42 binding kinase-α (MRCKα) and is predominantly expressed is heart (Tan et al. 2001). MYPT3 is widely distributed in cardiac muscles, brain and kidney as a membrane associated protein (Skinner et al. 2001). TIMAP is highly expressed in endothelial and hematopoietic cells and it is a positive regulator of endothelial barrier equilibrium (Csortos et al. 2008). In addition, all members of the MYPT family were found in the human uterus (Lartey et al.).

Structure of MYPT proteins

MYPT proteins represent high sequence similarity and share several conserved domains (Fig. 3). MYPTs include the PP1c binding RVxF motif on their N-terminus and the conserved central region of PP1c is associated to MYPTs via this region (Terrak et al. 2004). Binding of MYPTs to PP1cδ is supported by additional conserved regions such as residues

10-17 called MyPhoNE (myosin phosphatase N-terminal element), which is a consensus RxxQV/I/LK/RxY/W sequence (Terrak et al. 2004). RVxF motif is followed by eight or less ankyrin repeat domain (Fig. 3) and the ankyrin repeats 1, 5, 6 and 7 attach to C-terminus of PP1cδ during interaction with PP1c. Besides catalytic subunit binding, ankyrin repeats serve the major platform for substrate coupling.

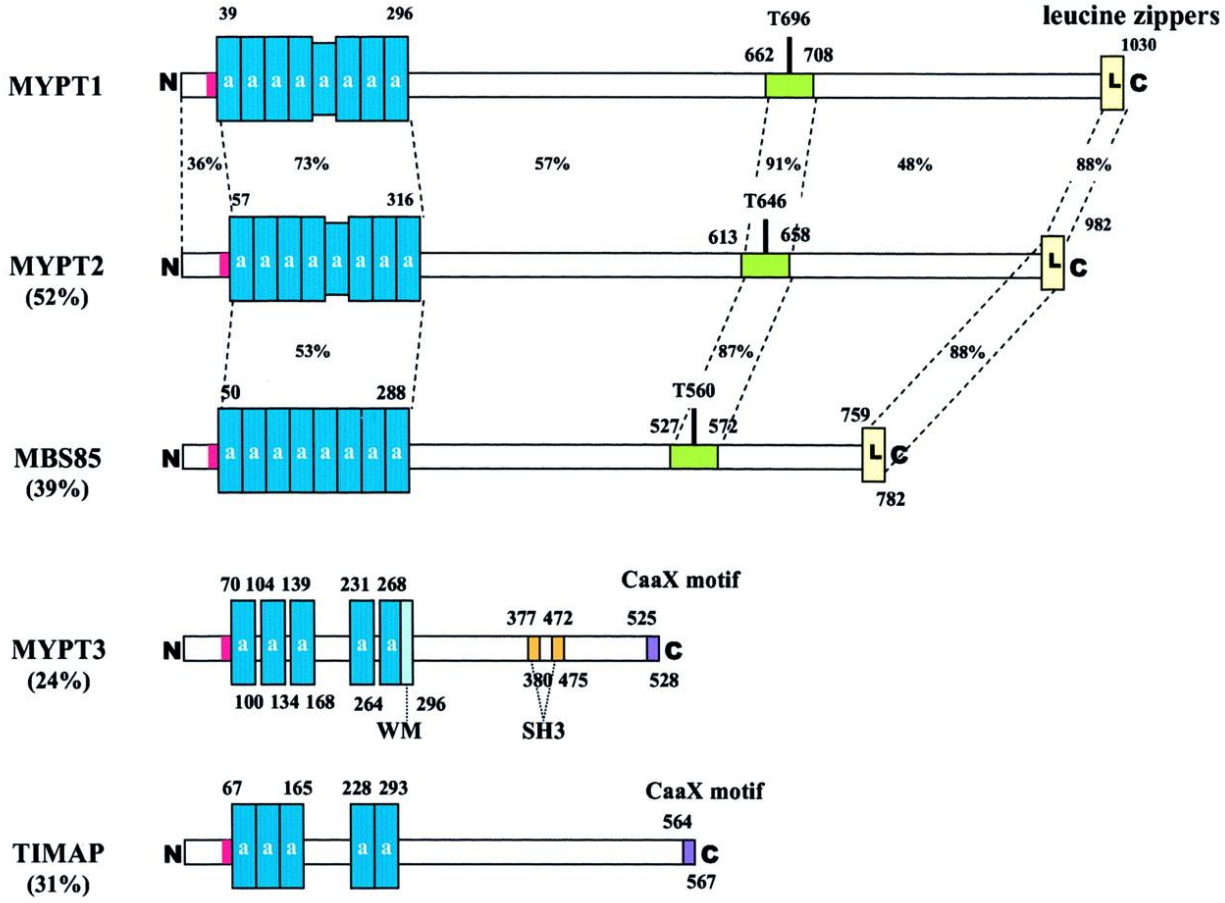

Figure 3. Schematic structure of MYPT family members.

Sequence homology in percentage, different regions and position of phosphorylation sites compared to MYPT1 are indicated. Regions: PP1c-binding motif, red area at N-terminal edge of ankyrin (a) repeats; L, leucine zipper region; WM, Walker motif (ATP/GTP-binding site); CaaX, putative prenylation site; SH3, class I ligand binding consensus site. (Hartshorne et al. 2004)

The ankyrin repeat domain is followed by the central region containing conserved phosphorylation sites from which Thr^{696} and Thr^{853} (by human sequence) are the best characterized ones, found in MYPT1 and MYPT2. MBS85 comprises the Thr^{696} site but neither MYPT3 nor TIMAP contains any of the side chains (Fig. 3). C-terminal halves of MYPT proteins are more diverse. Leucine zipper sequence takes part of protein-protein

interactions and dimerization and it is found in MYPT1, MYPT2 and MBS85 but not in MYPT3 or TIMAP (Fig. 3). The latter two proteins comprise a prenylation motif on their C-terminus, referred to as CaaX box (Fig. 3), which anchors MYPT3 and TIMAP to the cell membrane. The most closely related members are MYPT1 and MYPT2 certified by sequence comparisons performed between human MYPT proteins (Ito et al. 2004). The sequence of MYPT1 shows 52% homology with MYPT2, and in spite of their conserved motifs, N-terminal region is the most distinct with 36% similarity. MBS85 sequence is mainly resembles to MYPT2 (Ito et al. 2004). The sequence of MYPT3 is similar to MYPT1 and 2 only on its N-terminal region (Skinner et al. 2001). Sequence homology between MYPT3 and TIMAP is approximately 45% (Cao et al. 2002).

MYPT1 (also called myosin binding protein, MBP or M130) provides the regulatory subunit of myosin phosphatase (MP or myosin light chain phosphatase, MLCP) holoenzyme (Fig. 4), which is a trimer consisting of a 35-38 kDa PP1cδ catalytic subunit and a 20 kDa subunit (M20) based on sequences cloned from chicken gizzard (Alessi et al. 1992) and rat aorta (Chen et al. 1994). In human, several isoforms of MYPT1 are generated by alternative splicing from one gene located at chromosome 12q15-q21.2 (Takahashi et al. 1997). MYPT1 isoforms differ in the absence or presence of the central insert (amino acid 512-552) or variably expressed leucine zipper domain demonstrating distinct molecular weight from 110 to 133 kDa (Dirksen et al. 2000). MYPT1 contains 7 or 8 ankyrin repeats between the segments of 39-296 with a conserved β-hairpin-helix-loop-helix structure (Fig. 4). Each of the repeats is composed of nearly 33 residues (Terrak et al. 2004). The region of 171-197 residues is less homolog but similar to ankyrin repeats (Shimizu et al. 1994). The ankyrin repeat domain serves as a platform for multiple protein interactions (Bennett et al. 2001). Two bipartite nuclear localization signals (NLS, Fig. 5) were also identified in MYPT1 sequence. First of them is located between the 27-33 amino acids on the N-terminus next to the PP1c binding RVxF motif and contributes to karyopherin-mediated import of MYPT1 to the nucleus (Wu et al. 2005). C-terminal NLS is positioned from the 843 to 852 region, just before the Thr^{853} phosphorylation site. The central segment of MYPT1 sequence is abundant in acidic side chains (362-372), in Ser/Thr amino acids (770-793) and contains sections with ionic features (719-793 and 814-848). The function of M20 subunit of MP is unknown and its binding to the C-terminal region of MYPT1 (amino acids 934-1006) does not affect the activity of the holoenzyme (Johnson et al. 1996; Hirano et al. 1997). In addition, M20 was found neither in skeletal muscle nor in brain (Moorhead et al. 1998).

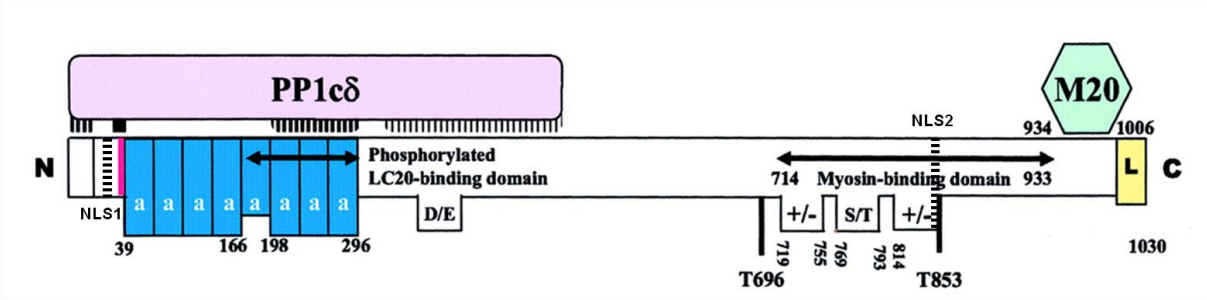

Figure 4. Illustration of human myosin phosphatase holoenzyme.
For the holoenzyme, interactions of varying strengths between MYPT1 and PP1cδ are indicated. Arrows indicate the suggested binding sites for phosphorylated myosin light chain and myosin. Regions of MYPT1: KVKF (red area), PP1c-binding motif; a, ankyrin repeat; D/E, acidic region; +/–, ionic region; S/T, Ser- and Thr-rich region; L, leucine zipper. Thr^{696} and Thr^{853} phosphorylation sites, nuclear localization signals (NLSs) and some residue numbers are indicated. Modified from (Hartshorne et al. 2004)

Diverse functions of myosin phosphatase

Basic role of myosin phosphatase in cytoskeletal processes

Regulation of myosin II by phosphorylation is essential in muscle contraction or non-muscle cell functions *e.g.* shape changes, cell division and cytokinesis, cell adhesion, cell migration or regulation of ion channels. Filamentous contractile motor protein myosin II is organized by the engagement of two 200 kDa heavy chains and two pairs of light chains with a 17 and a 20 kDa subunit and it was found to be a key protein in the above mentioned cellular movements. After phosphorylation of the 20 kDa myosin light chain (MLC20), myosin II reversibly binds to actin filaments via cross-bridges initiating contractile or motile events (Chacko et al. 1977). MLC20 phosphorylation depends on the balance between Ca^{2+}/calmodulin-dependent myosin light chain kinase (MLCK) and myosin phosphatase (MP) (Ikebe et al. 1985). Phosphorylation of MLC20 at Ser^{19} mainly by MLCK triggers the contraction of the acto-myosin complex and its dephosphorylation by MP is followed by relaxation (Fig. 6). MLC20 can be also phosphorylated at Thr^{18} which presumably impedes dephosphorylation of Ser^{19} that is necessary to sustain contractile force, however, the phosphorylation of Thr^{18} alone does not evoke contraction (Sutherland et al. 2012).

Initial studies focused on smooth muscle myosin phosphatase but the same regulatory mechanism was described in skeletal and cardiac muscles, too. In smooth muscle contraction, an increase in the intracellular Ca^{2+} concentration ($[Ca^{2+}]_i$) activates the formation of the Ca^{2+}-calmodulin complex, which triggers the activation of MLCK. Activated MLCK catalyses phosphorylation of myosin light chain at Ser^{19} creating a cross-bridge to actin and it is followed by contraction. When $[Ca^{2+}]_i$ restores to basal 120-150 nM, the balance shifts

towards myosin dephosphorylation and the dissociation of myosin from actin causes relaxation (Fig. 6). An agonist-dependent signaling can also provoke muscle contraction at a constant Ca^{2+} level in a $[Ca^{2+}]_i$ independent manner,(Somlyo et al. 2003). During Ca^{2+} sensitization (Fig. 6) ROK phosphorylates MYPT1 on its inhibitory sites in response to external stimuli and decreases the myosin phosphatase activity that induces the contraction of cytoskeletal elements. On the other hand, myosin phosphatase can also be activated by cAMP-PKA or cGMP-PKG signaling pathway during Ca^{2+} desensitization (Fig. 6). Activation of PKA/PKG induces the phosphorylation of MYPT1 on Ser^{695}, which prevents the subsequent phosphorylation of inhibitory Thr^{696} site and activates myosin phosphatase (Wooldridge et al. 2004). The activation of MP upon PKA/PKG leads to an increase in the dephosphorylation of MLC20 and relaxation in a Ca^{2+}-independent manner (Wu et al. 1996).

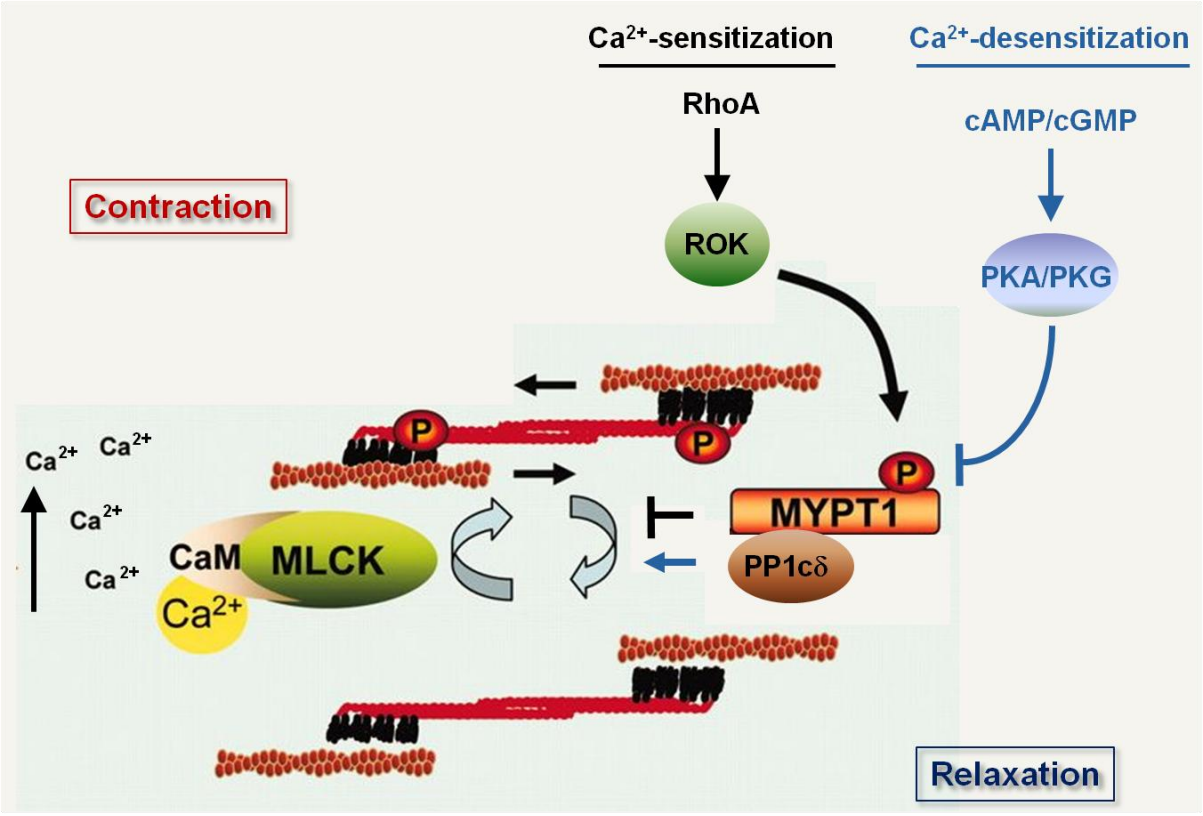

Figure 6. Regulation of smooth muscle contractility.
Modified diagram of smooth muscle contraction based on (Ratz et al. 2005).

Several additional cytoskeletal partners were identified and their interaction with MP is evolved through different segment of the enzyme. As previously mentioned, N-terminal ankyrin repeat domain is the major platform for protein interactions but C-terminal part of MYPT1 can also serve as a supporting or individual binding surface during interactions. Cytoskeletal adducin binds to the ankyrin repeats (Kimura et al. 1998) while moesin interacts

with the C-terminal region (Fukata et al. 1998). It was demonstrated that proteins of microtubule assembly, Tau and MAP2, are also substrates of myosin phosphatase (Amano et al. 2003). Several substrates of MP are known to be phosphorylated by ROK, including adducin, moesin, Tau, MAP2 and myosin.

Novel role of myosin phosphatase in neurotransmitter release

In the past few years, several studies focused on the novel function of myosin phosphatase in neurotransmitter release. In the nervous system, as in other organized systems, phosphorylation level of neuronal proteins depends on the balance between the catalytic activities of protein kinases and phosphatases. Many of protein kinases were identified as key regulators of neuronal protein phosphorylation but less information is available regarding protein phosphatases responsible for the reversibility of the process (Mayford et al. 1999). PP1cα and PP1cγ_1 catalytic subunit isoforms were identified in postsynaptic densities and dendritic spines (Ouimet et al. 1995; Strack et al. 1999) while in soma periphery and in neuronal cell nuclei the presence of PP1cδ was demonstrated (Strack et al. 1999). Neuronal targeting subunits of PP1cα and PP1cγ_1 such as neurofilament-L (Terry-Lorenzo et al. 2000), neurabin-I (MacMillan et al. 1999) and neurabin-II (Allen et al. 1997) were revealed in postsynaptic densities.

The regulatory subunit MYPT1 of myosin phosphatase (type PP1) was detected in rat brain and primary cell cultures of neurons (Lontay et al. 2004) and the activity of MP holoenzyme was also proved. Synaptosomes derived from cerebral cortex presented significant myosin phosphatase activity (Lontay et al. 2004) but the MP was thought to be predominantly present in the presynaptic projections (Lontay et al. 2012). The complex of MYPT1 and PP1cδ was co-localized and co-precipitated with synaptophysin, a presynaptic marker protein, which is phosphorylated by Ca^{2+}/calmodulin-dependent kinase II (Rubenstein et al. 1993). The ROK and myosin phosphatase were found to act on both pre- and post-synaptic target proteins influencing neurotransmission (Lontay et al. 2012). Application of PP1-specific inhibitors on cortical synaptosome preparations resulted in the suppression of the depolarization-induced exocytosis and neurotransmitter release, while increased exocytosis was evoked by the inhibition of ROK. Previously, it has been shown that SNARE (soluble N-ethylmaleimide sensitive factor attachment protein receptor) complex member syntaxin-1 is phosphorylated by casein kinase-2 at Ser^{14} (Gil et al. 2011) and synapsin-I, which modulates neurotransmitter release and reversibly docks actin to synaptic vesicles, can be phosphorylated at Ser^{9} by PKA (Hilfiker et al. 2005). Besides this, ROK- and MP-dependent

phosphorylation of syntaxin-1 Ser^{14} and synapsin-I Ser^{9} was observed (Lontay et al. 2012) suggesting the regulatory role of ROK and MP in neurotransmitter release.

Role of myosin phosphatase in cell proliferation

Nuclear retinoblastoma protein (pRb) is a tumor suppressor protein that is expressed from the retinoblastoma gene and plays a central role in cell proliferation and cell death (Chew et al. 1998). Loss of pRb function is a recognized initiator in cancer development (Murphree et al. 1984) and the regulatory role of pRb effects through protein-protein interactions. Hypo-phosphorylated pRb binds to the transcription factor EF2 (elongation factor 2) and blocks cell cycle but when pRb is hyper-phosphorylated by cyclin-dependent kinases, pRb-EF2 complex disintegrates and the independent EF2 initiates the expression of proteins regulating G1/S transition (Chellappan et al. 1991). Retinoblastoma protein attaches to and blocks EF2 again after dephosphorylation. Early studies established low expression level and hyper-phosphorylation of pRb in leukemic cells causing increased proliferation and decreased chemosensitivity of the cells (Kornblau et al. 1998). Yamamoto and co-workers have described the increase of PP1 and PP2A activity in leukemic cells (Yamamoto et al. 1999). Colocalization and association of MYPT1 with pRb was detected in THP-1 leukemic cells suggesting that MYPT1 targets catalytic subunit PP1c to pRb (Kiss et al. 2008). The absence of MYPT1 increased pRb phosphorylation and resulted in a decrease in the cell death of THP-1 cells concluding that myosin phosphatase mediates chemoresistance of leukemic cells during cell cycle through the dephosphorylation of pRb (Kiss et al. 2008).

Cytoskeletal merlin protein encoded by neurofibromatosis type 2 gene shares homology with the members of ezrin-radixin-moesin family of cytoskeleton (Trofatter et al. 1993). The name merlin is an acronym, which comes from moesin-ezrin-radixin-like. Merlin is a scaffolding protein linking actin filaments to the cell membrane or membrane-associated glycoproteins (McClatchey et al. 2005) and it inhibits cell proliferation. Merlin was first identified as a tumor suppressor which is inactive in a dominantly inherited disorder, namely neurofibromatosis type 2 (NF2) (Rouleau et al. 1993). Merlin can be phosphorylated at the C-terminal Ser^{518} by PAK 1 and 2, which initiates the translocation of merlin from the cell membrane to the cytoplasm (Kissil et al. 2002; Xiao et al. 2002). Moreover, merlin is a substrate of PKA which catalyzes its phosphorylation at Ser^{518} (Alfthan et al. 2004). Jin and co-workers have found that myosin phosphatase can activate merlin by dephosphorylating Ser^{518}. Moreover, myosin phosphatase inhibitor CPI-17 increased merlin phosphorylation

resulting in the loss of merlin function and initiating tumorigenic transformation (Jin et al. 2006).

Functions of myosin phosphatase during development

Additional studies demonstrated the essential importance of MYPT1 and myosin phosphatase during embryonic development as well as in pregnancy mediated adaptation of vertebrates. Global loss of MYPT1 was shown to be lethal within eight days during the development of mouse embryos (Okamoto et al. 2005) and caused severe defects in convergent extension of zebrafish embryos (Weiser et al. 2009). Investigations during zebrafish gastrulation confirmed the regulatory role of MP in development via actomyosin activity modulation which supports the balance between Rho-dependent amoeboid cell movement and mesenchymal cell behaviors (Weiser et al. 2009; Pankova et al. 2010). Failure in cell movements was observed during gastrulation of *Caenorhabditis elegans* due to MYPT1 deletion (Piekny et al. 2003).

Besides the cellular processes during vertebrate gastrulation, contractile changes of maternal vascular and smooth muscles during pregnancy were also linked to myosin phosphatase. MYPT1 was found to be up-regulated in the uterine artery of late-stage pregnant rats (Li et al. 2007). Increased myosin phosphatase activity was also measured during pregnancy and it was found to be the consequence of the increased MYPT1 protein and mRNA expression level in mouse and human (Lontay et al. 2010). In addition, the expression of MYPT1 at protein level was augmented not only in pregnant state but in response to smoothelin-like 1 protein (SMTNL1) deletion in neonates resulting in an exaggerated increase of MYPT1 (Lontay et al. 2010). Changes in the expression level of MYPT1 during pregnancy and SMTNL1 deletion promote uterine relaxation and reduced systemic blood pressure via desensitization of uterine and vascular smooth muscle to Ca^{2+} (Lontay et al. 2010). Besides this, MYPT1 was exclusively expressed in type 2a muscle fibers in pregnant mice and human (Lontay et al. 2010) suggesting the role of MYPT1 in skeletal muscle plasticity during pregnancy.

After birth, twofold increase in MYPT1 expression and MP activity was observed between postnatal days 6 and 12 in rodents (Payne et al. 2006). In the same study, a switch in MYPT1 splice variant isoforms was revealed from C-terminal leucine zipper positive (LZ+) to negative (LZ-) with a concomitant switch from a cGMP-sensitive to a cGMP-resistant vascular relaxation, may regulating the portal vein smooth muscle differentiation.

Further mechanisms of myosin phosphatase

An unconventional substrate of MP is histone deacetylase 7 (HDAC7) that is a transcriptional repressor. HDAC7 can regulated by various signal transduction processes (McKinsey et al. 2001) and is highly expressed in $CD4^+/CD8^+$ thymocytes and shows nuclear localization involved in T-lymphocyte differentiation (Dequiedt et al. 2003). Upon phosphorylation at Ser^{155}, Ser^{318} and Ser^{448} sites by protein kinase D1, HDAC7 translocates to the cytoplasm from the nucleus in a complex with 14-3-3 proteins (Kao et al. 2001; Dequiedt et al. 2005; Parra et al. 2005). Nuclear export of HDAC7 promotes the transcriptional suppression of its gene targets such as pro-apoptotic receptor Nur77. HDAC7 is dephosphorylated at the phospho-Ser residues by myosin phosphatase holoenzyme in the cytoplasm promoting its nuclear redistribution (Parra et al. 2007).

Myosin phosphatase has a number of additional interacting partners, substrates and regulators such as M-RIP or myosin phosphatase-Rho interacting protein (Riddick et al. 2008), interleukin-16 (Bannert et al. 2003), AMPK-related kinase NUAK1 (Zagorska et al.), 14-3-3 protein (Koga et al. 2008), 27 kDa heat shock protein (Patil et al. 2006) or proline-directed kinases like cdc2 (Yamashiro et al. 2008). The above illustrated examples clearly demonstrate the putative role of myosin phosphatase in a wide range of cellular processes, motility, cell cycle, development and in tumorigenesis.

Regulation of myosin phosphatase

Regulation of myosin phosphatase by phosphorylation

Phosphorylation of MYPT1 on Ser/Thr residues by a variety of protein Ser/Thr kinases is one of the principal regulatory mechanisms of myosin phosphatase functions causing enzyme activation or inhibition. Several phosphorylation sites were found on the MYPT1 regulatory subunit including, but not limited to Ser^{432}, Thr^{435}, Ser^{445}, Ser^{472}, Ser^{473}, Ser^{601}, Ser^{695}, Thr^{696}, Ser^{852}, Thr^{853} and Ser^{910} (numbering for human sequence, Fig. 5). There are two major and well characterized inhibitory sites in the sequence of MYPT1, namely Thr^{696} and Thr^{853} (Kimura et al. 1996). Several kinases were identified as a regulator of these residues, and RhoA-associated protein kinase (ROK) was first found to catalyze phosphorylation on both of them (Feng et al. 1999). Phosphorylation of MYPT1 on Thr^{696} or on Thr^{853} attenuated the activity of myosin phosphatase (Ichikawa et al. 1996; Muranyi et al. 2005) and the phosphorylation of Thr^{853} by ROK cause the dissociation of MYPT1 from its substrate myosin (Velasco et al. 2002). It is important to note that the sequence around Thr^{696} or Thr^{853} is similar to the sequence around Ser^{19} phosphorylation site of 20 kDa light chain of

myosin (MLC20), whereby this region of MYPT1 after phosphorylation on Thr^{696} or Thr^{853} may anchor the active site of PP1cδ blocking its affinity to myosin (Khromov et al. 2009). There are two serine residues, Ser^{695} and Ser^{852}, immediately adjacent to the two threonine inhibitory phosphorylation sites overlapping with the consensus sequence (RRxS) of cAMP- and cGMP-dependent protein kinase (PKA and PKG). Phosphorylation of Ser^{695} by PKA/PKG was found to hamper subsequent phosphorylation of Thr^{696} by ROK, releasing the inhibitory effect of myosin phosphatase (Wooldridge et al. 2004). Based on *in vitro* and *in situ* experiments in rat caudal artery, dual Ser^{695}/Thr^{696} or Ser^{852}/Thr^{853} phosphorylation did not influence the activity of myosin phosphatase but phosphorylation of Thr^{696} and Thr^{853} by ROK preceded phosphorylation of serines by PKA (Grassie et al. 2012).

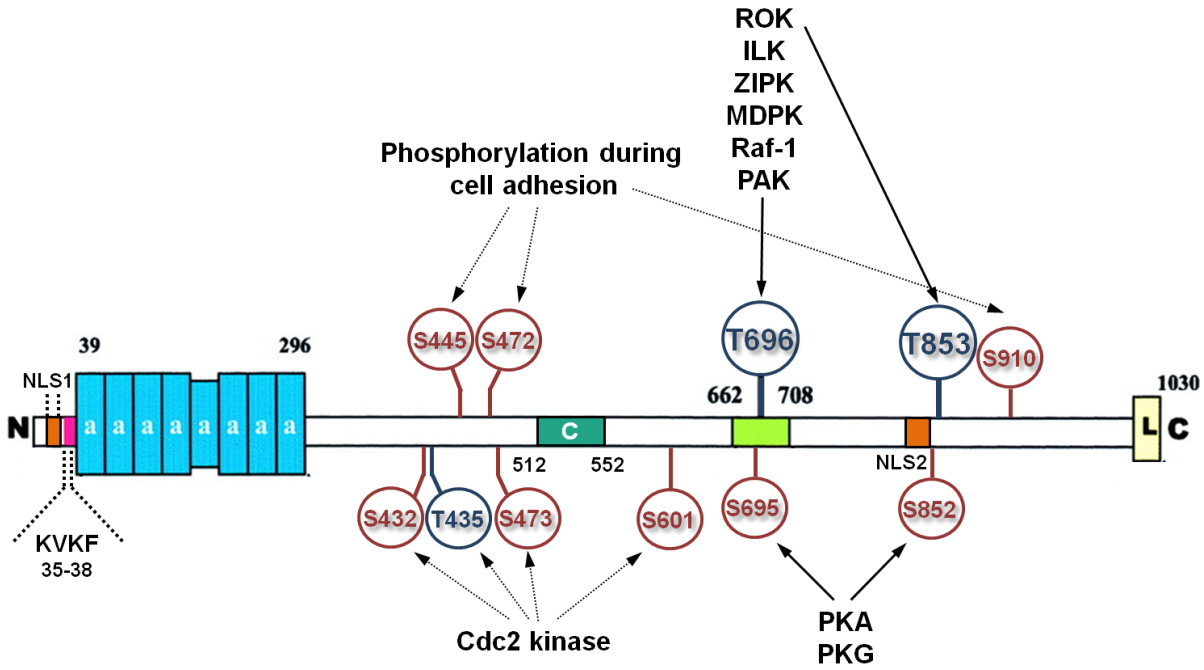

Figure 5. Regulation of MYPT1 by phosphorylation.
Indicated regions of MYPT1: NLS1 and NLS2 (orange boxes), nuclear localization signals; KVKF (pink box), PP1c-binding motif; a, ankyrin repeat; C (green box), central insert; L, leucine zipper. Phosphorylation sites and kinases are indicated. Modified illustration based on (Hartshorne et al. 2004).

Many other kinases are known to phosphorylate MYPT1 on Thr^{696}, *e.g.* zipper-interacting protein kinase (ZIPK) (MacDonald et al. 2001; Niiro et al. 2001), integrin-linked kinase (ILK) (Kiss et al. 2002; Muranyi et al. 2002) , myotonic dystrophy protein kinase (MDPK) (Muranyi et al. 2001), Raf-1 (Broustas et al. 2002) and p21-activated kinase (PAK) (Takizawa et al. 2002) (Fig. 5). Phosphorylation of MYPT1 on Ser^{445}, Ser^{472} and Ser^{910} has an inhibitory effect on cell adhesion (Zagorska et al. 2010). Mitosis-specific phosphorylation of MYPT1 causes

the activation of the holoenzyme. During mitosis, MYPT1 phosphorylation on Thr^{435} and/or Ser^{432} by cdc2 kinase enhances the affinity of the holoenzyme towards phosphorylated myosin increasing MP activity (Totsukawa et al. 1999). Additional phosphorylation sites of cdc2 kinase such as Ser^{473} and Ser^{601} were also found during mitosis (Yamashiro et al. 2008) (Fig. 5).

Regulation of myosin phosphatase by interacting proteins

Two small heat stable proteins, inhibitor-1 (I-1) and -2 (I-2) were first described as inhibitor proteins of protein phosphatase 1 (Huang et al. 1976) (Table 1). Inhibitor-1 is a phosphorylation-dependent inhibitor, which can be phosphorylated at Thr^{57} by PKC (Eto et al. 1999) or ILK (Deng et al. 2002), while I-2 does not require phosphorylation (Cohen et al. 1977). Both proteins bind to free PP1c subunit hampering its activity while if PP1c is in complex with MYPT1, their inhibitory effect decreases or even disappears. On the other hand, phosphorylation-dependent CPI-17 inhibitor affects on MP holoenzyme as well as on isolated PP1c (Eto et al. 1995). CPI-17 is a 17 kDa protein expressed in smooth muscle and brain (Eto et al. 1997) and the phosphorylation of its Thr^{38} residue by PKC elevated the inhibitory potency by about 1000 fold (Eto et al. 2001). Several other kinases were also found to phosphorylate *in vitro* the Thr^{38} of CPI-17: ROK (Koyama et al. 2000), ILK (Deng et al. 2002), PAK (Takizawa et al. 2002), PKA (Dubois et al. 2003), PKG (Erdodi et al. 2003) and protein kinase N1 (Hamaguchi et al. 2000) from which ROK, ILK and PAK also phosphorylate MYPT1 on Thr^{696} inhibitory site at least in *in vitro* conditions. Another member of CPI-17 family, kinase-enhanced protein phosphatase type 1 inhibitor (KEPI) also attenuates PP1c activity (Liu et al. 2002). KEPI was isolated from rat brain, but is also expressed in heart or muscle and it is activated by its phosphorylation at Thr^{73} by PKC (Liu et al. 2002) through an action similar to CPI-17. Additional small regulatory protein is dopamine- and cAMP-regulated phosphoprotein of 32 kDa (DARPP-32) that is primarily expressed in brain and shows sequence homology with I-1 (Williams et al. 1986). After its phosphorylation at Thr^{34}, DARPP-32 binds close to the catalytic center of PP1c inhibiting its catalytic activity in a phosphorylation-dependent manner (Hemmings et al. 1984). 14-3-3β protein is a small acidic regulatory protein that is widely expressed in all eukaryotic cells investigated (van Heusden 2009). 14-3-3β was found to contribute cytoskeletal reorganization with binding to MYPT1, which diminishes the association of MYPT1 to myosin II and cause dissociation of MP complex from its substrate increasing phosphorylation of MLC20 (Koga et al. 2008).

Telokin was found to activate MP without altering phosphorylation of Thr^{696} or Thr^{853} of MYPT1 (Khromov et al. 2012). It is a 17 kDa protein containing C-terminal domain of myosin light chain kinase (Gallagher et al. 1991) and is highly expressed in phasic smooth muscle (Choudhury et al. 2004). Telokin does not have any kinase activity but its phosphorylation on Ser^{13} by PKG or PKA is required for MP activation (MacDonald et al. 2000; Khromov et al. 2006). However, it is still undefined how telokin activates myosin phosphatase. Tumor suppressor prostate apoptosis response (Par)-4 protein was also found to support activation of MP. In vascular smooth muscle cells Par-4 co-localizes with the actin filament bundles (Vetterkind et al. 2009) and directly binds to and interacts with MYPT1 (Vetterkind et al. 2010). Association of Par-4 with MYPT1 blocks the access of ZIPK to the inhibitory phosphorylation site Thr^{696} of MYPT1 and maintains MP in an activated state. After phosphorylation of Par-4 at Thr^{155} by ZIPK, phospho-Par-4 dissociates from MYPT1 allowing ZIPK to inhibit MP through the phosphorylation of MYPT1 at the inhibitory site (Vetterkind et al. 2010).

Table 1. Regulatory proteins of myosin phosphatase

Protein	Target subunit	Type of regulation
prostate apoptosis response-4 protein (Par-4)	MYPT1	Activation
telokin	?	Activation
14-3-3β	MYPT1	Inhibition
CPI-17	PP1c	Inhibition
dopamine- and cAMP-regulated phosphoprotein of 32 kDa (DARPP-32)	PP1c	Inhibition
inhibitor 1 (I-1)	PP1c	Inhibition
inhibitor 2 (I-2)	PP1c	Inhibition
kinase-enhanced protein phosphatase type 1 inhibitor (KEPI)	PP1c	Inhibition
smoothelin-like 1 protein (SMTNL1)	?	Inhibition

A novel inhibitory protein of myosin phosphatase was recently identified in smooth muscle contraction namely the smoothelin-like 1 protein (SMTNL1) (Borman et al. 2004). SMTNL1 is the member of smoothelin family of muscle proteins and contains a C-terminal calponin homology (CH) domain (Borman et al. 2004). SMTNL1 mediates sex-dependent adaptations of smooth and skeletal muscle induced by exercise (Wooldridge et al. 2008) and inhibits myosin phosphatase activity (Borman et al. 2009; Lontay et al. 2010). Characteristics of SMTNL1 protein and its effect towards MYPT1 and MP will be detailed later (see *Smoothelin-like 1 protein* section).

Smoothelin-like 1 protein (SMTNL1)

Structure of smoothelins and SMTNL1

Smoothelin-like 1 protein (SMTNL1), originally termed as calponin homology-associated with smooth muscle (CHASM), was first isolated from rabbit ileum smooth muscle as a target of cGMP-dependent protein kinase, PKG (Borman et al. 2004). It was identified as a new member of smoothelin family of muscle proteins, which contains two additional members, namely smoothelin A (SMTN-A) and smoothelin B (SMTN-B) expressed from a single *smtn* gene (van Eys et al. 1997; Rensen et al. 2002). SMTNL1 is encoded separately by a unique gene (Ulke-Lemee et al. 2011). SMTN-A, a 59 kDa short isoform is expressed in visceral smooth muscle (van der Loop et al. 1997) and the 100 kDa long isoform, SMTN-B is expressed in vascular smooth muscle (Wehrens et al. 1997; Kramer et al. 1999). Smoothelins are often used as indicators for differentiated and contractile smooth muscle cells (van der Loop et al. 1997). The three members of SMTN family shares sequence similarity (Fig. 7) mainly at their carboxyl-termini containing a single type-2 calponin homology (CH) domain (Ishida et al. 2008) referring to smooth muscle calponin which shows high binding affinity towards cytoskeletal actin (Horowitz et al. 1996). Although SMTNL1 contains the CH-domain, it was not able to bind filamentous actin by co-sedimentation assay (Borman et al. 2004). Apart from the CH-domain, smothelins have other novel actin-binding domains (double within SMTN-B, single within SMTN-A) and both isoforms contain additional tropomyosin-binding domain (Fig. 7) (Quensel et al. 2002). Interestingly, SMTNL1 was also found to bind tropomyosin and this interaction promoted its localization to the thin filament (contractile muscle filament including actin, tropomyosin and troponin) through the CH-domain in combination with the intrinsically disordered amino-terminus of SMTNL1 (MacDonald et al. 2012). Moreover, SMTNL1 is also able to interact with calmodulin (CaM) through an IQ motif (based on the consensus sequence IQxxxRGxxxR) at the N-termini of the CH-domain (apo-CaM-binding site or CBD2) and by another CaM-binding region namely Ca^{2+}-CaM-binding domain (CBD1, Fig. 7) (Ishida et al. 2008; Ulke-Lemee et al. 2014). CBD1 prefers to interact with calcium-bound CaM while CBD2 prefers binding to calcium-free (apo-) CaM (Ulke-Lemee et al. 2014). According to current knowledge, SMTNL1 has a single serine phosphorylation site, Ser^{301}, which is responsible for PKA and PKG (Borman et al. 2004) and plays a central role in SMTNL1 function.

Smoothelin-like 2 protein (SMTNL2) should be mentioned as another smoothelin-like protein expressed from *smtnl2* gene (Strausberg et al. 2002; Kimura et al. 2006). SMTNL2 is

a functionally uncharacterized protein containing a single CH-domain and a predicted D-site as a MAPK substrate (Gordon et al. 2013). In the study of Gordon *et al.* SMTNL2 was found to be phosphorylated by ERK and JNK *in vitro*, and the presence of SMTNL2 was detected in all the tested adult mouse tissue types, prominently in skeletal muscle at mRNA level as well as at protein level during myogenic differentiation of C2C12 muscle myoblasts (Gordon et al. 2013). SMTNL2 was found to be downregulated in kidney and breast tumors compared to corresponding normal tissues (Galvez-Santisteban et al. 2012).

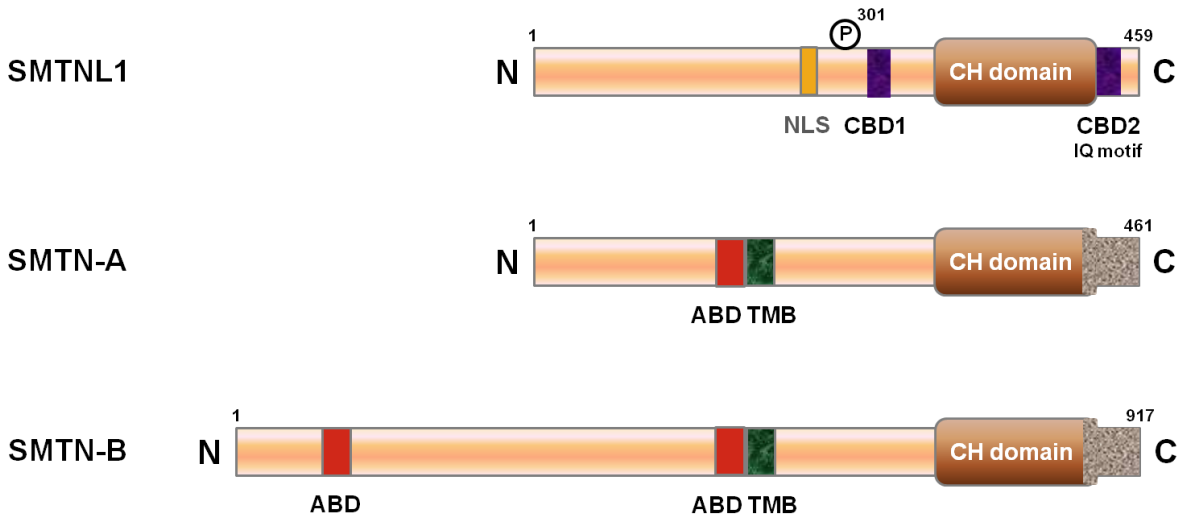

Figure 7. Schematic structure of SMTN family proteins.
Marked fragments are: CH-domain, calponin homology domain; ABD, actin-binding domain; TMB, tropomyosin-binding domain; CBD1, Ca^{2+}-CaM-binding region; CBD2, apo-CaM-binding region with IQ motif; NLS, putative nuclear localization signal. Illustration was made on (Turner et al. 2014).

Molecular functions of SMTNL1

SMTNL1 was identified during Ca^{2+} desensitization (cyclic nucleotide-induced relaxation) in permeabilized rabbit ileum smooth muscle, and it was phosphorylated at Ser^{301} by PKG during muscle relaxation (Borman et al. 2004). Initial studies focused on the interactions between SMTNL1 and the contractile apparatus although SMTNL1 is also expressed in steroid hormone sensitive tissues such as endometrium and myometrium of uterine (Lontay et al. 2010). It is known that adaptive responses during pregnancy are under the control of steroid hormones. Bodoor *et al.* established the binding of SMTNL1 to progesterone receptor (PR) *in vivo* and *in vitro* (Bodoor et al. 2011). Elevated expression level of SMTNL1 was detected in vascular and myometrial smooth muscle during pregnancy and pseudo-pregnancy (Lontay et al. 2010) while increased protein level of PR was found in both reproductive and non-reproductive murine tissues when SMTNL1 was knocked out (Bodoor

et al. 2011). Smtnl1 knock out mice were characterized by a reproductive phenotype by decreased fertility with higher embryonal lethality, longer intervals between pregnancies, difficulties to get pregnant (Bodoor et al. 2011). Direct role in the regulation of PR was confirmed since RNA interference of SMTNL1 caused significant increase in PR expression and gene expression analysis suggested a co-regulator effect of SMTNL1 on PR transcriptional activity (Bodoor et al. 2011). In addition, SMTNL1 translocated from the cytosol to the nucleus upon phosphorylation at Ser^{301} (Lontay et al. 2010) and the translocation attenuated its binding to the B isoform of PR and inhibited transcriptional activity of PR-B (Bodoor et al. 2011).

Based on recent findings of SMTNL1 as a co-regulator of progesterone receptor the following model of myosin phosphatase regulation by SMTNL1 in smooth muscle cells was set up (Fig. 8) (Lontay et al. 2010): Non-phosphorylated SMTNL1 associates to MYPT1, the regulatory subunit of MP and blocks myosin phosphatase activity inhibiting dephosphorylation of MLC20. When SMTNL1 is phosphorylated at Ser^{301} by PKA or PKG, it translocates to the nucleus after dissociation from MYPT1 resulting muscle relaxation via phospho-MLC20 dephosphorylation by active MP. In the nucleus, phospho-SMTNL1 may bind to transcriptional factors, which modulates (decrease) the expression of MYPT1. In the nucleus of reproductive tissue cells, SMTNL1 interacts with nuclear hormone receptors that may also regulate MYPT1 expression.

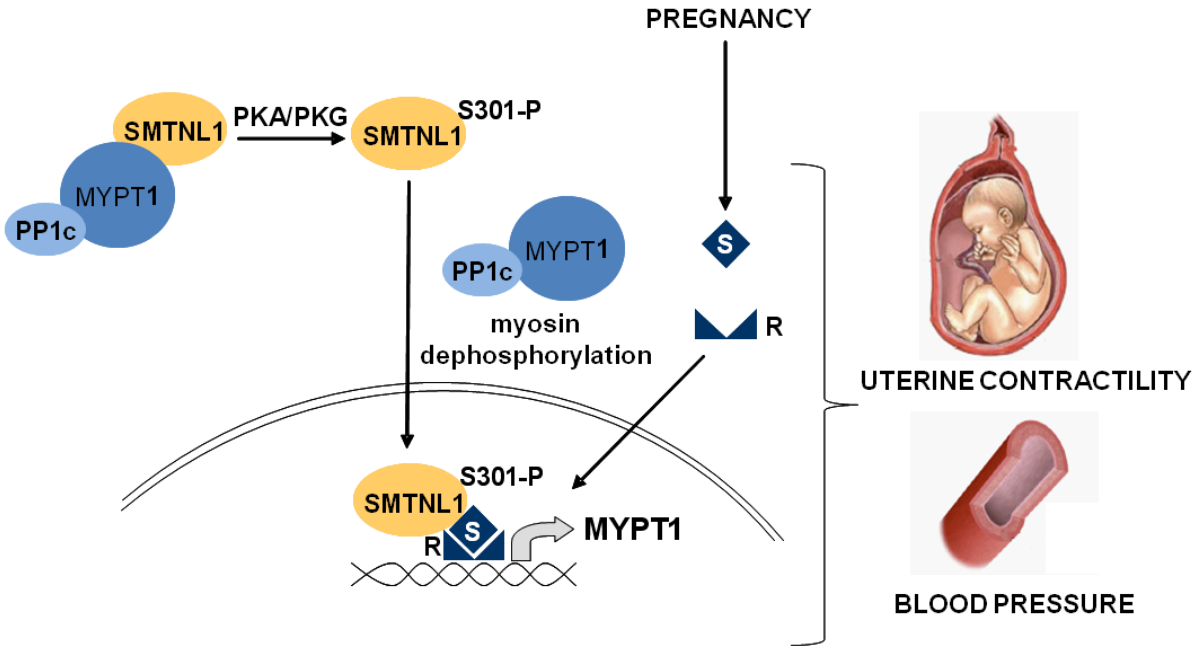

Figure 8. Model for the regulation of MYPT1 by SMTNL1.
(Lontay et al. 2010)

The other phenotype beside the reproductive one of the *smtnl1* knock out mouse strain was characterized with an exercise-adapted phenotype. In SMTNL1 KO mice performed better in exercise on treadmill training than their wild type littermates (Wooldridge et al. 2008). In addition, exercise training on itself caused decreased expression of SMTNL1 both in smooth or skeletal muscle. SMTNL1 also showed differences in the expression level between different types of smooth muscle and between genders suggesting a type- and sex-dependent contractile response of muscles (Wooldridge et al. 2008). Further experiments exhibited a more relaxed phenotype connected to increased myosin phosphatase activity during SMTNL1 deletion or SMTNL1 phosphorylation at Ser^{301} (Wooldridge et al. 2008) indicating the inhibitory effect of unphosphorylated SMTNL1 towards myosin phosphatase. Borman *et al.* verified the inhibitory effect of full length SMTNL1 on MP activity towards phosphorylated MLC20 but did not found any effect on the activity of MLCK during *in situ* experiments (Borman et al. 2009). The inhibitory effect of SMTNL1 seems to be CH-domain-dependent as truncated mutant of SMTNL1 lacking CH-domain did not reduced MP activity (Borman et al. 2009).

The skeletal muscle fibers are characterized based on their phenotypic and metabolic properties. One criteria for classification is the way of adenosine triphosphate (ATP) production which is essential during contraction (Peter et al. 1972). Slow twitch (type I fibers) muscle fibers produce ATP in the presence of oxigen, since fast twitch (type IIA and B) fibers have a high glycolytic enzime activity and produce ATP during anaerob catabolism of carbohydrates. Type IIA fibers have both aerobic and anaerobic metabolic pathways. Skeletal muscle fiber types are also different in the time of contraction, which depends on the combination of myosin heavy chain and light chains (Aagaard et al. 1998). One muscle fiber contains one type of myosin heavy chain and different types of light chains therefore the type of myosin heavy chain (MHCI, IIA or IIB) serves as muscle fiber marker (Table 2). Type IIB glycolytic fibers are characterized by the less contraction time. Muscles containing IIB fast twitch fibers are capable of the greatest effort and are the most exhaustible ones, while repeated low level contraction and higher endurance is typical when the muscle contains slow twitch fibers (Lieber et al. 2002). Type IIA fast twitch fibers have fast contraction time and medium resistance to fatigue with a less force production than type IIB fibers. Skeletal muscle is capable to transform from oxidative to glycolytic isotype and this process can be characterized by the distribution of the various fiber types. The above described plasticity of muscle could be triggered upon physiological and pathological conditons such as pregnancy or hypertension and hyperthyreodism, respectively.

Table 2. Characteristics of skeletal muscle fiber types

Characteristics of the three muscle fiber types			
Fiber type	**Slow twitch (I)**	**Fast twitch A (IIA)**	**Fast twitch B (IIB)**
Contraction time	Slow	Fast	Very fast
Activity used for	Aerobic	Anaerobic	Anaerobic
Force production	Low	High	Very high
Oxidative capacity	High	High	Low
Glycolytic capacity	Low	High	High
Type of myosin heavy chain	MHCI	MHCIIa	MHCIIb

SMTNL1 was characterized as a skeletal muscle protein showing IIA fiber type specific expression pattern and sensitivity to pregnancy hormones. Moreover, it has been characterized as a major regulator of muscle isotype switch in exercise training in mice. Summing up, SMTNL1 can be designated as a modulator of vascular smooth muscle as well as cardiovascular and skeletal muscle contraction and adaptation to exercise, pregnancy or development through the inhibition of MP and regulation of gene expression through the progesterone receptor.

AIMS

Cytoskeletal regulator and muscle contractility mediator myosin phosphatase (MP) impacts through the dephosphorylation of phosphorylated 20 kDa light chain of motor protein myosin II (Ikebe et al. 1985) and governs contractility, cell motility and migration processes of muscle or non-muscle cells. Extensive regulatory role of MP is indicated by the additional substrates besides myosin II and supported by the diverse subcellular localization of the regulatory subunit of MP (MYPT1) in different cell types (Boudrez et al. 1999). Possible translocation of MYPT1 from the cytosol to the plasma membrane (Shin et al. 2002) and to the nucleus (Lontay et al. 2005) upon phosphorylation was previously reported and active nuclear conduction of MP was proved *in vitro* (Lontay et al. 2005) suggesting a possible regulatory role of MP in different nuclear processes. Based on the above mentioned preliminary data our goal was:

- To gain more information about nuclear roles of myosin phosphatase by investigating the exact subnuclear localization of MYPT1.
- To screen novel substrates of MP through the determination of the nuclear interactome of MYPT1.
- To determine the regulatory effect of myosin phosphatase towards its nuclear substrates.

On the other hand, smoothelin-like 1 protein (SMTNL1) was demonstrated as a regulator of MP activity during exercise adaptation and pregnancy (Lontay et al. 2010) but the molecular background of it is still undetermined. In the second part of the present study our aims were the followings:

- To investigate the possible direct interaction between SMTNL1 and MYPT1 by binding assays and to determine the regions of MYPT1 are responsible for the interaction.
- To describe the molecular mechanism regulated by SMTNL1 and the physiological relations connected to SMTNL1 in skeletal muscle adaptation during pregnancy.

MATERIALS AND METHODS

Chemicals and reagents

Chemicals and reagents were purchased as listed below. L-glutamine, fetal bovine serum (FBS), Non Essential Amino Acids (NEAA), Dulbecco's Modified Eagle Medium (DMEM), Minimum Essential Medium (MEM) for human cell line culturing were from PAA Laboratories; trypsin-EDTA 0.05% (GIBCO); polyethyleneimine (PEI) transfection reagent (Polysciences Inc.); pReceiver-M11 encoding human wild-type PRMT5 transcript variant 1 (NM_006109.3, GeneCopoeia Inc.); recombinant human PRMT5 (Sino Biological Inc.); pcDNA 3.1 encoding N-terminal Flag-tagged (FT-) SMTNL1 (NP_077192.1) (Lontay et al. 2010); QuickChange II XL Site-Directed Mutagenesis Kit (Agilent Technologies); CM5 sensorchips (Biacore AB); active Rho-kinase (ROK) from rat, protein kinase C (PKC) and A (PKA) (Merck Millipore); Pierce BCA protein assay kit (Thermo Scientific); 0.45 μM pore size nitrocellulose membrane (Bio-Rad Hungary Ltd.); Ac-DEVD-AMC substrate (Calbiochem); rat tail collagen-coated cover slips (BD Biosciences); ProLong Gold Antifade Reagent (Molecular Probes); SomaPlex reverse phase protein microarray slides (Protein Biotechnologies); TRI reagent (Molecular Research Center Inc.); RNase free DNase I, Maxima Hot Start PCR Master Mix, siMYPT1 sequences, ON-TARGETplus Non-targeting siRNA #1, Dharmafect 2 reagent, Pierce Protein Desalting Spin Columns (Thermo Fisher Scientific); qPCRBIO cDNA synthesis kit (PCR Biosystems); Epigenase PRMT methyltransferase (type II-specific) activity/inhibitory assay kit (Epigentek); Protein-A Sepharose CL-4B (GE Healthcare); Flag peptide, anti-flag M2 affinity gel, protease inhibitor cocktail Complete Mini, histone mixture from calf thymus, Periodic acid-Schiff (PAS) staining system and all other chemicals were obtained from Sigma Aldrich. Microcystin-LR (MCY-LR) was generously given by the Department of Botany, University of Debrecen.

Antibodies

Antibodies were as follows: anti-MYPT1$^{1\text{-}296}$ was prepared as described previously (Lontay et al. 2004); anti-PP1cδ, anti-nucleolemma, anti-nucleoli, anti-spliceosome, anti-PRMT5 from Upstate Millipore; anti-MYPT1 (E-19), anti-PP1cα/γ (E-9); anti-Lamin A/C, monoclonal anti-α-tubulin from Santa Cruz Biotechnology; anti-H2AR3me2s from Abcam; anti-MEP50, anti-phospho-Thr, anti-histone H2A, -histone H4, -H4R3me2s and HRP-linked anti-mouse IgG from Cell Signaling Technology; anti-*c*-Myc and horseradish-peroxidase (HRP) conjugated anti-rabbit IgG from Sigma Aldrich; anti-retinoblastoma protein from BD

biosciences, HRP-conjugated Clean-blot IP detection reagent from Thermo Scientific Inc.; anti-SMTNL1, anti-phospho-SMTNL1^{S301} from Proteintech Inc.; anti-MHC1, anti-MHC2a, anti-MHC2b from Developmental Studies Hybridoma Bank, University of Iowa, USA; To-Pro-3 iodide, Alexa Fluor 633-conjugated Phalloidin (F-actin), Alexa Fluor 488-conjugated anti-rabbit, Alexa Fluor 546-conjugated anti-goat and anti-mouse IgG from Molecular Probes.

Anti-phospho-PRMT5^{T80} antibody

Rabbit polyclonal phospho-specific PRMT5 antibody was made by Abmart Inc. using the Thr^{80} phosphorylated PRMT5 synthetic peptide with a sequence of GRDWN(pT)LIVGK during rabbit immunization and for affinity purification of the antibody. We validated the antibody by dot blot and by immunoblot following manufacturer's suggestions (ab-mart.com). The phospho-PRMT5^{Thr80} specific antibody recognized neither the wild type (wt) nor the Thr80Ala (T80A) mutant peptide of PRMT5 but the Thr^{80} phosphorylated PRMT5 synthetic peptide by dot blot analysis (Fig. 9A). The antibody was also found to be specific to the ROK-phosphorylated Flag-PRMT5 (FT-PRMT5) but showed no cross-reaction with either the non-phosphorylated FT-PRMT5 or the non-phosphorylated and phosphorylated form of FT-PRMT5^{T80A} mutant (Fig. 9B).

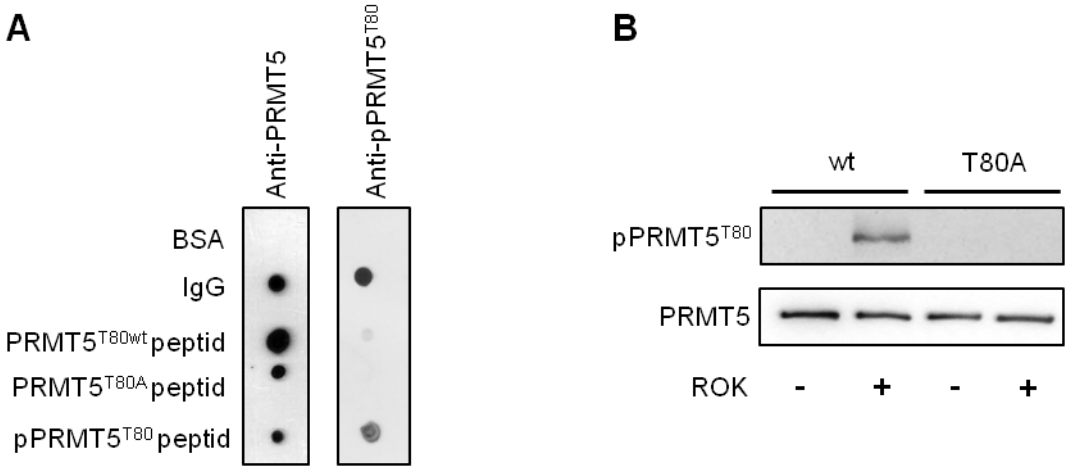

Figure 9. Validation of anti-phospho-PRMT5^{T80} antibody.

(A) *Specificity of the anti-PRMT5 and anti-phospho-PRMT5^{T80} antibodies was verified by dot blot analysis using wild type (T80wt), alanine mutant (T80A) and phosphorylated wild type (pT80) synthetic peptides of PRMT5 from Abmart. BSA and anti-rabbit IgG were applied as negative and positive control, respectively.* ***(B)*** *Validation of anti-phospho-PRMT5^{T80} antibody by immunoblot using non-phosphorylated and ROK-phosphorylated FT-PRMT5^{wt} (wt) and FT-PRMT5^{T80A} (T80A) proteins.*

Recombinant proteins

Recombinant PP1cδ (Hirano et al. 1995), GST-MYPT1$^{1\text{-}1004}$, GST-MYPT1$^{667\text{-}1004}$ (Feng et al. 1999) and N-terminal hexahistidine tagged (His-) MYPT1$^{1\text{-}633}$ (Hirano et al. 1997) were expressed in E. coli and purified as described before (Toth et al. 2000; Kiss et al. 2002). ^{32}P-MLC20 was purified as described previously (Erdodi et al. 1995). Recombinant inhibitor-2 (I-2) was prepared as described before (Zhang et al. 1994). Recombinant human PRMT5 (NP_006100.2) fused with a polyhistidine-tag at C-terminus and a Flag-tag at the N-terminus (FT-His-PRMT5) was purchased from Sino Biological Inc. for SPR and phosphorylation assays for MS analysis and was free from MEP50 (Fig. 10F). FT-PRMT5^{wt}, -PRMT5^{T80A}, FT-MYPT1 and FT-SMTNL1 were purified from transfected tsA201 lysates using anti-Flag M2 affinity gel applying the manufacturer's protocol. FT-PRMT5^{wt} and -PRMT5^{T80A} proteins were bound to anti-Flag M2 affinity gel during kinase or phosphatase assays and *in vitro* protein arginine methyltransferase assays. FT-PRMT5 was in complex with MEP50. PP1c-free FT-MYPT1 was produced for phosphatase assays and for *in vitro* protein arginine methyltransferase assays. FT-MYPT1 bound to the anti-Flag M2 affinity gel was incubated with MYPT1$^{1\text{-}296}$ peptide (Lontay et al. 2004) several times to dissociate the PP1c subunit then FT-MYPT1 was eluted from the beads with 300 μg/ml Flag-peptide. The lack of PP1c in the FT-MYPT1 preparation was validated by Western blot with anti-PP1c antibody and phosphatase assay with ^{32}P-MLC20 substrate. The purity of GST-MYPT1$^{1\text{-}1004}$, GST-MYPT1$^{667\text{-}1004}$ (Fig. 10A), His-MYPT1$^{1\text{-}633}$ (Fig. 10B), rPP1cδ (Fig. 10C), FT-SMTNL1 (Fig. 10D) and FT-PRMT5s (Fig. 10E) was judged by sodium dodecyl sulfate-polyacrylamide gel electrophoresis (SDS-PAGE) followed by Coomassie Blue staining.

Surface plasmon resonance (SPR)

SPR-based binding studies were carried out using a Biacore 3000 instrument to monitor the interaction of MYPT1 with PRMT5 or SMTNL1. Tris-based buffer of FT-His-PRMT5 and FT-SMTNL1 or His-MYPT1$^{1\text{-}633}$ was replaced by Pierce Protein Desalting Spin Columns to a buffer consists of 10 mM HEPES, 150 mM NaCl, pH 7.4 or to 10 mM sodium acetate, pH 5.0, respectively. GST-MYPT1$^{1\text{-}1004}$ and GST-MYPT1$^{667\text{-}1004}$ were immobilized on CM5 sensor chips coupled with anti-GST. The surface of the chips were activated by the injection of 35 μl solution containing 200 mM EDC and 50 mM NHS for 7 min at a flow rate of 5 μl/min. 30 μg of anti-GST antibody was diluted in 1 ml of immobilization buffer (10 mM Na-acetate, pH 5.0) and was injected to the surface at 10 μl/min flow rate for 7 min. The remaining reactive sites were eliminated applying 35 μl 1M ethanolamine (pH 8.5).

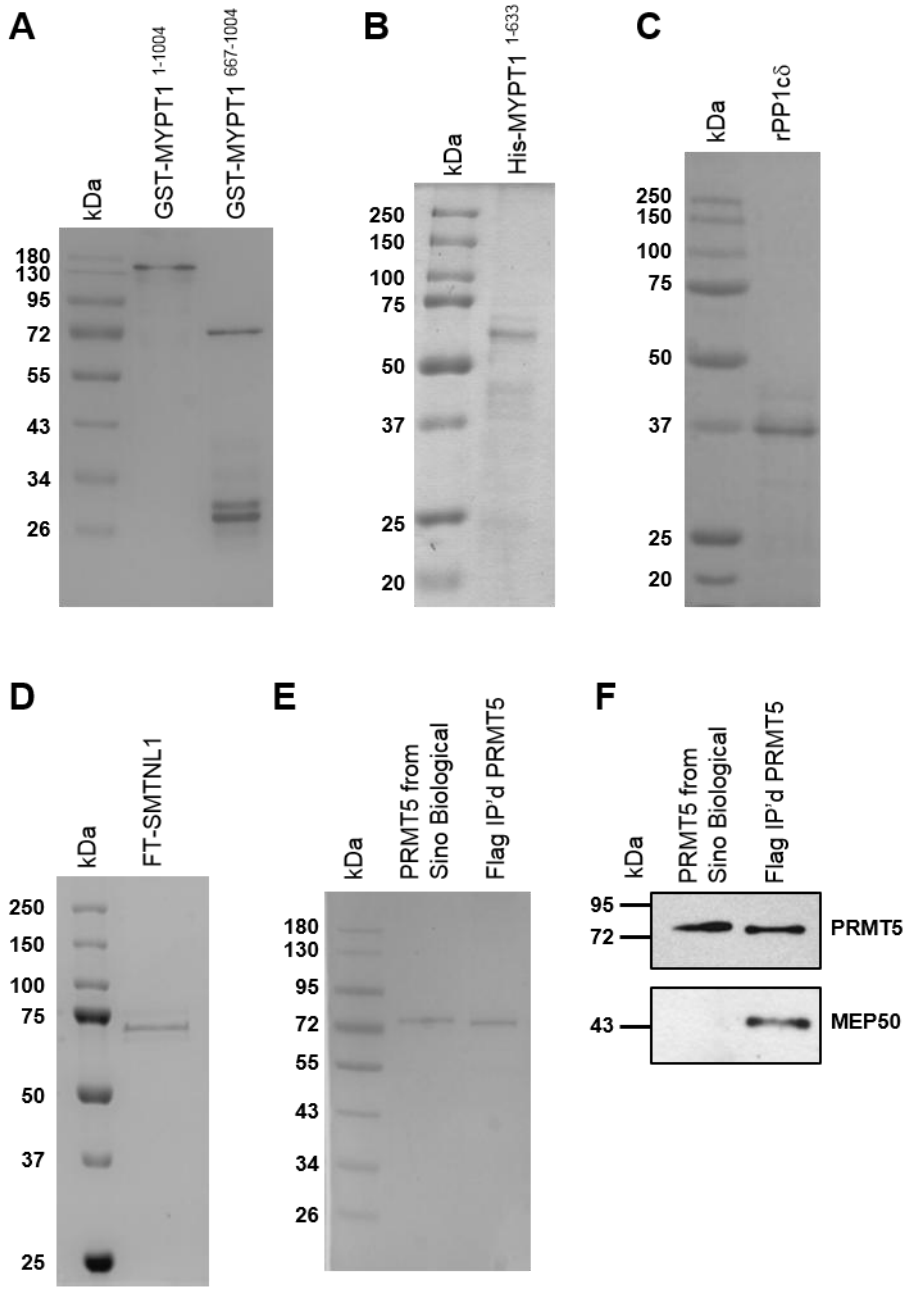

Figure 10. Purity of recombinant proteins.

Coomassie stained gels represent the purity of GST-MYPT1$^{1-1004}$ and GST-MYPT1$^{667-1004}$ ***(A)****, His-MYPT1$^{1-633}$* ***(B)****, rPP1cδ* ***(C)****, FT-SMTNL1* ***(D)****, FT-His-PRMT5 (Sino Biological) and the immunoprecipitated (IP'd) FT-PRMT5* ***(E)****. Immunoblot of MEP50-free FT-His-PRMT5 and Flag IP'd PRMT5 in complex with MEP50* ***(F)*** *by PRMT5 and MEP50 specific antibodies.*

Thereafter, recombinant GST as control surface, GST-MYPT1$^{1-1004}$ and GST-MYPT1$^{667-1004}$ were bound in running buffer (10 mM HEPES, pH 7.4, 150 mM NaCl, 3 mM EDTA, 0.005% Surfactant P20). His-MYPT1$^{1-633}$ was directly immobilized via amine-groups of protein by amine coupling. The amount of the captured ligands was determined by the changes of the resonance signal. A surface without any captured ligands and blocked by 1M ethanolamine

was used as control surface. FT-His-PRMT5 was injected over the cell surfaces in a concentration range of 0.3125-6.7 μM or FT-SMTNL1 was applied from 0.5 to 7.14 μM at a flow rate of 10 μl/min. Association of FT-His-PRMT5 or FT-SMTNL1 to the immobilized proteins was monitored for 7 min. The dissociation induced by the injection of running buffer without any analyte was monitored for an additional 6-7 min. Non-specific binding was determined by the screening of the control surface. Resonance signal was expressed as response units (RU). RU of the control surface was subtracted from data related to protein-coated surfaces. Interaction of PRMT5 or SMTNL1 with MYPT1 fragments was characterized by kinetic parameters of sensorgrams and association constant (K_a) values determined by BIAevaluation 3.1 software.

Site-directed mutagenesis

Expression vector pReceiver-M11 encoding wild-type human full-length PRMT5 (NM_006109.3) transcript variant 1 was purchased from GeneCopoeia Inc., USA. Point mutation of $PRMT5^{T80A}$ was performed using QuickChange II XL Site-Directed Mutagenesis Kit according to the manufacturer's instructions. Primers for mutagenesis are listed in Table 3. The sequence of the $PRMT5^{T80A}$ was verified by DNA sequencing, performed by UD-GenoMed Medical Genomic Technologies Ltd. (Debrecen, Hungary). DNA sequencing primers are listed in Table 4.

Table 3. Primer pair of PRMT5 site-directed mutagenesis

PRMT5 mutant	Forward primer (5' to 3')	Reverse primer (5' to 3')
$PRMT5^{T80A}$	TGTCAGGAAGGGACTGGAATGC GCTAATTGTGGG	CCCACAATTAGCGCATTCCAGT CCCTTCCTGACA

Table 4. Primers for DNA sequencing of PRMT5 mutant

PRMT5 forward # 1 353	5' – GTCTTCCAGCTTTCCTGCTG – 3'
PRMT5 forward # 2 858	5' – CTTAAGCCAGAACCGTCCTC – 3'
PRMT5 forward # 3 1357	5' – GCCCAGCACTTCCTAAAAGA – 3'
PRMT5 reverse 447	5' – GGAAGAGTGATGGCCAGTGT – 3'

Cell cultures

Human liver hepatocellular carcinoma (HepG2) and human embryonal kidney (tsA201) cells from The European Collection of Cell Cultures (ECACC) were grown using DMEM with high glucose content supplemented with 2 mM L-glutamine and 10 % heat-

inactivated FBS. Human breast adenocarcinoma (MCF-7) cells purchased from ECACC were maintained in MEM completed with 2 mM L-glutamine, 1% NEAA and 10 % heat-inactivated FBS. All three human cell lines were subcultured in 37 °C incubator with humidified atmosphere of 5 % CO_2 between 60-90% confluency, and were passed after 2-3 days by trypsin-EDTA solution.

Transient transfections

The endogenous MYPT1 expression was knocked down using the mixture of double-stranded siRNAs (Table 5) and a non-target sequence (ON-TARGETplus Non-targeting siRNA #1) with the G–C content of siMYPT1 was used as a control. Transfection mixture containing 50 nM siRNAs and Dharmafect 2 reagent was added to serum-free medium comprising HepG2 or MCF-7 cells. After 30 min, the medium was completed with 10% FBS and cells were incubated for 6 h and transfection medium was replaced to complete medium. After 42 h of incubation cells were processed.

TsA201 cells were transfected with pReceiver-M11 plasmids containing FT-PRMT5^{wt}, FT-PRMT5^{T80A} and FT-MYPT1 inserts or pcDNA 3.1 plasmid with FT-SMTNL1 insert using 1 mg/ml PEI transfection reagent in serum-free medium, based on the transient transfection protocol of adherent cells by PolyPlus-transfection. After 6 h incubation medium was replaced to complete DMEM and after an additional 24 h cells were lysed.

Table 5. siRNA sequences for MYPT1 silencing

siRNA #1	5’ – CAACUAAACAGGCCAAAUA – 3’
siRNA #2	5’ – GCUAAAUAGUGGUCAUAUA – 3’
siRNA #3	5’ – ACAAAGAGACGUUGAUUAU – 3’
siRNA #4	5’ – CGGAUUCCAUUUCUAGAUA – 3’

Cell lysis and protein measurement

To prepare total cell lysates, HepG2 and transfected tsA201 cells were collected and washed by Dulbecco's phosphate-buffered saline (PBS: pH 7.2; 2.7 mmol/L KCl, 1.5 mmol/L KH_2PO_4, 136.9 mmol/L NaCl, 8.9 mmol/L $Na_2HPO_4 \cdot 7H_2O$) and lysed in a buffer (50 mM Tris HCl, pH 7.4, 150 mM NaCl, 1 mM EDTA, 1% (v/v) Triton X-100) compatible with anti-Flag M2 affinity purification and it was followed by 3 x 10 sec sonication (30% amplitude, 2 pulse/sec) on ice with 15 sec intervalls. After centrifugation (16,000 × g for 15 min at 4 °C), protein concentration of the supernatants were measured by bicinchoninic acid (BCA) colorimetric method using ELISA reader (Labsystem Multiscan MS) at 540 nm. Working

reagents and diluted bovine serum albumin (BSA) as a standard were prepared following the manufacturer's descriptions.

Cell fractionation method

HepG2 and MCF-7 cells were grown to 80% confluency, washed with ice-cold PBS, collected and centrifuged at 4°C at 1,500 x g for 3 min. After the removal of PBS, cells were homogenized in 400 µl buffer A (10 mM Hepes, pH 7.9, 10 mM KCl, 0.1 mM EDTA, 0.1 mM EGTA, 1 mM DTT, 0.5 % (v/v) Nonidet P-40, 0.5 mM PMSF, 1 x concentrated protease inhibitor cocktail) by suspending with a 26 gauge needle 10 times for HepG2, 5 times for MCF-7 cells using a 1 ml syringe. The lysates were vortexed for 15 sec. The efficiency of lysis was judged by trypan blue staining monitoring the intact nuclei. The lysate was centrifuged at 4°C at 16,000 x g for 1 min and the supernatant was used as cytosolic fraction. The pellet was resuspended in 200 µl buffer A and passed through a 26G needle 5 times as a washing step. After centrifugation at 4°C at 16,000 x g for 1 min, 100 µl buffer B (20 mM Hepes, pH 7.9, 420 mM NaCl, 0.5 mM EDTA, 0.5 mM EGTA, 1 mM DTT, 0.5 mM PMSF, 1 x concentrated protease inhibitor cocktail) was added to the pellet and it was sonicated (3 x 10 sec, 30% amplitude, 2 pulse/sec) on ice with 15 sec intervalls and used as nuclear fraction. The fractionation method was based on protocols previously described (Phung et al. 1997; Marciniak et al. 1998).

Cell viability assay

Untreated, non-target control and MYPT1 knocked down HepG2 cells were plated into 96-well tissue culture plates to determine changes in cell viability by MTT assay. To prepare MTT reagent, 5 mg of 3-(4,5-dimethylthiazol-2-yl)-2,5-diphenyltetrazolium bromide was solved in 1 ml PBS. Before adding 20 µl MTT reagent to the cells, culture medium was replaced by 200 µl fresh medium in the wells. Cells were incubated at 37°C in 5% CO_2 atmosphere for 30-90 min until formazan crystals became visible by light microscope. After the MTT medium was removed, the formazan salt was dissolved in DMSO (100 µl/well) and the intensity of the color was measured at 540 nm by an ELISA reader. Cell viability was expressed as a percentage, where 100% was considered as the viability of untreated cells.

Caspase assay

Untreated, non-target control and MYPT1-silenced HepG2 cells were grown in 6-well plates for caspase-3 activity assay. Cells were washed in ice-cold PBS and lysed in caspase lysis buffer (10 mM HEPES, 2 mM EDTA, 0.1% CHAPS, 5 mM DTT, 1 x concentrated

protease inhibitor cocktail and 1 mM PMSF, pH 7.4). Caspase reaction buffer (100 mM HEPES, 10% sucrose, 0.1% CHAPS, 5 mM DTT, pH 7.25) containing the fluorogenic substrate were added to the lysates in 1:1 ratio and incubated for 1 hour at 37°C. Aminomethylcoumarin (AMC) -conjugated caspase-3-specific peptides (Ac-DEVD-AMC) were used as substrates of the reaction. Liberation of AMC due to the cleavage of the substrate was directly proportional to the enzyme activity of caspase-3 which was detected by measuring the fluorescence using 380 nm excitation and 460 nm emission wavelengths. Caspase-3 activity was given in percentage, where 100% was the caspase-3 activity of untreated cells.

Mouse colony maintenance and pregnancy studies

Congenic 129 SvEv *smtnl1-/-* mouse (Wooldridge et al. 2008) strain was generated and pregnancy and pseudo-pregnancy studies were conducted by the Haystead group at Duke University, NC as described (Lontay et al. 2010). For pregnancy studies, 8 week old mice were sacrificed at day 14-17 of the pregnancy. Animal studies were approved by the Duke University Institutional Animal Care & Use Committee. Human skeletal muscle biopsies were collected at the East Carolina University and the procedure was approved by the University and Medical Center Institutional Review Board at East Carolina University.

Homogenization of tissue samples

For Western blotting murine plantaris muscles were frozen in liquid N_2 and stored at -80^{o}C until their processing. Tissue samples were homogenized on ice in glass dounce homogenizer with 40-50 strokes in ice-cold homogenization buffer (50 mM Tris-HCl, pH 6.8, 1% (m/v) SDS, 10% (v/v) glycerol, 20 mM DTT, 127 mM 2-mercaptoethanol supplemented with protease and phosphatase inhibitors). After 20 min incubation on ice samples were centrifuged at 13,000 x g for 5 min on 4°C, protein concentration of the supernatants was determined by the BCA method and samples were heated for 5 min on 100°C completed with 5x sample buffer (0.2 M Tris-HCl, pH 6.8, 10% (m/v) SDS, 20% (v/v) glycerol, 10 mM DTT, 0.05% bromophenol blue).

Immunohistochemistry

Non-pregnant, pseudopregnant or pregnant mouse plantaris muscle and human rectus abdominalis (RA) samples of pre-menopausal patients with hysterectomy (non-pregnant) or with C-sectioning (caesarean delivery) were utilized for fiber typing of skeletal muscle (SKM) by immunohistochemistry. Isopenthane-frozen tissue samples were fixed by 4%

formalin and analyzed by immunofluorescent staining using antibodies specific for SMTNL1, MHC1, MHC2a and MHC2b. Images were taken on Zeiss LSM 510 confocal laser scanning microscope and were processed using LSM 5 Examiner software program.

Periodic Acid-Schiff staining

To determine glycogen content of skeletal muscle, Periodic Acid Schiff (PAS) staining was applied on mouse plantaris and human rectus abdominalis muscle tissues following the instructions of manufacturer. Sections were deparaffinized and rehydrated in distilled water then incubated in Periodic Acid solution for 5 min at room temperature (RT). After 2-3 times repeated rinse by distilled water slides were immersed in Schiff's reagent for 15 min at RT and following five minute wash by tap water for 5 min was next. Counterstaining was performed with Hematoxylin solution for 90 sec followed by washing step in running tap water. Sections were dehydrated and mounted in xylene based mounting media. Glycogen was detected as bright red signal by light microscopy. The intensity of the signal was measured by Image J software and was normalized to the data of WT non-pregnant tissues. A representative set of images of n = 5-7 experiments are shown.

Proteomic studies

Plantaris muscle samples of WT and SMTNL null mice in day 0 and 14 of pregnancy were homogenized in glass homogenizer in sample buffer (5M urea, 4% CHAPS, 1 mM DTT) and centrifuged at 15000 x g for 15 min. Samples were subjected parallel to multi-dimensional proteomic analysis using micro anion-exchange separation, 1D SDS PAGE and LC-MALDI TOF-TOF MS/MS analysis. Proteins were visualized with silver staining and gels were dried. Proteins showing increased recovery between each condition were excised for identification by MALDI-TOF TOF mass spectrometry (Table S1). Changes in individual proteins were determined using a combination of densitometry and iTRAQ (Shadforth et al. 2005; Schmidt et al. 2009).

SDS-PAGE and immunoblotting

Protein samples made for Western analysis were supplemented by 5x SDS sample buffer (0.2 M Tris-HCl, pH 6.8, 10% (m/v) SDS, 20% (v/v) glycerol, 10 mM DTT, 0.05% bromophenol blue) or proteins bound to affinity beads were eluted by 1 x SDS sample buffer (0.0625 M Tris-HCl, pH 6.8, 2% SDS, 10% glycerol, 5% β-mercaptoethanol, 0.02 % bromophenol blue). All of the samples were incubated for 5 min at 100°C after addition of 1x or 5x SDS sample buffer. Protein separation by molecular weight was performed by sodium

dodecyl sulfate-polyacrylamide gel electrophoresis (SDS-PAGE). After SDS-PAGE, separated proteins were revealed by Coomassie blue staining method to verify purity of proteins or by MS compatible silver staining to subjected samples to LC-MS/MS analysis. In every other cases samples were transferred to 0.45 μM pore size nitrocellulose membranes at 100 V for 90 min. The remaining binding sites of the membranes were blocked by 5% (m/v) nonfat dry-milk powder solved in PBS (137 mM NaCl, 2.7 mM KCl, 1.8 mM KH_2PO_4, 10 mM Na_2HPO_4, pH 7.2) with 0.1% (v/v) Tween20 (PBST). PBST was replaced by TBST (50 mM Tris-HCl, pH 7.4, 150 mM NaCl, 0.1% (v/v) Tween20) when phosphorylation specific antibodies were applied. After blocking, membranes were incubated with primary antibodies for overnight at 4°C with gentle agitation, washed 3 x 10 min by PBST or TBST and it was followed by incubationing them with either HRP-conjugated anti-rabbit, or with anti-mouse or clean blot IP detection reagent at least for 2 h at room temperature. Immunoreactions were detected by enhanced chemiluminescence (ECL) either by FluorChem AIC system (Alpha Innotech) or by autoradiography films. For quantitative comparisons samples were derived from the same experiments. For quantification of PRMT5 Thr^{80} or SMTNL1 Ser^{301} phosphorylation membranes were stripped and assayed for PRMT5 or SMTNL1 content as it is described (see Membrane stripping for reprobing). Internal controls were either assayed on the same gel or were processed in a parallel experiment. Densitometry of the proteins of interest were performed by Image J. 1.46 and normalized to an internal control protein and plotted as relative numbers as detailed in figure legends.

Membrane stripping for reprobing

Membranes were washed four times for 5 min each in TBST and were incubated from 30 min at 50°C in stripping buffer (62 mM Tris, 2% (m/v) SDS, 0.7% (v/v) 2-mercaptoethanol, pH 6.8 with slight agitation. Then membranes were washed six times for 5 min with TBST before blocking them again.

Immunofluorescence microscopy

HepG2 cells were grown on rat tail collagen-coated cover slips and were fixed by dehydration using 90% ethanol and permeabilized by 0.5% Triton-X-100 for 3 min at room temperature. Cells were washed three times for 5 min by TBS between the different steps then blocked by 1% BSA for 60 min at 4°C. Primary and secondary antibodies were applied in 1:100 and 1:200 dilutions, respectively, at least for 60 min at 4°C. To-Pro-3 iodide (1:1000) or DAPI (1:2000) were added as nuclear dyes as indicated in figure legends. After the

washing steps, cover slips were mounted with ProLong Gold Antifade Reagent. Images were taken by Leica X8 confocal microscope and were processed using Leica X8 software program and PhotoShop Imaging software.

Immunoprecipitation and pull-down assays

For immunoprecipitation (IP) anti-MYPT1$^{1-296}$, anti-PRMT5 antibodies and non-immune rabbit serum were incubated with Protein-A Sepharose (PAS) at 4°C for 2h with continuous gentle shaking in IP binding buffer consisting of 30 mM Tris, 150 mM NaCl, 1 mM EDTA, 0.1% Triton-X-100 supplemented with protease inhibitor cocktail, pH 7.4. In parallel HepG2 total lysate diluted to 1 mg/ml final concentration was precleared with 100 µl PAS at 4°C at least for 30 min. Precleared HepG2 lysate was distributed equally among PAS coupled by anti-MYPT1$^{1-296}$, anti-PRMT5 or serum control and incubated overnight at 4°C agitation. Finally, samples were washed two times by IP binding buffer, once with TBS and the buffer was completely removed from PAS beads. Proteins were eluted by adding 50 µl 1 x SDS sample buffer directly to the beads followed by boiling. Samples were loaded onto SDS-PA gels and were applied for Western blot analysis. Membranes were probed with anti-MYPT1$^{1-296}$ and -PRMT5 antibodies followed by Clean-blot IP detection reagent.

Flag-peptide as a control and FT-MYPT1 were bound to anti-Flag M2 affinity gel for LC-MS/MS analysis to identify the interacting proteins of FT-MYPT1. Samples were precleared on anti-Flag M2 affinity gel prior to affinity isolation. After washing with TBS three times, beads were incubated with HepG2 nuclear extract for 2 hr on 4°C. FT-MYPT1 and its interacting proteins were eluted from the beads by 300 µg/ml Flag-peptide. Eluted samples were subjected to SDS-PAGE. Bands of interest were visualized by MS compatible silver staining and the proteins were prepared for LC-MS/MS by in-gel digestion using trypsin.

FT-PRMT5^{wt}, -PRMT5^{T80A} and FT-MYPT1 were purified from transfected tsA201 lysates using anti-flag M2 affinity gel applying the manufacturer's protocol. FT-PRMT5^{wt} and -PRMT5^{T80A} proteins were bound to anti-flag M2 affinity gel during kinase and phosphatase assays and *in vitro* protein arginine methyltransferase assays. FT-MYPT1 was eluted from the beads with 300 µg/ml Flag peptide and applied for phosphatase assays and *in vitro* protein arginine methyltransferase assays.

Identification of MYPT1 interacting proteins from LC-MS/MS data

Bands of interest were subjected to *in-gel* digestion (for protocol see https://msf.ucsf.edu/protocols.html) using side-chain protected porcine trypsin (37 ˚C, 4h). For the identification of MYPT1 interacting proteins, the resulting peptide mixtures were analyzed directly by data-dependent „triple play" LC-MS/MS using a 3D-ion trap mass spectrometer (LCQ-Fleet, Thermo Fisher Scientific). Peak lists generated from the MS/MS data by the Mascot Distiller software (v2.2.1.0) were searched against the human subset of the NCBI database (downloaded 02/20/2010; 183553 protein sequences) using the Mascot search engine. Search parameters: enzyme: trypsin with maximum 2 missed cleavage sites per peptide; fixed modification: carbamidomethyl (Cys); variable modifications: acetylation (protein N-terminus), oxidation (Met), pyroglutamic acid formation (peptide N-terminal Gln); mass accuracy: 0.6 Da and 1 Da for precursor and fragment ions (both monoisotopic), respectively. Acceptance parameters: peptide score>38 ($p<0.05$), minimum 2 unique peptides/protein. LC-MS/MS analysis was performed by the Laboratory of Proteomics Research in the Biological Research Centre of Szeged.

Protein phosphatase assay for HepG2 fractions

Protein phosphatase activity of total lysate, cytosolic and nuclear extracts of HepG2 cells (at 0.05 mg/ml final concentration) was determined using 1 μM γ-^{32}P-labelled 20 kDa light chain of myosin (γ-^{32}P-MLC20) as a substrate as detailed previously (Cohen 2002). Briefly, the reaction was initiated by the addition of the substrate and the 1.5 min incubation was terminated by the addition of 200 μl 10 % TCA and 200 μl 6 mg/ml BSA. After centrifugation, γ-$^{32}P_i$ liberated from the substrate into the supernatant was determined in a liquid scintillation counter.

Protein kinase and phosphatase assays using recombinant PRMT5

Radioactive phosphorylation of recombinant human FT-His-PRMT5 from Sino Biological Inc. was initiated by 0.2 mM γ-^{32}P-ATP or in a non-radioactive manner for LC-MS/MS analysis by 0.5 mM ATP in the absence (control) or in the presence of 0.4 U/ml ROK, 0.1 μg/ml PKA or 0.1 μg/ml PKC at 30°C for 120 min. ROK was applied in ROK assay buffer (20 mM MOPS, pH 7.2, 25 mM beta-glycerophosphate, 0.5 mM EGTA, 0.5 mM DTT, 5 mM $MgCl_2$). PKA assay buffer contained 50 mM HEPES, pH 6.4, 6 mM $MgCl_2$, 1 mM EGTA, 10 mM NaF. PKC assay buffer composed of 20 mM HEPES, 10 mM $MgCl_2$, 1 mM DTT, 0.03% Triton-X100 and 0.65 mM $CaCl_2$, pH 7.5 plus micelles. All kinase assay

buffers contained 1 μM MCY-LR to inhibit protein phosphatase activity. The reaction mixtures were subjected to SDS-PAGE and bands were detected by autoradiography. Non-radiant PRMT5 phosphorylated by ROK was visualized by MS/MS compatible silver-staining previously described (Shevchenko et al. 1996), bands were cut out and subjected to LC-MS/MS analysis.

For Western blots, non-radioactive phosphorylation reaction by ROK (0.4 U/ml) was also carried out in the absence or in the presence of 10 μM H1152 with 0.5 mM ATP, 5mM $MgCl_2$ and 1 μM MCY-LR at 30°C for 30 min using FT-PRMT5^{wt} or FT-PRMT5^{T80A} bound to anti-Flag M2 affinity gel. The kinase assay medium was removed and beads were washed by TBS. Dephosphorylation of FT-PRMT5^{wt} that was phosphorylated by ROK and was bound to the beads (the product of the kinase assay) was initiated by adding 25 nM FT-MYPT1, 5 nM rPP1cδ or the combination of these two proteins at 30°C for 15 min. Beads were washed by TBS and were incubated at 100°C for 5 min in 1 x SDS sample buffer followed SDS-PAGE. Phosphorylation level of Thr^{80} of PRMT5 was detected by phospho-PRMT5^{T80} specific antibody by Western blot and analysed by densitometry normalized to the input of PRMT5.

Identification of PRMT5 phosphorylation sites from LC-MS/MS data

For phosphorylation studies, approximately 80% of the peptide mixtures were subjected to phosphopeptide-enrichment using TiO_2 (Larsen et al. 2005) and the phosphopeptide fractions as well as the remaining 20% of the original samples were analyzed by data-dependent LC-MS/MS using an Orbitrap Elite mass spectrometer (MS spectra acquired in the Orbitrap, MS/MS spectra in the linear ion trap). Collision-induced dissociation (CID) was applied as ion activation technique by neutral gas molecules (Sleno et al. 2004). Peak lists generated from the MS/MS data by the PAVA software (v2010/september) were searched against the Swissprot database (downloaded 06/27/2013; 540546 protein sequences) using the ProteinProspector search engine. Search parameters: enzyme: trypsin with maximum 1 missed cleavage site per peptide; fixed modification: carbamidomethyl (Cys); variable modifications: acetylation (protein N-terminus), oxidation (Met), pyroglutamic acid formation (peptide N-terminal Gln) allowing maximum 2 variable modifications per peptide; mass accuracy: 5 ppm and 0.6 Da for precursor and fragment ions (both monoisotopic), respectively. Subsequently another search was conducted on the subset of confidently identified proteins using the same search parameters except that maximum 2 missed cleavages per peptides were allowed, and phosphorylation on Ser/Thr/Tyr was also set as variable

modification allowing maximum 3 variable modifications/peptides. For all searches the following acceptance criteria were applied: score>22 and 15, and E-value<0.01 and 0.05 for protein and peptide identifications, respectively. For phosphopeptide sites assignments, SLIP threshold (Baker et al. 2011) was set to 6. All phosphopeptide identifications were inspected manually. LC-MS/MS analysis was performed by the Laboratory of Proteomics Research in the Biological Research Centre of Szeged.

***In vitro* protein arginine methyltransferase assays**

FT-PRMT5^{wt} was bound to anti-Flag M2 affinity gel following phosphorylation by ROK and was applied for the methylation assay. Methyltransferase assays were carried out in a buffer containing 50 mM Tris, 150 mM NaCl supplemented with protease inhibitor cocktail, pH 7.4 and 2 μM S-adenosyl-L-methionine (SAM) and 0.02 mg/ml of histone mixture were added to the reaction in a total volume of 50 μl. Methylation reaction was allowed to proceed for 2 hours at 30°C in the presence or in the absence of 5 nM rPP1cδ, 25 nM FT-MYPT1 or the combination of rPP1cδ and FT-MYPT1 (assumed as MP holoenzyme). Products of the methylation reactions were analyzed by Western blots using antibodies specific for symmetrical dimethylated H2AR3 and H4R3. Membranes were stripped in each case and were assayed with anti-H2A and -H4 antibodies. Changes of symmetrical dimethylation levels were calculated by densitometry normalized to H2A and H4 internal controls.

Nuclear PRMT5 activity of HepG2 and MCF-7 cells was quantified by colorimetric Epigenase PRMT methyltransferase (type II-specific) activity/inhibitory assay kit following the instructions of the manufacturer. After MYPT1 expression was depleted in HepG2 and MCF-7 cells, nuclear extracts were prepared. During the assay, SAM as a methyl donor, PRMT assay buffer (content of kit) and 5 μg of the nuclear extracts were added onto microplate wells coated with type II PRMT substrate. Methyltransferase reaction was allowed to proceed for 90 min at 37°C. Colorimetric measurement was conducted at 450 nm by conventional microplate reader. PRMT5 activity was expressed as optical density [(OD)/min/mg] in a time dependent manner. PRMT5 activity of MYPT1-silenced nuclear extracts was compared to its non-target control RNA-silenced nuclear extracts.

Gene expression analysis and microarray processing

For total RNA extraction from adherent cells, non-target control and MYPT1-silenced HepG2 cells were grown on 6 well culture plates. Cells were washed 3 x times by PBS and were lysed adding 1 ml TRI reagent per well. Cells were suspended and incubated for an

additional 5 min and were transferred into microcentrifuge tubes. Samples were supplemented with 200 µl chloroform, vortexed for 15 sec and incubated at RT for 4 min. The lysate were centrifuges for 15 min,13,000 x rpm at 4°C then the upper phase containing the RNA was removed and the RNA was precipitated by the addition of 500 µl 2-propanol and incubated for 10 min at RT. After at least 20 min incubation on -70°C, samples were centrifuged for 10 min at 13,000 x rpm at 4°C. 2-propanol was removed and 1 ml of 75% (v/v) ethanol was added following a 5 min 13,000 x rpm centrifugation at 4°C. The alcohol was completely removed and the RNA pellet was dissolved in nuclease free water. NanoDrop ND-1000 spectrophotometer (Thermo Fisher Scientific) was used to determine the RNA concentration. RNA was treated with RNase free DNase I and reverse transcription was performed with qPCRBIO cDNA synthesis kit. PCR amplification was carried out with Maxima Hot Start PCR Master Mix based on the manufacturer's description. RT-PCR products were analyzed by agarose gel electrophoresis. The expression level of the genes of interest was quantified by Image J. 1.45s, normalized to GAPDH and represented as relative numbers. The primer pairs used in the RT-PCR experiments are summarized in Table 6. The expression pattern of the non-target and the MYPT1-silenced HepG2 cells was examined using total RNA extracts. Microarray processing and data analysis was performed by UD-GenoMed Medical Genomic Technologies Ltd. (Debrecen, Hungary). Statistically significant difference was considered as $p < 0.05$ and the fold change cut off value was 1.5.

Table 6. RT-PCR primer pairs

Target	Forward primer (5' to 3')	Reverse primer (5' to 3')
PPP1R12A	CCACAACCCTGACTACAACTAC	TCTCCTTCTTTCTCCTCTTCTCT
PRMT5	CGGAGAAGGGCAGACTA	CAATTTCAAGAGCCACTGC
RAP1A	ATAAGAGTATGTGTCTCACTGC	TCTTCATTCCTGTAATCTGGC

Tissue array analysis

SomaPlex reverse phase protein microarray slides containing human cancer liver and normal tissue samples from 25 clinical cases and 15 common cancer cell line lysates in triplicates were purchased from Protein Biotechnologies. Microarray slides were handled following the manufacturer's instructions. Protein slides were blocked by 3% bovine serum albumin dissolved in TBST assayed with anti-phospho-PRMT5^{T80}, -phospho-MYPT1^{T850} and -histone H2A antibodies at 4°C. Slides were incubated with HRP-labeled secondary antibodies for 2 hours and the antibody binding was developed by enhanced chemiluminescence (ECL) using x-ray films. Each slide was stripped and incubated by

antibodies raised against PRMT5, MYPT1$^{1-296}$, H2AR3me2s and α-tubulin. Dots of interest were analyzed by densitometry and were all normalized to their adequate tubulin internal controls. Values of the phosphorylation of PRMT5 at Thr^{80}, -MYPT1 at Thr^{850} and H2AR3me2s were normalized to PRMT5, MYPT1 and H2A, respectively. Values of cancer tissues were related to normal tissue data and plotted as relative numbers.

Statistical analysis

Normalized data were analyzed using either unpaired parametric Student's t-test (for two groups) or analysis of variance (one-way ANOVA, for >2 groups) or by general linear models (GLM, for >2 groups). Post hoc testing for one-way ANOVA was determined by Tukey's test. In GLMs, we tested all possible interaction terms and report here the final models obtained by excluding non-significant ($p > 0.05$) interactions. When any covariate or factor was significant in GLMs, we applied Tukey's procedure to test for pair-wise differences in group means. Groups sharing the same letter do not show significant deviations. All of normalized variables used in statistical analyses were found to be normally distributed. Tests were conducted using GraphPad for Windows or R statistical program. All data presented in this work represent mean± SE or SEM, *n* means the number of independently performed experiments.

RESULTS

Subnuclear localization of myosin phosphatase in HepG2 cells

Nuclear localization of MYPT1 has been published previously (Tran et al. 2004; Lontay et al. 2005) but its nuclear role or exact subnuclear localization is still undefined. Subcellular localization of MYPT1 and different isoforms of PP1c subunits in human hepatocarcinoma cells (HepG2) was exhibited by Western analysis using antibodies specific for MYPT1, for PP1cδ or for both PP1cα and PP1cγ1. Subcellular compartment-specific α-tubulin and lamin A/C antibodies were used to verify the purity of extracts. MYPT1, PP1cα/γ1 and PP1cδ were distributed in cytoplasmic and nuclear subcellular fractions (Fig. 11A). PP1 and PP2A enzyme activities were determined in HepG2 total lysate, cytosolic and nuclear fraction (Fig. 11B) using ^{32}P-labeled myosin light chain (^{32}P-MLC20) which was shown to be a substrate of both enzymes. Cytosolic protein phosphatase activity was more than 20% higher than in the nuclear fraction. Phosphatase activity of fractions was determined similarly in the presence of 2 μM inhibitor-2 (I-2), which can selectively inhibit PP1 but does not influence PP2A (Bollen et al. 1987). Specific activity values measured in response to 2 μM I-2 suggested that ~60% of total phosphatase activity of nuclear fraction was due to PP1, while PP2A was the dominant protein phosphatase in the cytosolic fraction and represented ~75% of the phosphatase activity. To verify the subcellular and subnuclear localization of the PP1cδ isoform and MYPT1 in HepG2 cells fluorescent confocal microscopy was applied and the colocalization of MYPT1 to PP1cδ and to the subnuclear compartments was determined. MYPT1 and PP1cδ showed nuclear colocalization (Fig. 11C, bottom panel) indicating the nuclear presence of MP. MYPT1 and PP1cδ isoform exhibited staining in the cytoplasm as well. The study of subnuclear localization of MYPT1 using anti-MYPT1$^{1\text{-}296}$ and subnuclear compartment-specific antibodies showed that MYPT1 accumulated in spliceosomes and colocalized with histone H1b protein (Fig. 11C, middle panels) but did not localize to the nuclear membrane or to the nucleoli (Fig. 11C, upper panels). These data suggest that MYPT1 is a putative PP1-targeting subunit during pre-mRNA splicing and it may play a role in the regulation of chromatin structure.

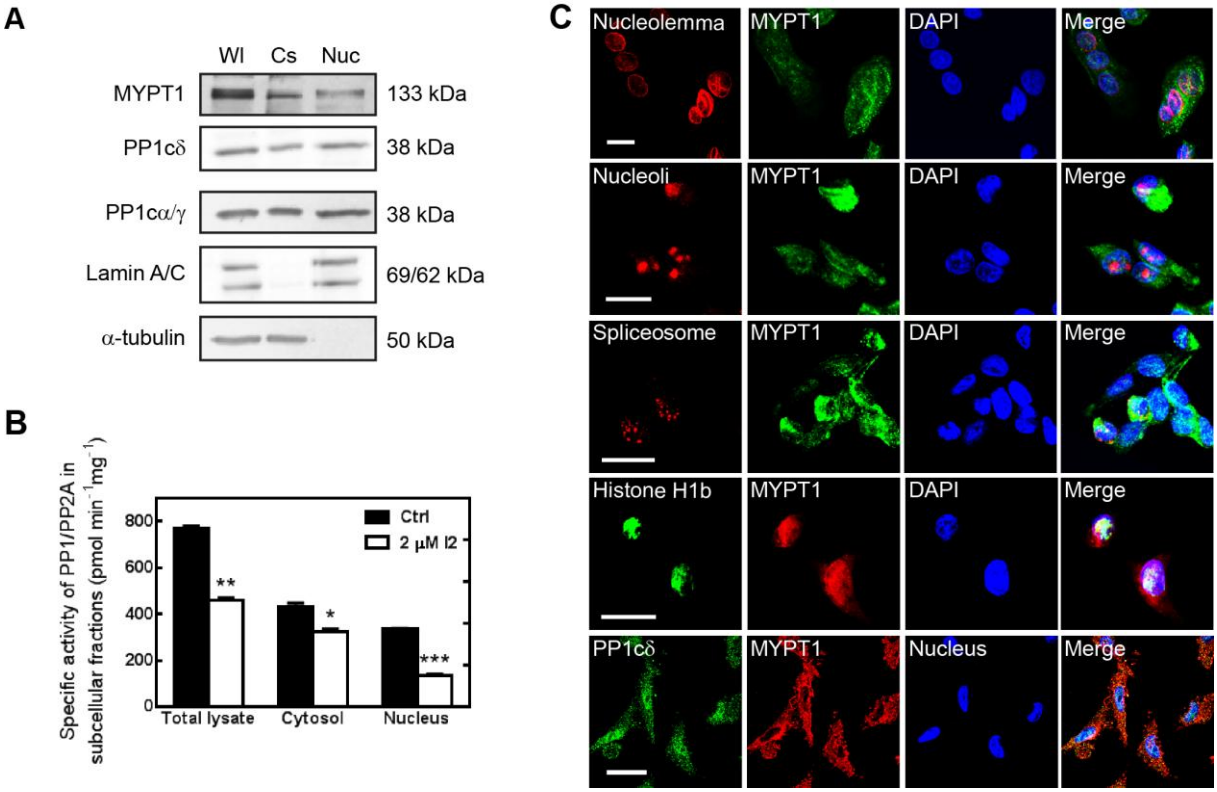

Figure 11. Subcellular distribution of MYPT1 in HepG2 cells.

(A) *HepG2 whole cell lysate (Wl), cytosol (Cs) and nuclear (Nuc) fractions were analyzed by Western blot using antibodies specific for MYPT1, PP1cδ and PP1cα/γ as well as for subcellular fraction-specific markers such as α-tubulin for cytosol and Lamin A/C for nucleus. Samples derived from the same experiment and were processed in parallel.* ***(B)*** *Protein phosphatase activity of cytosolic and nuclear fractions was determined in the absence and in the presence of 2 μM inhibitor-2 (I2) using ^{32}P-MLC20 as substrate. Values represent mean ± SEM; n=3; *p<0.05, **p<0.01, ***p<0.001 by student t-test.* ***(C)*** *Subnuclear distribution of MYPT1 by immunofluorescent microscopy using anti-MYPT1$^{1-296}$ (green) or anti-MYPT1 (E19) (red), anti-histone H1 (green), anti-PP1cδ (green) and subnuclear-specific markers such as anti-nucleolemma (red), anti-nucleoli (red), anti-spliceosome (red) specific antibodies. Nucleus is stained with DAPI (blue). Scale bars: 20 μm.*

MYPT1 nuclear interactome: interaction with the methylosome complex

To get closer to the nuclear processes possibly regulated by MP, nuclear interactome of Flag (FT)-MYPT1 was established by pull-down method followed by mass spectrometry. Pull-down assays were carried out using Flag-MYPT1 protein bound to anti-Flag M2 affinity gel incubated with nuclear extract of HepG2 cells. Proteins filtrated by FT-MYPT1 were eluted from the beads, separated by SDS-PAGE then the silver-stained protein bands were cut out from the gel and subjected to LC-MS/MS analysis. The MYPT1-interacting proteins are listed in Table 7 with their identified peptide sequences and their functions. The distribution of the MYPT1-binding proteins by cellular roles has also been revealed by gene ontology analysis (Table 8).

Table 7. FT-MYPT1 binding proteins of HepG2 nuclear fraction

NCBI gi#	Protein	MW, Da	Peptides	Function
4505317	Protein phosphatase 1 regulatory subunit 12A isoform a (MYPT1)	115610	63 GADINYANVDGLTALHQACIDDNVDMVK 90 162 QGVDIEAAR 170 162 QGVDIEAARKEEER 175 183 QWLNSGHINDVR 194 250 ILVDNLCDMEMVNK 263 299 SPLIESTANMDNNQSQK 315 319 NKETLIIEPEKNASR 333 442 KTGSYGALAEITASK 456 443 TGSYGALAEITASK 456 494 LAYVAPTIPR 503 505 LASTSDIEEKENR 517 558 RQDDLISSSVPSTTSTPTVTSAAGLQK 584 585 SLLSSTSTTTK 595 694 RSTQGVTLTDLQEAEKTIGR 713 695 STQGVTLTDLQEAEK 709 695 STQGVTLTDLQEAEKTIGR 713 908 SGSYSYLEER 917 908 SGSYSYLEERKPYSSR 923 935 LYEQILAENEK 945	Signal transduction
13699824	Kinesin family member 11	120111	147 LTDNGTEFSVK 157 222 TTAATLMNAYSSR 234 258 IGKLNLVDLAGSENIGR 274 261 LNLVDLAGSENIGR 274 298 VITALVER 305 319 ILQDSLGGR 327 811 ISQETEQRCESLNTR 825	Motor protein, mitosis
338443	Beta-spectrin	275259	444 LVSQDNFGFDLPAVEAATK 462 905 VAVVNQIAR 913 1548 SQNIVTDSSSLSAEAIR 1564	Protein targeting
20070220	Protein arginine methyltransferase 5 isoform a	73322	2 AAMAVGGAGGSR 13 69 SDLLLSGRDWNTLIVGK 85 202 IAVALEIGADLPSNHVIDR 220 228 AAILPTSIFLTNK 240 334 YSQYQQAIYK 343 369 GPLVNASLR 377 386 IKLYAVEK 393	Transcription regulation
4507361	Mitogen-activated protein kinase kinase kinase 7 isoform A	64930	72 KAFIVELR 79 412 SIQDLTVTGTEPGQVSSR 429 520 KQELVAELDQDEKDQQNTSR 539	Signal transduction, transcription regulation
4506583	Replication protein A1	68723	184 VVPIASLTPYQSK 196 490 VIDQQNGLYR 499	DNA replication, DNA damage
4505995	Protein phosphatase 1B isoform 1	53180	91 SGSALELSVENVK 103 91 SGSALELSVENVKNGIR 107 130 SGSTAVGVMISPK 142 180 IQNAGGSVMIQR 191 201 ALGDYDYK 208 361 NVIEAVYSR 369	Signaling pathways, cell stress response pathways
62897939	Methylosome protein 50 variant	37469	36 YRSDGALLLGASSLSGR 52 38 SDGALLLGASSLSGR 52	Gene expression, cell proliferation
8571390	Chlorid ion current inducer protein I(Cln)	26340	19 QQPDTEAVLNGK 30 31 GLGTGTLYIAESR 43	Gene expression, spliceosomal snRNP assembly
307383	RNA helicase A	143405	64 DFVNYLVR 71 435 AAECNIVVTQPR 446 837 ELDALDANDELTPLGR 852	Translation initiation, splicing, spliceosome assembly

Table 7. continued

29881667	Splicing factor proline/glutamine-rich	76255	299 LFVGNLPADITEDEFK 314 320 YGEPGEVFINK 330 320 YGEPGEVFINKGK 332 343 ALAEIAKAELDDTPMR 358 366 FATHAAALSVR 376 414 GIVEFASKPAAR 425 480 FAQHGTFEYEYSQR 493 667 FGQGGAGPVGGQGPR 681	Splicing
11067747	CDC5-like protein	92422	207 GVDYNAEIPFEK 218 478 LGLLGLPAPK 487	Cell cycle control, transcription regulation
288100	Initiation factor 4B	69240	166 IRVDVADQAQDKDR 179 357 AASIFGGAKPVDTAAR 372	Translation initiation
4885225	Ewing sarcoma breakpoint region 1 isoform 2	68721	269 QDHPSSMGVYGQESGGFSGPGENR 292 411 GDATVSYEDPPTAK 424	Gene expression, cell signaling, RNA processing
693937	Polyadenylate binding protein II	58709	25 RSLGYAYVNFQQPADAER 42 26 SLGYAYVNFQQPADAER 42 43 ALDTMNFDVIK 53 70 KSGVGNIFIK 79 71 SGVGNIFIK 79 114 GYGFVHFETQEAAER 128 162 AKEFTNVYIK 171 207 GFGFVSFER 215 266 YQGVNLYVK 274 287 KEFSPFGTITSAK 299 288 EFSPFGTITSAK 299 491 SKVDEAVAVLQAHQAK 506	Gene expression, RNA processing
56237027	Insulin-like growth factor 2 mRNA binding protein 1 isoform 1	63783	200 LLVPTQYVGAIIGK 213 526 DQTPDENDQVIVK 538	Translation regulation, mRNA transport
4504447	Heterogeneous nuclear ribonucleoprotein A2/B1 isoform A2	36041	192 GGNFGFGDSR 201 202 GGGGNFGPGPGSNFR 216 314 NMGGPYGGGNYGPGGSGGSGGYGGR 338	Gene expression, mRNA processing
4504445	Heterogeneous nuclear ribonucleoprotein A1 isoform A	34289	16 LFIGGLSFETTDESLR 31 285 SSGPYGGGGQYFAKPR 300	mRNA processing and transport, RNA splicing
356168	Histone H1b	21721	54 SGVSLAALKK 63 64 ALAAAGYDVEK 74	DNA-binding, nucleosome assembly

The potential nuclear MYPT1-binding proteins mostly play roles in RNA processing and splicing and in gene expression (Table 8). Mitogen-activated protein kinase and magnesium-dependent protein phosphatase 1B (PP1B/PP2C) were also among the interacting partners of MYPT1. Surprisingly, all three members of the methylosome complex were identified, namely the protein arginine methyltransferase 5 (PRMT5/JBP1), the PRMT5/JBP1-interacting protein (pICln), and the methylosome protein 50 (MEP50/WDR77). PRMT5 is one of the nine PRMTs in mammalian cells and plays a unique and specific role in the generation of the ω-N^G, N^G-symmetric dimethylarginine (SDMA) as a type II PRMT. It has

multiple cytosolic and nuclear binding partners and is implicated in the regulation of transcription, RNA transport and cellular signaling (McBride et al. 2000).

Table 8. Distribution of FT-MYPT1 binding proteins by their cellular roles

Cellular role	Percentage (%)
RNA processing, splicing, spliceosome assembly	27.58
Gene expression	17.24
Signal transduction	13.79
Transcription regulation	10.34
Translation regulation	10.34
DNA-binding, nucleosome assembly	3.44
DNA replication, DNA damage	3.44
Others (mitosis, protein targeting, protein refolding, embryogenesis, cell proliferation, cell cycle control)	13.79

PRTM5 of the methylosome complex interacts with MP

PRMT5, an enzyme responsible for the symmetric demethylation of numerous proteins was identified as one of the nuclear MYPT1-intercating proteins. We considered necessary to apply additional methods verifying the interaction of PRMT5 as a MYPT1 since *Mellacheruvu et al.* recognized PRMT5 as a nonspecific interacting protein in affinity purified Flag-tagged complexes from HeLa and tsa201 cell lysates (Mellacheruvu et al. 2013). Nuclear and cytoplasmic colocalization of MYPT1 to the methylosome proteins MEP50 and PRMT5 was established by confocal microscopy in HepG2 cells (Fig. 12A). PRMT5 accumulated to a lesser extent in the nucleus than in the cytoplasm (Fig. 12A, upper panel) while MEP50 performed a homogenous staining throughout the cell but predominantly in the cytoplasm (Fig. 12A, lower panel). Both of the methylosome proteins exhibited significant nuclear colocalization with MYPT1 quantified by the Pearson's correlation coefficient (PCC). PCC proved to be 0.5975 of MYPT1 with PRMT5 and 0.618 with MEP50. Since PRMT5 is a key component in the methylosome complex giving the catalytic activity of the complex and it was also defined by the highest peptide number by mass spectrometry (8 peptides for PRMT5 and 2-2 peptides for MEP50 and pICln) from the FT-MYPT1 nuclear interactome, we focused on PRMT5 in our further experiments. Antibodies specific for MYPT1$^{1\text{-}296}$ and PRMT5 were used to confirm their associationby immunoprecipitation in HepG2 cells (Fig. 12B). PRMT5 and MYPT1 were identified in each precipitates as judged by Western blots implying that these proteins were co-precipitated. No cross reactions were detected in the non-immune serum control (Fig. 12B).

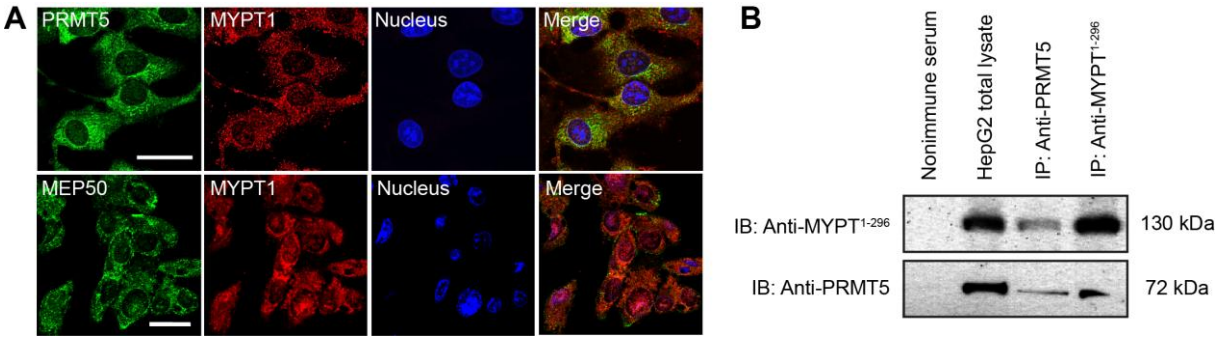

Figure 12. Interaction of MYPT1 with PRMT5.

(A) *Nuclear colocalization of MYPT1 and the members of the methylosome complex by immunofluorescent microscopy of HepG2 cells using anti-MYPT1 (red), anti-PRMT5 (green) and anti-MEP50 (green) antibodies. Nucleus was stained with To-Pro-3 iodide (blue). Scale bars: 20 μm.* ***(B)*** *Immunoprecipitations were carried out using anti-MYPT1$^{1-296}$ and anti-PRMT5 antibodies as well as non-immune rabbit serum as negative control. Immunoprecipitates and HepG2 total lysate were analyzed by Western blot using antibodies specific for MYPT1 and PRMT5.*

To investigate the molecular background of the MYPT1-PRMT5 interaction, binding of PRMT5 to the N- and C-terminal regions of MYPT1 and to the full length MYPT1 was investigated by surface plasmon resonance (SPR)-based binding assays. Full-length GST-MYPT1$^{1-1004}$ as well as the N-terminal MYPT1 of 1 to 633 residues (His-MYPT1$^{1-633}$) and the C-terminal fragment of residues 667 to 1004 (GST-MYPT1$^{667-1004}$) were immobilized and purified FT-PRMT5 was flown through the surface as an analyte. PRMT5 interacted with full-length GST-MYPT1$^{1-1004}$ in a concentration range of 0.3125–5 μM and the association

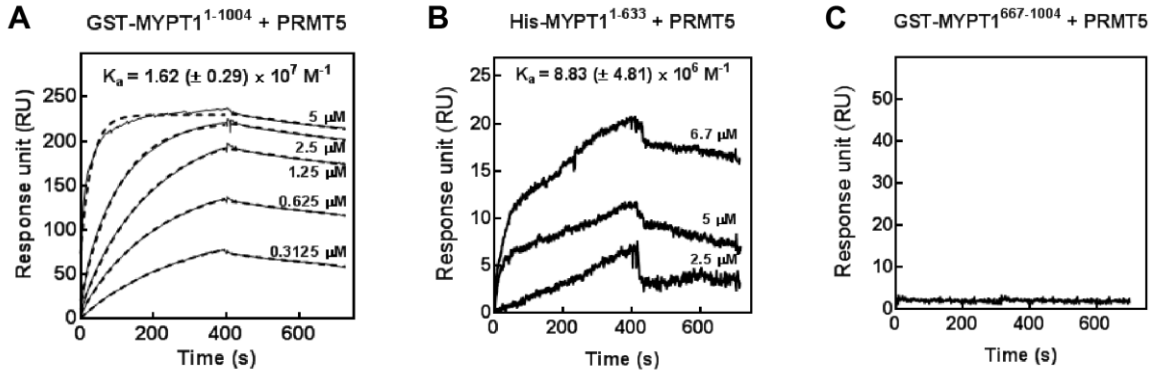

Figure 13. SPR analysis of the interaction of MYPT1 with PRMT5.

GST-MYPT1$^{1-1004}$ ***(A)****, GST-MYPT1$^{667-1004}$ C-terminal fragment* ***(C)*** *and His-MYPT1$^{1-633}$* ***(B)*** *were bound on CM5 sensor chip. FT-PRMT5 was applied in the indicated concentrations. The interaction was monitored using Biacore 3000. The association constant (K_a) values are indicated in the figure.*

constant of the binding was K_a=(1.62 ± 0.29) × 10^7 M^{-1} (Fig. 13A), while no signal for binding with GST-MYPT1$^{667\text{-}1004}$ (Fig. 13C) was obtained. PRMT5 bound to the N-terminal His-MYPT1$^{1\text{-}633}$ (Fig. 13B) with an association constant K_a= (8.82 ± 0.31) × 10^6 M^{-1}, determined by using the first phase of the association curves in the evaluation. Fitting the sensorgram of GST-MYPT1$^{1\text{-}1004}$ with a 1:1 binding model resulted in overlaps with the experimental curves suggesting a 1:1 molar ratio in the GST-MYPT1$^{1\text{-}1004}$- PRMT5 complex. Binding of PRMT5 to the N-terminus of MYPT1 but not to the C-terminal fragment suggests that PRMT5 forms a stable complex with MYPT1 through its N-terminal region.

PRMT5 is a substrate of ROK and MP

The putative phosphorylation sites of PRMT5 were screened and the protein kinases potentially target these sites were predicted by a P-Si Predictor algorithm developed by Kinexus (http://www.phosphonet.ca/). Protein kinase A (PKA), protein kinase C (PKC) and ROK were suggested as potential phosphorylating enzymes therefore they were probed in an *in vitro* phosphorylation assays. The autoradiogram in Figure 14A shows that PRMT5 was phosphorylated by ROK but not by PKA or PKC in kinase assays when radioactive ATP (γ-^{32}P-ATP) was used as phosphoryl donor substrate.

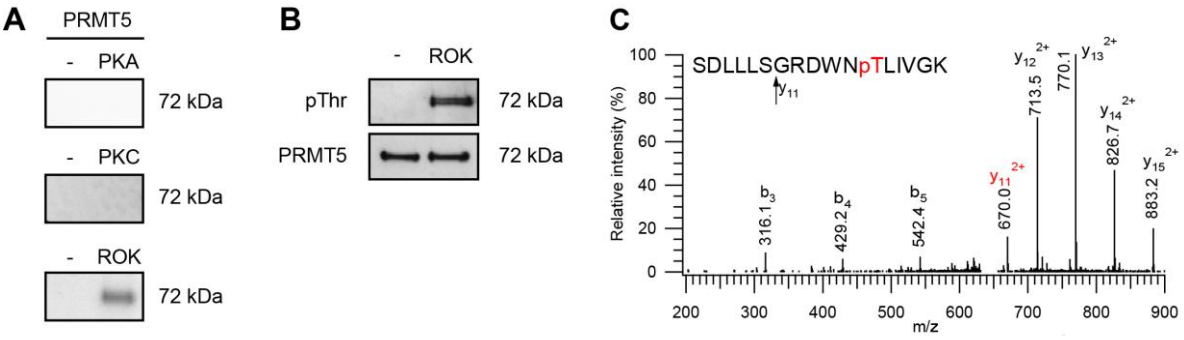

Figure 14. ROK phosphorylates PRMT5 at Thr^{80}.

(A) *Autoradiograms of PRMT5 phosphorylated in the absence or in the presence of 0.1 μg/ml protein kinase A (PKA, upper panel), 0.1 μg/ml protein kinase C (PKC, middle panel) or 0.4 U/ml Rho-associated kinase (ROK, lower panel) with ^{32}P-ATP.* ***(B)*** *Western blot analysis of ROK-phosphorylated PRMT5 using antibody specific for phospho-Thr. After stripping the membrane, anti-PRMT5 antibody was applied to detect PRMT5 as an input control.* ***(C)*** *Ion trap collision-induced dissociation (CID) spectra of PRMT5 phosphopeptides. CID of m/z: 656.338 (3+) identified as SDLLLSGRDWNpTLIVGK representing [69-85] of the wild type protein. Thr^{80} was identified as the modification site (see fragment ion y_{11} (phosphorylated)). Peptide fragments are labeled according to the nomenclature by Biemann (Biemann 1990).*

Western blot analysis of ROK-phosphorylated PRMT5 by an antibody specific for phosphorylated Thr (Fig. 14B) indicated that ROK phosphorylates PRMT5 on Thr residue/s.

Thr^{80} residue was also identified as a ROK phosphorylation site in PRMT5 by mass spectrometry analysis of ROK-phosphorylated FT-PRMT5 samples compared to non-phosphorylated ones (Fig. 14C). Ser$^{15/16}$, Thr^{67} and Ser^{69} were also identified as potential phosphorylation sites of PRMT5 from LC-MS/MS data. However, only Thr^{80} phosphorylation was unambiguously linked to the ROK-treatment since the phosphorylation of Ser$^{15/16}$ was also identified in control samples which were incubated without ROK and the Thr^{67} and Ser^{69}

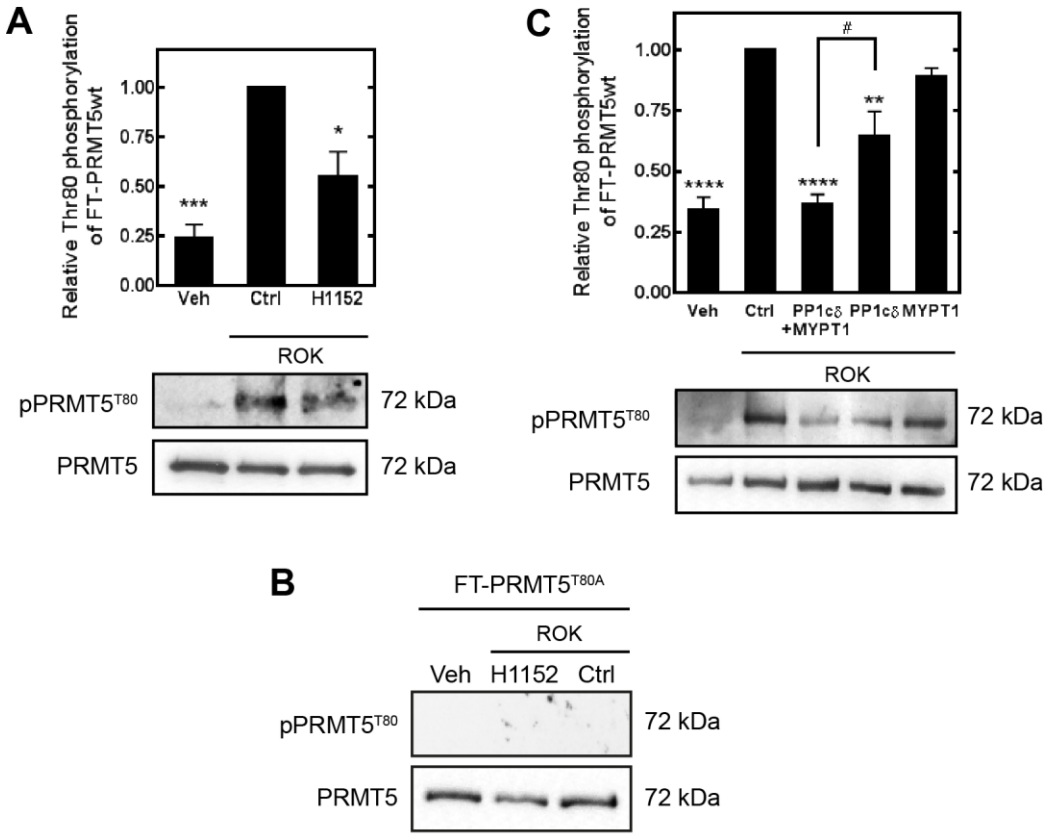

Figure 15. ROK phosphorylates, MP dephosphorylates PRMT5 at Thr^{80}.

(A) *Effect of ROK inhibitor (10 μM H1152) on the phosphorylation level of PRMT5 during in vitro ROK assay. Negative and positive control samples were prepared in the absence and presences of ROK, respectively. Relative phosphorylation level of Thr^{80} was judged by Western blot using anti- pPRMT5^{T80} antibody and blots for PRMT5 served as loading control.* ***(B)*** *Alanine mutant of PRMT5^{T80} (PRMT5^{T80A}) was analyzed by Western blot using anti-phospho-PRMT5^{T80} and PRMT5 antibody after in vitro phosphorylation by ROK in the presence or in the absence of 10 μM H1152, a selective ROK inhibitor.* ***(C)*** *Effect of 25 nM FT-MYPT1 and 5 nM rPP1cδ or their combination on the phosphorylation level of PRMT5 at Thr^{80} as judged by Western blot. Data were compared to ROK-phosphorylated PRMT5. Gels have been processed under the same experimental conditions. Values represents mean ± SEM; *p<0.05, **p<0.01, ***p<0.001, ****p<0.0001, $^{\#}$p<0.05, one-way ANOVA followed by Tukey's multiple comparison test, n=3.*

phosphorylation sites were uncertain even after the enrichment using titanium-oxide chromatography.

ROK-specific phosphorylation of PRMT5^{T80} was confirmed by ROK-assay (Fig. 15A), in which the relative Thr^{80} phosphorylation level of wild type PRMT5 determined by anti-phospho-PRMT5^{T80} antibody (anti-pPRMT5^{T80}) was significantly reduced (nearly 50%) in response to H1152, a selective Rho-kinase inhibitor. The phosphorylation of the alanine mutant of PRMT5^{T80} (PRMT5^{T80A}) was probed in ROK assay in the presence and absence of H1152. No signal was detected with Western blot by anti-pPRMT5^{T80} antibody confirming the Thr^{80} specificity of ROK in PRMT5 phosphorylation (Fig. 15B). To prove the regulatory role of MP on PRMT5, FT-PRMT5 was phosphorylated by ROK and an *in vitro* phosphatase assays was carried out using recombinant PP1cδ and purified FT-MYPT1 proteins or their combination representing MP holoenzyme (Fig. 15C). FT-MYPT1 by itself had no effect on the phosphorylation level of PRMT5 at Thr^{80}, whereas recombinant PP1cδ or the mixture of PP1cδ and FT-MYPT1 caused ~36% and ~63% decrease in the phosphorylation level of PRMT5^{T80}, respectively, comparing to the ROK-phosphorylated samples judged by Western blot analysis using anti-pPRMT5^{T80}. The increased dephosphorylation of PRMT5 at Thr^{80} by PP1cδ in the presence of FT-MYPT1 indicates that the phosphorylated PRMT5 is a substrate of MP holoenzyme and MYPT1 has a targeting role in this process.

Methyltransferase activity of PRMT5 is regulated via phosphorylation and dephosphorylation of its Thr^{80} residue

To explore the effect of Thr^{80} phosphorylation of PRMT5 on its methyltransferase activity we assayed PRMT5 activity by determining symmetric dimethylation of histone 2A and 4 (H2A and H4) on their common arginine 3, the so called "R3 motif". Significant changes in symmetrical dimethylation of H2AR3 or H4R3 were not detected when FT-MYPT1 or PP1cδ were applied (Fig. 16A and B). Nevertheless, the symmetrical dimethylation of H4R3 was decreased by 46% when the mixture of FT-MYPT1 and PP1cδ was added during methyltransferase assay (Fig. 16B). Change in symmetrical dimethylation level of H2AR3 (Fig. 16A) was even more profound when the mixture of PP1cδ and FT-MYPT1 was added suggesting that PP1cδ requires MYPT1 for its phosphatase activity. Since MEP50 is an essential component of the methyltransferase activity of PRMT5, we tested if the phosphorylation at Thr^{80} increases the affinity of MEP50 to PRMT5 resulting the enhanced activity upon ROK phosphorylation. The phosphorylation by ROK with or

without the inhibition of ROK by H1152 had no effect on the amount of the MEP50 bound to the wt PRMT5 (Fig. 17A).

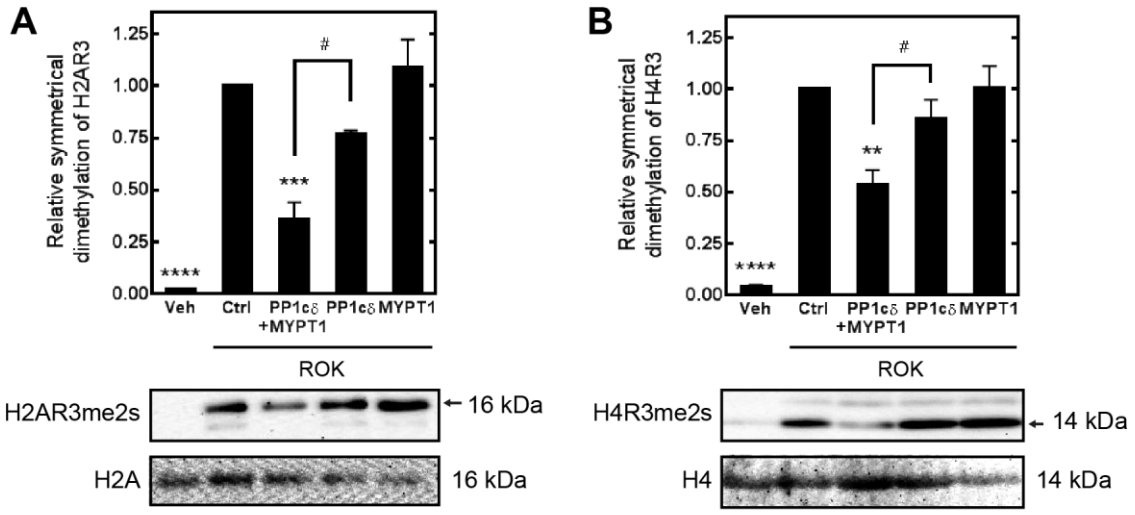

Figure 16. ROK and MP regulate the methyltransferase activity of PRMT5 through phosphorylation/dephosphorylation at Thr^{80}.

*In vitro arginine methyltransferase assay of unphosphorylated and ROK-phosphorylated PRMT5 measured by the symmetric dimethylation level of histone H2A Arg3 (H2AR3me2s, **A**) or histone H4 Arg3 (H4R3me2s, **B**) in the presence of 25 nM FT-MYPT1, 5 nM rPP1cδ or their combinations.*

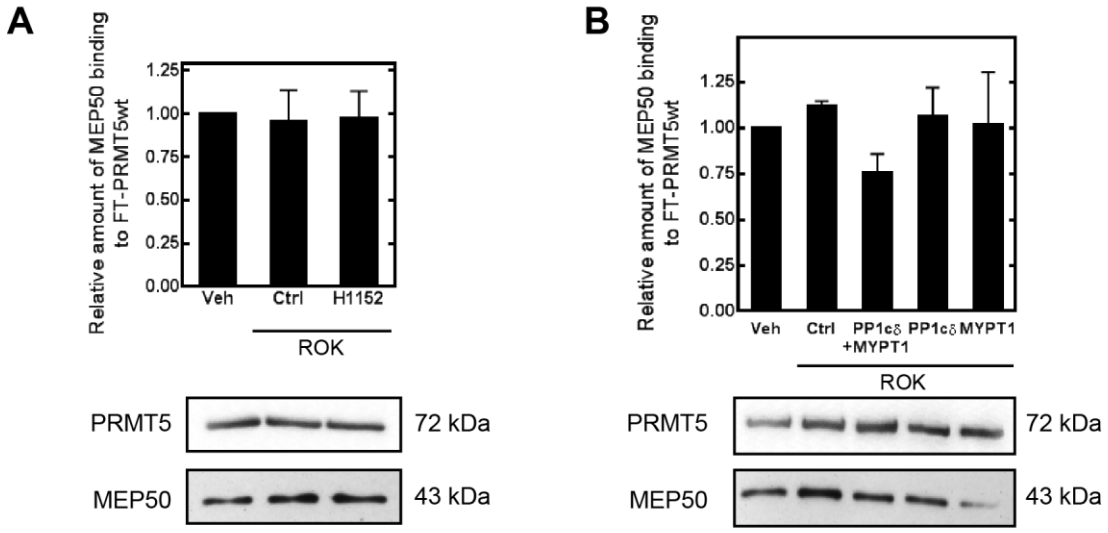

Figure 17. Effect of PRMT5 Thr^{80} phosphorylation on MEP50-binding.

*Amount of MEP50 bound to FT-PRMT5 during ROK-phosphorylation **(A)** and dephosphorylation by MP **(B)** compared to unphosphorylated control samples. MEP50 was detected by anti-MEP50 antibody on Western blot and relative amount was normalized to the level of PRMT5. Gels have been processed under the same experimental conditions. Values represent mean ± SEM; **p<0.01, ***p<0.001, ****p<0.0001, $^{\#}$p<0.05, one-way ANOVA followed by Tukey's multiple comparison test, n=3.*

The relative amount of MEP50 binding to wt PRMT5 showed no significant differences either upon ROK phosphorylation or dephosphorylation by MP (Fig. 17B) implying that the phosphorylation of PRMT5 at Thr^{80} has no effect on MEP50 binding. These data indicate that Thr^{80} residue is a regulatory phosphorylation site of PRMT5 and the phosphorylation increases, while the dephosphorylation decreases its methyltransferase activity.

Silencing of MYPT1 increased Thr^{80} phosphorylation of PRMT5 and dimethylation of histone R3 motifs in HepG2 cells

Histone 2AR3 and -4R3 are symmetrically dimethylated by PRMT5 which shifts the balance from an activating asymmetric (ADMA) to a suppressive symmetric dimethylarginine (SDMA) mark at these motifs regulating gene expression (Feng et al. 2011). The fact that MP dephosphorylated PRMT5 at the ROK-specific phosphorylation site *in vitro* led us to study whether MP plays a role in the regulation of gene expression through the arginine methylation of H2A and 4 at the gene repression sites. Transfection with MYPT1-specific siRNAs (siMYPT1) resulted in a decrease in the protein expression of MYPT1 by >65% in HepG2 cells (Fig. 18A) compared to control experiments where non-targeting siRNAs were applied. MYPT1-silencing was not associated with any significant decrease either in the survival (Fig. 18B) or in the apoptotic properties measured by caspase-3 activity (Fig. 18C). Upon MYPT1-silencing drastic changes in cell morphology and in formation of stress fibers were detected by immunofluorescent staining (Fig. 18D). Neither protein expression (Fig. 19B) nor subcellular localization (Fig. 19A) of PRMT5 was altered in response to silencing of MYPT1, however, the phosphorylation of PRMT5 at Thr^{80} was increased by 46% (Fig. 19C). The dimethylation level of H2AR3 (Fig. 19E) and H4R3 (Fig. 19G) was elevated by 40% and 45%, respectively, whereas the expression of both histone proteins remained constant upon MYPT1 silencing (data are not shown). Fluorescent mean intensity of H2AR3 symmetrical dimethylation (Fig. 19D) increased from 12.8 to 21.79 (arbitrary unit) due to MYPT1-silencing. Difference in symmetrical dimethylation was more considerable in case of H4R3 (from 8.19 to 22.58, Fig. 19F) compared to non-significant intensity changes of H2A or H4 expression (data are not shown).

To clarify our data on PRMT5 regulation by MP, we applied the nuclear extract of non-target and MYPT1-silenced HepG2 on quantitative methyltransferase assay (Fig. 20A). We found that knocking down MYPT1 enhanced the specific activity of PRMT5 by ~65% comparing to the control samples and we also verified these data on human breast cancer cell

line (MCF7 cells) (Fig. 20B). Our results reflect the role of MP in the methyltransferase activity of PRMT5 and thus influence the dimethylation of histone repression marks.

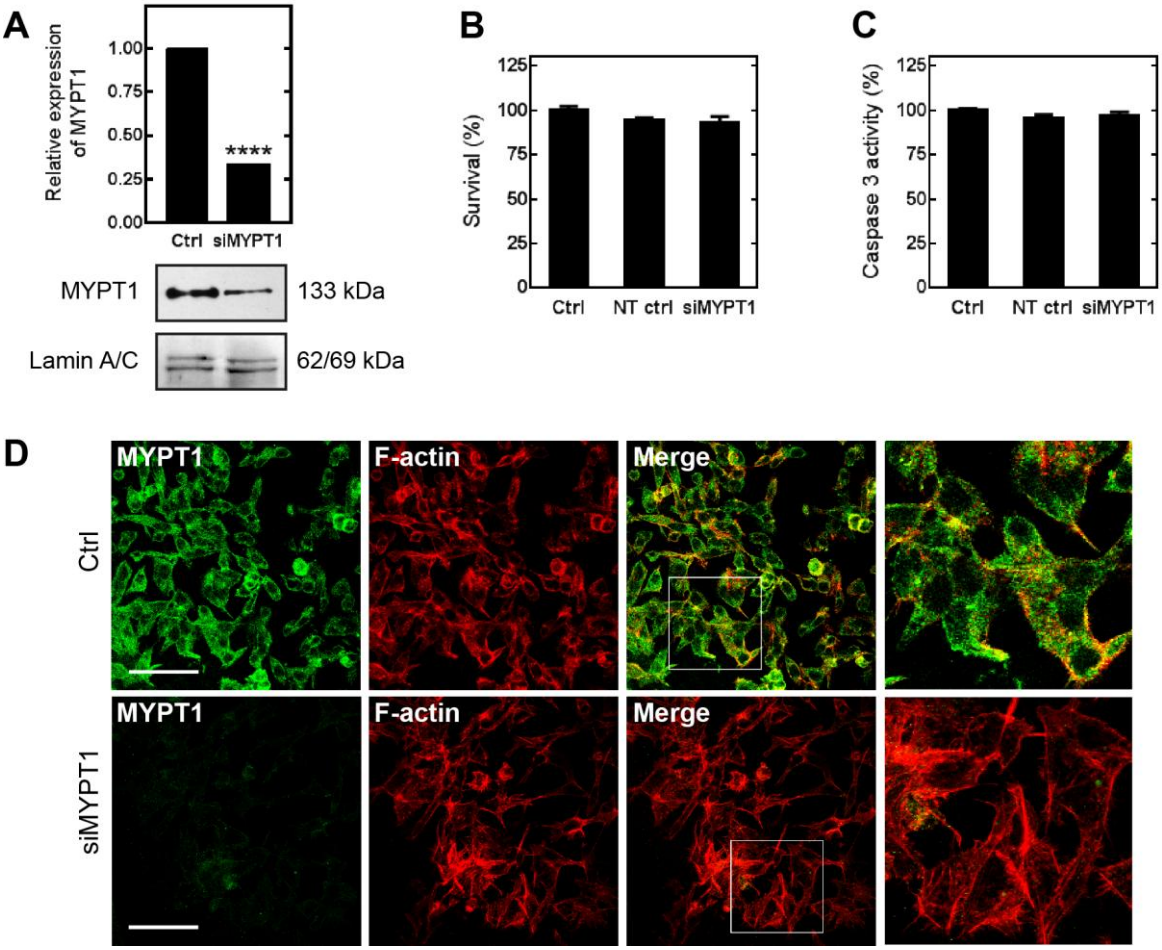

Figure 18. MYPT1 silencing in HepG2 cells.

(A) *Western blot analysis of nuclear fractions of non-target control (Ctrl) and MYPT1-silenced (siMYPT1) HepG2 cells by anti-MYPT1$^{1-296}$ and lamin A/C. The relative expression of MYPT1 was normalized to lamin A/C as internal control. Mean ± SEM; n=3; ****p<0.0001 by student t-test.* ***(B-C)*** *Effect of MYPT1 silencing on cell survival of HepG2 cells. Viability (B) and Caspase-3 activity (C) of untreated (Ctrl), non-target control (NT ctrl) and MYPT1-silenced (siMYPT1) HepG2 cells were determined by MTT or Caspase-3 activity assays. Values obtained for untreated control cells were taken as 100%. Values represent mean ± SEM; n=3.* ***(D)*** *Immunofluorescent staining of non-target control (Ctrl) and MYPT1-silenced (siMYPT1) cells using antibodies specific for MYPT1$^{1-296}$ and F-actin. Scale bars: 50 μM. Enlargement of framed regions in merged images are shown on the right.*

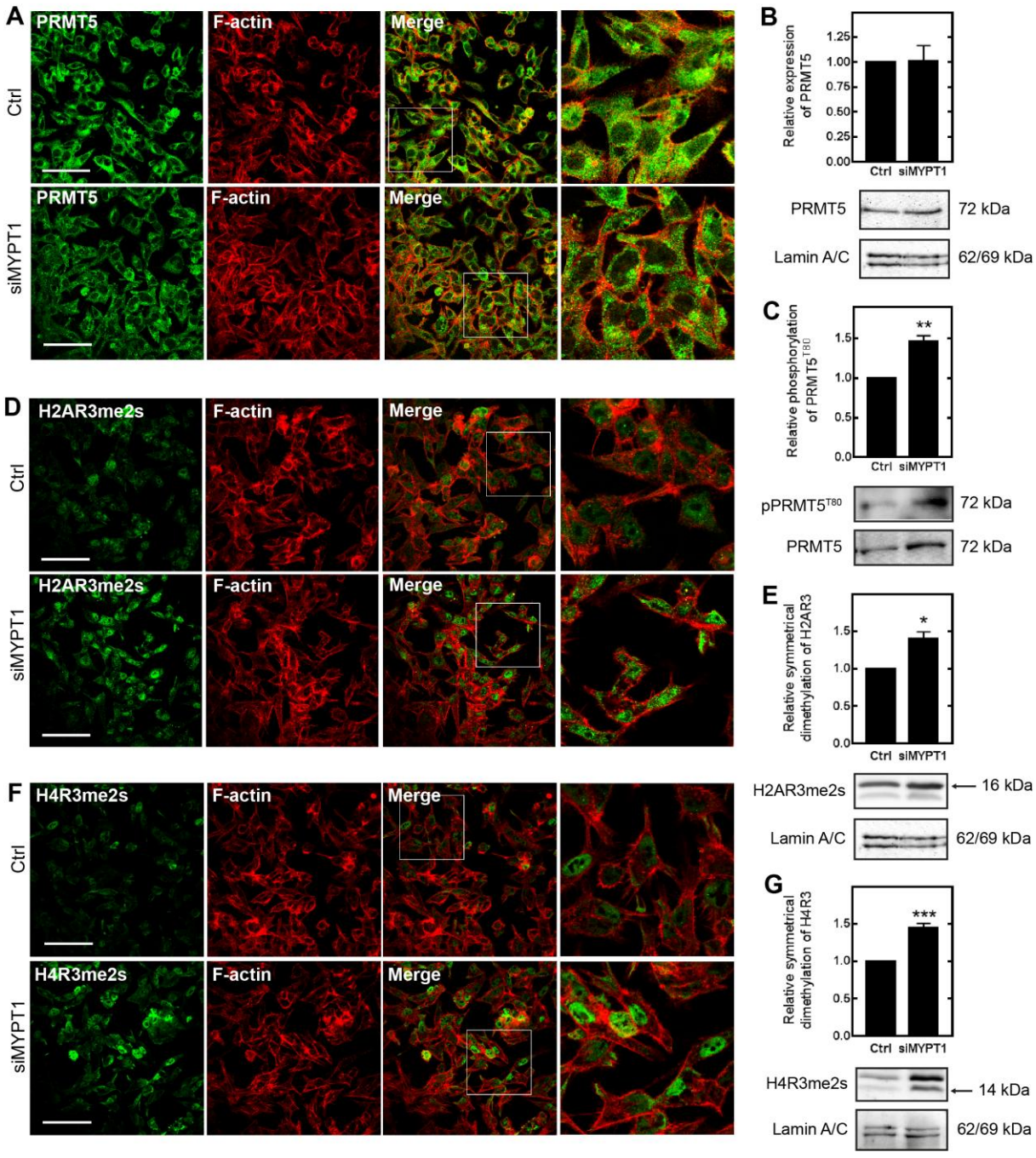

Figure 19. Effect of MYPT1 silencing on the methyltransferase activity of PRMT5 in HepG2 cells.

Immunofluorescent staining of non-target control (Ctrl) and MYPT1-silenced (siMYPT1) cells by anti- PRMT5 ***(A)****, -histone H2A symmetric dimethyl Arg3 (H2AR3me2s)* ***(D)*** *-histone H4 symmetric dimethyl Arg3 (H4R3me2s)* ***(F)*** *and –F-actin. Scale bars: 50 μM. Enlargement of framed regions in merged images are shown on the right on A, D and F panels. Non-target (Ctrl) and MYPT1-silenced (siMYPT1) HepG2 nuclear fractions were analyzed by immunoblot using PRMT5* ***(B)****, pPRMT5^{T80}* ***(C)****, H2AR3* ***(E)*** *H4R3* ***(G)*** *specific antibodies. The relative expression of PRMT5 and the relative symmetric dimethylation of H2AR3 or H4R3 were normalized to lamin A/C. Samples derived from the same experiment and the blots were processed in parallel or assayed after stripping. Relative phosphorylation of PRMT5^{T80}*

*was normalized to the expression level of PRMT5 and then to lamin A/C by densitometry. Mean ± SEM; n=3; *p<0.05, **p<0.01, ***p<0.001 by student t-test.*

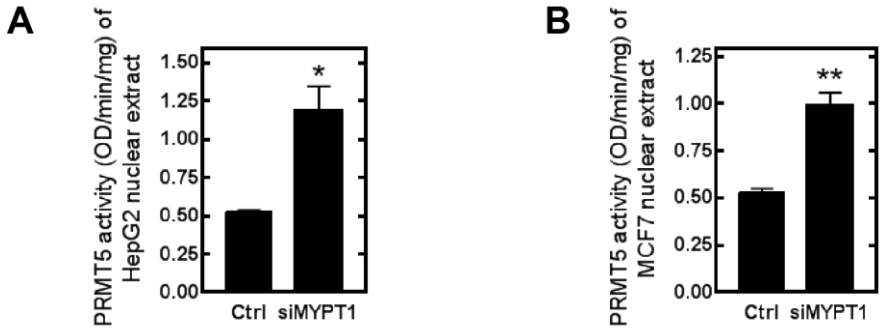

Figure 20. PRMT5 activity of HepG2 and MCF7 nuclear extracts.
Quantitative PRMT5 activity of nuclear fractions from non-target control (Ctrl) and MYPT1-silenced (siMYPT1) HepG2 ***(A)*** *and MCF7* ***(B)*** *cells was measured by colorimetric Epigenase PRMT Methyltransferase (Type II-Specific) assay kit. Activity is expressed in optical density (OD)/min/mg.*

Silencing of MYPT1 results in altered gene expression pattern and downregulates the expression of tumor suppressors in HepG2 cells

To define more precisely the role of MP in functions related to the regulation of dimethylation of histone proteins, we performed microarray analysis using the Affymetrix Human Gene 1.0 ST Array for the study of gene expression. Over 39,000 transcripts/single array were examined encompassing the entire expressed human genome. Total RNA was isolated from non-target control (Ctrl) and MYPT1-silenced (siMYPT1) HepG2 cells. The comparison of control and siMYPT1 samples identified 2429 genes differentially regulated between the two groups. Complete list of genes is available at www.figshare.com website (https://figshare.com/s/dc7bb286c3e1525c4c1f). Table 9 shows a list of genes that were up- or downregulated by more than 1.5-fold (n = 3) in the siMYPT1 samples when compared to gene expression pattern. Hierarchical cluster analysis was performed on all differentially expressed genes using average linkage with Pearson's dissimilarity and the number of induced and repressed genes were presented in a heat map (Fig. 21).

Table 9. List of differentially expressed genes in siMYPT1 HepG2 with 1.5 fold change cut-off limit and tumor suppressor genes (with 1.5 or less fold change, marked by blue colour).

Gene symbol	Gene description	Regulation	Fold change
PPP1R12A	protein phosphatase 1, regulatory (inhibitor) subunit 12A (MYPT1)	down	2.0050275
EPHA2	EPH receptor A2	up	1.5645913
SLC2A1	solute carrier family 2 (facilitated glucose transporter), member 1	up	1.6917205
TGFBR3	transforming growth factor, beta receptor III	up	1.5754458
TMCO1	transmembrane and coiled-coil domains 1	down	1.9577281
KLF6	Kruppel-like factor 6	up	1.6079206
ANKRD1	ankyrin repeat domain 1 (cardiac muscle)	up	2.1838295
HEPACAM|HEPN1	hepatocyte cell adhesion molecule | HEPACAM opposite strand 1	down	1.6288424
OAS1	2',5'-oligoadenylate synthetase 1, 40/46kDa	up	1.6448771
SLC2A1	solute carrier family 2 (facilitated glucose transporter), member 1	up	1.6917205
TGFBR3	transforming growth factor, beta receptor III	up	1.5754458
TMCO1	transmembrane and coiled-coil domains 1	down	1.9577281
KLF6	Kruppel-like factor 6	up	1.6079206
ANKRD1	ankyrin repeat domain 1 (cardiac muscle)	up	2.1838295
HEPACAM|HEPN1	hepatocyte cell adhesion molecule | HEPACAM opposite strand 1	down	1.6288424
OAS1	2',5'-oligoadenylate synthetase 1, 40/46kDa	up	1.6448771
DUSP6	dual specificity phosphatase 6	up	1.5159508
LPAR6	lysophosphatidic acid receptor 6	up	1.5162095
IRF9	interferon regulatory factor 9	up	1.6238389
IFI27	interferon, alpha-inducible protein 27	up	1.6448994
KIAA1199		up	2.1050441
SNORD68|RPL13	small nucleolar RNA, C/D box 68 | ribosomal protein L13	up	1.7279054
MIR21	microRNA 21	up	1.9698615
KRT23	keratin 23 (histone deacetylase inducible)	up	1.5333802
SLC16A6	solute carrier family 16, member 6 (monocarboxylic acid transporter 7)	up	2.1183825
DTNA	dystrobrevin, alpha	up	1.6605202
ICAM1	intercellular adhesion molecule 1	up	1.5522647
GDF15	growth differentiation factor 15	up	1.6862459
MFSD2B	major facilitator superfamily domain containing 2B	down	1.519762
SNX17	sorting nexin 17	down	1.6879824
FETUB	fetuin B	down	1.7819421
KNG1	kininogen 1	down	1.505488
FILIP1L	filamin A interacting protein 1-like	up	1.5426576
SLC7A11	solute carrier family 7, (cationic amino acid transporter, y+ system) member 11	up	1.6259567
ITGA2	integrin, alpha 2 (CD49B, alpha 2 subunit of VLA-2 receptor)	up	1.794632
EGR1	early growth response 1	up	1.6131204
SPRY4	sprouty homolog 4 (Drosophila)	up	1.6954104
GMDS	GDP-mannose 4,6-dehydratase	up	1.5297856
IER3	immediate early response 3	up	2.0160716
SERPINE1	serpin peptidase inhibitor, clade E (nexin, plasminogen activator inhibitor type 1), member 1	up	1.6623654
C8orf4	chromosome 8 open reading frame 4	up	1.5722965
ITGAD	integrin, alpha D	down	1.098526
PTK6	Protein Tyrosine Kinase 6	down	1.0911998
RAP1	Ras-related protein 1	up	1.1432405

Table 9. continued

NFATC2	nuclear factor of activated T-cells, cytoplasmic, calcineurin-dependent 2	down	1.2310033
DLEC1	deleted in lung and esophageal cancer 1	down	1.0655253
MAPK9	mitogen-activated protein kinase 9	down	1.326913
PRR11	proline rich 11	down	1.0980254
MXD3|PRELID1	MAX dimerization protein 3 | PRELI domain containing 1	down	1.0978435
SLC9A3	solute carrier family 9 (sodium/hydrogen exchanger), member 3	down	1.1432443
STAT5A	signal transducer and activator of transcription 5A	down	1.1359215
CST5	cystatin D	down	1.2583836
MYCNOS	v-myc myelocytomatosis viral related oncogene, neuroblastoma derived (avian) opposite strand	down	1.1683407

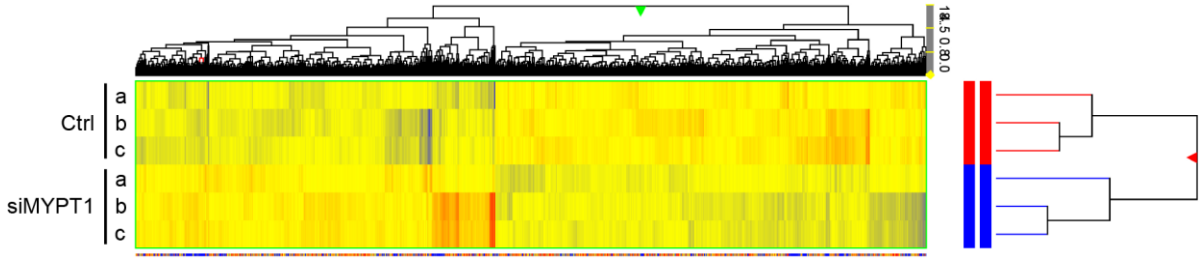

Figure 21. Microarray analysis of MYPT1-silenced HepG2 cells.
Heat map of genes related to MYPT1 silencing (siMYPT1) in HepG2 cells from three independent experiments (a, b, c) by microarray analysis. Induced genes are indicated by red and repressed genes are indicated by blue, ctrl: control.

Bioinformatic analysis was assigned to different canonical pathways such as LPS/IL-1 mediated inhibition of RXR function (PPAR α, γ, IL1R, JUN), antioxidant action of vitamin C (STAT5, MAPK3 and 9), cell cycle regulation (Not7, PPP2C, CDK2, E2F3, Rb protein) as well as IL-4 and IL-8 signaling. Knocking down of MYPT1 also influenced molecular and cellular functions such as lipid metabolism, molecular transport, cell growth and differentiation and cell death. Additionally, the siMYPT1-related genes were analyzed to identify diseases and disorders relevant to the list (Table 10). 39.5% of all related genes (960) were linked to cancer such as lymphohematopoietic, liver and breast cancer and renal-cell carcinoma formation. Genes related to infectious diseases and developmental disorders were also identified in 10.9% and 6.99%, respectively. Taken together, microarray analysis identified a number of signaling pathways strongly point to a role of MP in the regulation of gene expression.

Table 10. Ontology of the related genes and their classification by GO terms in MYPT1-silenced HepG2 cells.

	Name	p-value	# molecules
Diseases and Disorders	Cancer	4.37E-06 - 7.75E-03	960
	Infectious Disease	4.44E-06 - 6.46E-03	263
	Neurological Disease	9.35E-06 - 6.93E-03	350
	Skeletal and Muscular Disorders	9.35E-06 - 7.48E-03	278
	Developmental Disorder	3.02E-05 - 6.93E-03	170
Molecular and Cellular Functions	Lipid Metabolism	1.75E-07 - 7.60E-03	231
	Molecular Transport	1.75E-07 - 7.60E-03	339
	Small Molecule Biochemistry	1.75E-07 - 7.60E-03	266
	Cellular Growth and Proliferation	1.26E-06 - 7.75E-03	509
	Cell Death and Survival	1.93E-06 - 7.53E-03	474
Physiological System Development and Function	Hair and Skin Development and Function	2.38E-05 - 7.52E-03	41
	Organismal Survival	2.50E-05 - 5.29E-04	368
	Immune Cell Trafficking	4.01E-05 - 7.68E-03	185
	Tumor Morphology	4.92E-05 - 6.82E-03	68
	Digestive System Development and Function	6.69E-05 - 7.52E-03	133

The evaluation of genes related to MYPT1-silencing revealed the significant downregulation of several tumor suppressors and transcription factors. One of the substrates dephosphorylated by MP is tumor suppressor retinoblastoma protein (pRb) that plays a crucial role in the negative control of the cell cycle and in tumor progression as a major regulator of G1 checkpoint (Witkiewicz et al. 2014). Another factor is *c*-Myc that regulates the cell cycle progression and cellular transformation as a multifunctional transcription factor (Shalaby et al. 2016).The protein expressions of pRb and *c*-Myc were significantly decreased upon MYPT1 silencing and these were also confirmed by Western blot analysis (Fig. 22A and B). To clarify the connection between the MP activity and the PRMT5-regulated gene expression we screened for genes that are related to both PRMT5 and MP in the database of siPRMT5 (Gkountela et al. 2014) and siMYPT1 microarray analysis, respectively. One of the potential candidates was the Ras-related protein 1 (Rap1), a member of Ras-related protein family, which is a small GTPase that plays a critical role in signaling pathways controlling cell growth and differentiation (Bokoch et al. 1993). Rap1 gene expression was 2.3 fold reduced upon PRMT5 silencing in human embryonic stem cells and the expression of this gene was found to be significantly increased in siMYPT1 cells (Table 9; Fig. 22C).

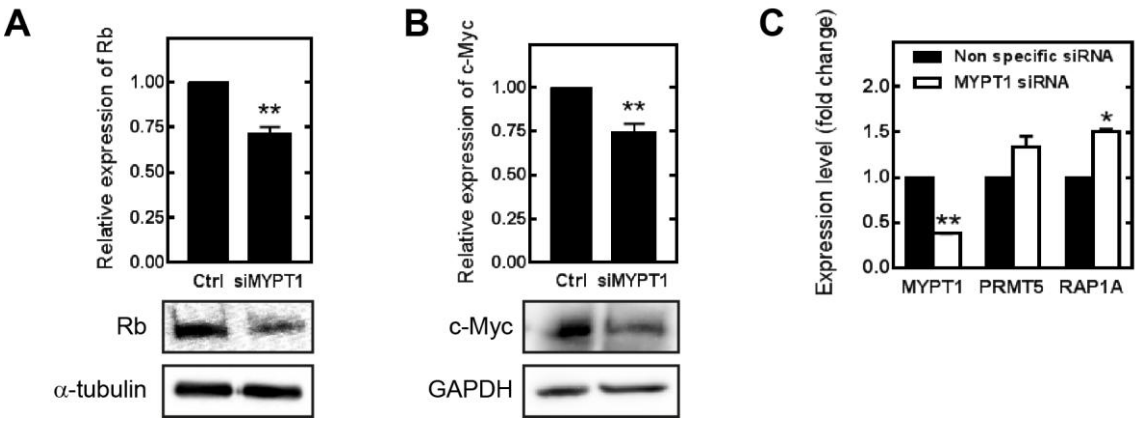

Figure 22. Protein level of Rb and c-Myc in MYPT1-silenced HepG2.

*Detection of retinoblastoma protein **(A)** and c-Myc **(B)** protein expression changes due to MYPT1 silencing of HepG2 whole cell lysates by Western blot. Protein expression levels were quantified by densitometry normalized to α-tubulin or GAPDH expression level. Samples derived from the same experiment and processed in parallel. **(C)** RT-PCR analysis of MYPT1, PRMT5 and RAP1A mRNA levels in non-specific siRNA treated and MYPT1 silenced HepG2 cells. GAPDH was used as an invariant gene. Values are mean ± SEM from three independent experiments; *p<0.05, **p<0.01 by student t-test.*

MP modulates indirectly the suppression mark of gene expression on histone 2A and 4 through the regulation of PRMT5 activity in human cancer

The microarray analysis indicated that in case of a decrease in the expression level of MYPT1 of myosin phosphatase cancer-related processes dominate. Therefore, protein tissuearray analysis was conducted in multiple tissue lysates of patients for the validation of changes in the protein levels and their posttranslational modifications in cancer. Tumor tissue lysates were obtained from a large group of human patients with grade 2 and 3 and state II and III (Fig. 23 light and medium gray columns, respectively) hepatocellular carcinoma (HCC, n=20), with four different types of metastatic liver cancers (Fig. 23 dark gray columns) as well as with 15 other types of cancer cell lines with their adequate normal cell type controls (Fig. 24). These arrays were analyzed using high throughput screening for multiple protein targets such as PRMT5 (Fig. 23/24A), pPRMT5^{T80} (Fig. 23/24B), MYPT1 (Fig. 23/24C), pMYPT1^{T850} (Fig. 23/24D), histone 2A (Fig. 23/24E) and histone 2A symmetric arginine methylation (Fig. 23/24F). Protein expression of PRMT5 showed an increase in ~75% of the investigated cancer tissues comparing to healthy controls. THP-1 monocytic leukemia, Raji Burkitt lymphoma, epidermoid and uterine carcinoma cells presented the largest increase and significant reduction was also detected in stomach, colon and prostate adenocarcinoma and HeLa cervix carcinoma cells (Fig. 24A). The relative phosphorylation of PRMT5 at Thr^{80} in cancer cell lines were significantly elevated in all cases especially in the leukemia, lymphoma,

lung, liver and breast carcinoma (Fig. 24B) as well as in HCC tissues (Fig. 23B). The relative MYPT1 expression exhibited a diverse expression pattern since it was downregulated in few cases, significantly in HeLa cervix carcinoma but in uterine carcinoma it showed a twofold increase (Fig. 24C), however, MYPT1 expression did not change in the majority of cancer types (60%). Since MP holoenzyme activity is primarily regulated through the phosphorylation of MYPT1 at the Thr^{850} inhibitory site, we measured the MYPT1 Thr^{850} phosphorylation related to the MYPT1 levels and found an increased phosphorylation level of $MYPT1^{T850}$ in almost all cases up to a 5-9-fold elevation in ovarian and prostate adenocarcinoma, cervix carcinoma and leukemia (Fig. 24D). The overexpression of histone proteins in cancer cells and the elevated symmetric dimethylation of them have been already described in colorectal, glioblastoma and numerous other cancer types (Zhang et al. 2015; Sheng et al. 2016). We also verified either no changes (Burkitt lymphoma, Jurkat lymphoma and hepatocellular adenomatoid) or a significant elevation in the histone protein expression (Fig. 23/24E) and 85% of all examined cancer types showed an increase in the repressive Arg3 symmetrical dimethylation mark. Our results imply that the decreased activity of MP indicates an obvious relation to the increased activity of PRMT5 and the increased level of the R3 gene repression mark on histones in almost every investigated cancer types particularly in THP1 monocytic leukemia, ovarian adenocarcinoma, hepatocellular, bladder and uterine carcinoma, MCF7 breast cancer and in kidney adenocarcinoma. The protein expression as well as the phosphorylation of PRMT5 at Thr^{80} (Fig. 23A and B), and also the arginine methylation of histone 2A increased in the higher grade and stage in hepatocellular carcinoma tissues (n=11-13) (Fig. 23F) exhibiting a strong direct correlation to the grade and state of the tumor. These data suggest the involvement of the ROK/MP/PRMT5/histone dimethylation pathway in tumorigenesis.

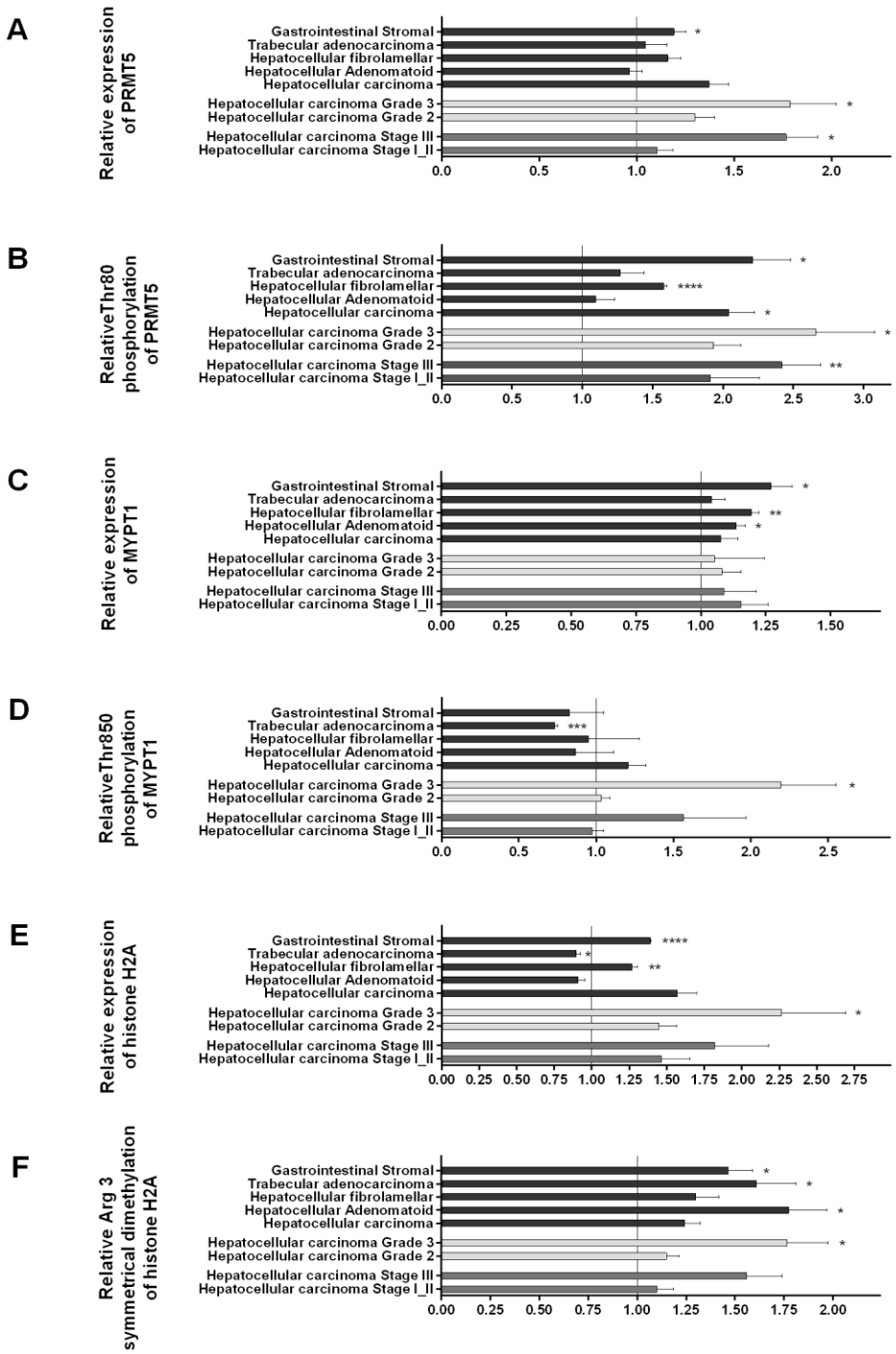

Figure 23. Protein expression profile of HCC tissue samples.

Protein microarray analysis was conducted to study the changes in protein expression and posttranslational modification of PRMT5 ***(A, B)****, MYPT1* ***(C, D)*** *and histone H2A* ***(E, F)*** *proteins in human healthy control and cancer liver tissues. HCC samples (n=20) were grouped based on their clinically verified stage (lower, medium gray columns) or the classification of the tumor's grade (middle, light gray columns) Average of HCC samples and other types of metastatic liver cancer tissues are shown next to each other (upper, dark gray columns). Value of 1 means average of relative expression, phosphorylation or symmetrical dimethylation of the given protein or residue to the corresponding non-tumor samples. Data are mean ± SEM; *p<0.05, **p<0.01, ***p<0.001, ****p<0.0001 by student t-test.*

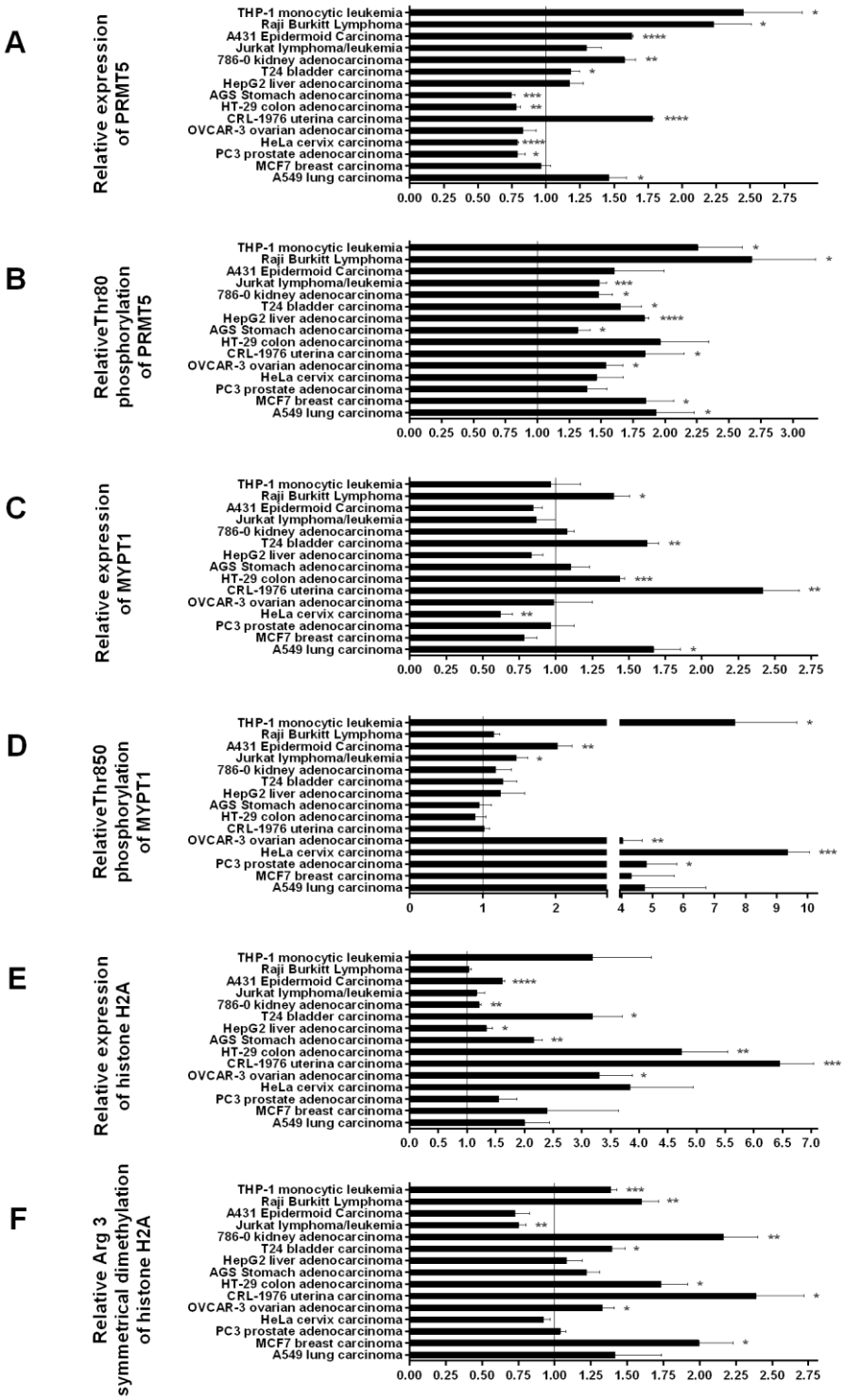

Figure 24. Protein expression profile of cancer cell lines.

Investigation of the changes in protein expression and posttranslational modification of PRMT5 ***(A, B)****, MYPT1* ***(C, D)*** *and histone H2A* ***(E, F)*** *proteins in cancer cell lines. Protein microarray contains 15 cancer cell lines and normal tissue lysate as controls of corresponding organs in triplicates. Value of 1 means average of relative expression, phosphorylation or symmetrical dimethylation of the given protein or residue to the corresponding non-tumor samples. Blots were processed under the same experimental procedure. Data are mean ± SEM; *p<0.05, **p<0.01, ***p<0.001, ****p<0.0001 by student t-test.*

Protein-protein interaction between MYPT1 and SMTNL1

Since MP plays a crucial role not only in the regulation of cytoskeletal elements but in other cellular processes such as gene expression, our aim was also to investigate its other regulatory possibilities by other interacting proteins such as SMTNL, a novel inhibitory protein (Borman et al. 2009; Lontay et al. 2010). SMTNL1 was identified as a MYPT1-binding protein from uterine smooth muscle by coimmunoprecipitation and its deletion was found to enhance myosin phosphatase activity (Lontay et al. 2010) but their interacting surfaces have not been characterized. We attempted surface plasmon resonance (SPR) binding studies between the two proteins using recombinant MYPT1 truncated fragments. To assess the interaction, full-length GST-MYPT1$^{1\text{-}1004}$, His-MYPT1$^{1\text{-}633}$ and GST-MYPT1$^{667\text{-}1004}$ were immobilized on sensor chips and FT-SMTNL1 was applied in variant concentrations ranging from 0.5 to 7.14 μM. Figure 25 represents sensorgrams obtained by detailed kinetic analysis of the binding of SMTNL1 on three different surfaces. Distinct interaction of SMTNL1 was observed with full-length GST-MYPT1$^{1\text{-}1004}$ with an association constant $K_a = (6.86 \pm 3.38) \times 10^5\ M^{-1}$ (Fig. 25A). SMTNL1 interacted with N-terminal mutant (His-MYPT1$^{1\text{-}633}$, Fig. 25B) or with C-terminal fragment represented by residues 667-1004 (Fig. 25C). The association reached saturation when GST-MYPT1$^{1\text{-}1004}$ or His-MYPT1$^{1\text{-}633}$ was bound to the sensor chip, but a lower response was detected with His-MYPT1$^{1\text{-}633}$ than with the full-length protein. Ankyrin repeat sequences on the N-terminus of MYPT1 provide the primary surface for

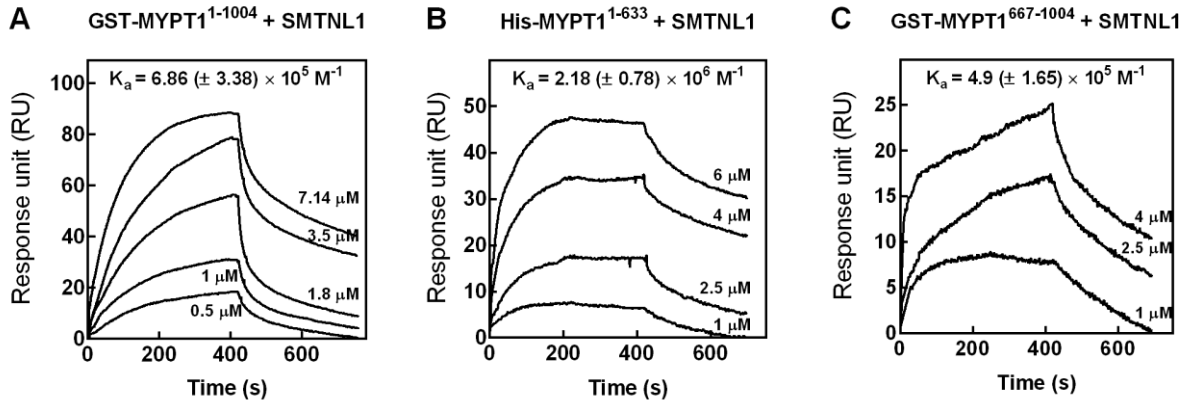

Figure 25. Interaction of SMTNL1 with MYPT1 derivatives via SPR* (*unpublished data*).** *Full-length GST-MYPT1$^{1\text{-}1004}$* ***(A)*, N-terminal His-MYPT1$^{1\text{-}633}$* ***(B)*** *and C-terminal GST-MYPT1$^{667\text{-}1004}$ fragments* ***(C)*** *were immobilized on CM5 sensor chips. Indicated concentrations of FT-SMTLN1 were applied on the surfaces. The association constant (K_a) values were derived from the sensorgrams using Biacore 3000 evaluation program. K_a values are marked in the figures.*

protein-protein interactions but C-terminal leucine zippers also contribute to the formation of a mutual interaction between MYPT1 and SMTNL1. In accordance with our expectations, we monitored strong binding of SMTNL1 to the MYPT1 N-terminal recombinant fragment (K_a= (2.18 ± 0.78) × 10^6 M^{-1}). Weaker but still significant binding of SMTNL1 to GST-MYPT1$^{667-1004}$ (K_a= (4.9 ± 1.65) × 10^5 M^{-1}) indicates that the C-terminus of MYPT1 enhances the interaction and it happens through multiple surfaces.

Increased expression and phosphorylation of SMTNL1 in pregnancy

Sex related differences referring to SMTNL1 in exercise-trained mice were previously shown in smooth muscle (Wooldridge et al. 2008). The expression of MYPT1 was also found to be dependent of the gender and the developmental stage of mice (Lontay et al. 2010). Moreover, the role of MP during pregnancy has also been described. To clarify the role of SMTNL1 as the regulator of MP in pregnancy, changes of SMTNL1 were examined in skeletal muscle during pregnancy by immunoblot analysis. To separate the effects of hormonal regulation of SKM from physical effects due to the increased body weight gain during pregnancy, pseudopregnant mice were also tested. Pseudo-pregnant mice proceed with the normal hormonal changes observed in pregnant animals but do not experience weight gain from the developing fetal mice *in utero*. SMTNL1 expression was remarkably enhanced in pregnant and pseudopregnant mice compared to plantaris muscle of non-pregnant females (t_{max} day 16±2, Fig. 26A).

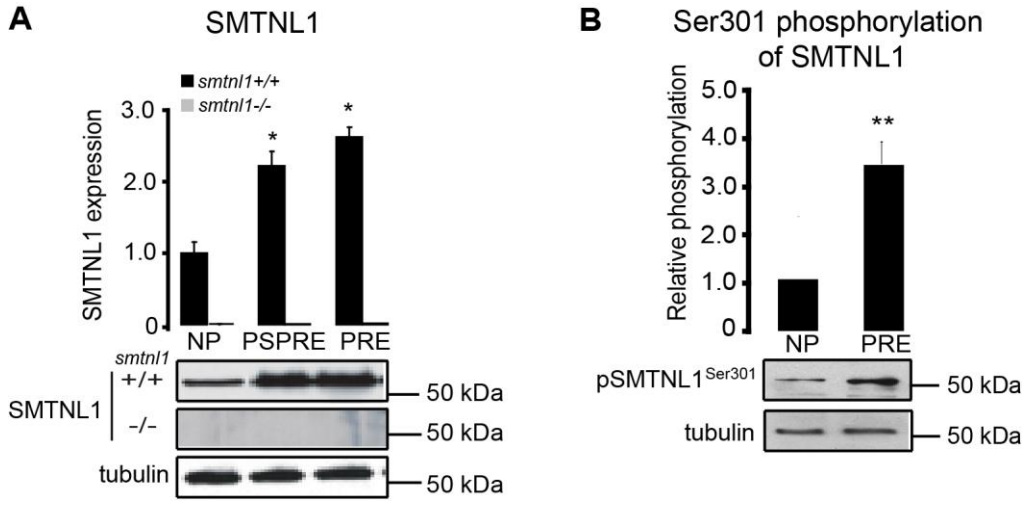

Figure 26. Expression and phosphorylation level of SMTNL1 in skeletal muscle
(A)*Expression of SMTNL1 in non-pregnant (NP), pregnant (PRE) and pseudopregnant (PSPRE) mice plantaris muscle by Western blot analysis.* ***(B)*** *Phosphorylation of SMTNL1 Ser^{301} in non-pregnant (NP) and pregnant (PRE) mice plantaris muscle. Tubulin served as a loading control. Data represents mean ± SEM, n= 4-5/group, *p<0.05 and **p < 0.001 by t-test.*

Increased SMTNL1 expression during pregnancy was also confirmed by immunohistochemistry in plantaris skeletal muscle (Fig. 27C). Translocation of SMTNL1 from the cytosol to the nucleus was observed upon its phosphorylation on Ser^{301} (Lontay et al. 2010). Phosphorylation of SMTNL1 on Ser^{301} was 3.5-fold increased in pregnant females (t_{max} day 12±2) in correlation with non-pregnant ones (Fig. 26B) suggesting that the phosphorylation state and the localization of SMTNL1 depends on hormonal changes in pregnancy.

Pregnancy and SMTNL1 regulate glycolytic fiber switching in mice and humans

During fiber typing experiments of murine and human SKM samples MHC2b showed increased expression in pregnant *smtnl1-/-* mice and concomitant reduction of MHC2a expression was detected by immunoblot (Fig. 27A and B). Similar tendency was shown when pseudopregnant mice were analyzed suggesting the regulatory role of sex hormones in these changes rather than to physical changes arising from the developing fetuses (Fig. 27A and B). Staining of SMTNL1 and type2a fibers of MHC by immunohistochemistry of plantaris (Fig. 27C) showed that SMTNL1 expression localized only in type2a muscle fibers in non-pregnant wild type females. Above all, SMTNL1 expression was not confined only to MHC2a fibers in plantaris of pregnant animals but SMTNL1 staining was detected in fibers different from type2a (see white arrows in Fig. 27C). These fibers are thought to belong to those type 2x fibers that are in the transition from type 2a to 2b fibers and provide a crucial state in muscle plasticity. MHC2a expression showed a decline in the mean proportion of type2a fibers (Fig. 27A and C) and this phenomenon was more pronounced in skeletal muscle of pregnant *smtnl1-/-* mice, which showed a >10% decline in type2a fibers relative to WT litter-mates (Fig. 27C, Table 11). If pregnancy and SMTNL1 deletion reduces MHC2a expression, this raises the question whether these conditions concomitantly increase MHC2b levels and numbers of type2b fibers? Based on results of quantitative fiber counting, Western blot and immunohistochemical analysis of MHC2b, pregnancy and pseudo-pregnancy induced a 15-20% increase in expression of type2b fibers (Fig. 27B, D and Table 11). In spite of the increasing expression of MHC2b during pregnancy both in mouse and human skeletal muscle (Fig. 27B, Fig. 28A), immunohistochemical experiments with anti-MHC2a and -MHC2b suggested that staining of SMTNL1 can also be found in fibers undergoing type2a/type2b transition (Fig. 27C and D). Expression of SMTNL1, MHC1 and MHC2a/2b in abdominis rectus muscle isolated from women undergoing hysterectomy (non-pregnant control) or C-

section (as pregnant) analyzed by immunohistochemistry suggested that pregnancy was also likely to promote similar fiber switching in humans (Fig. 28A).

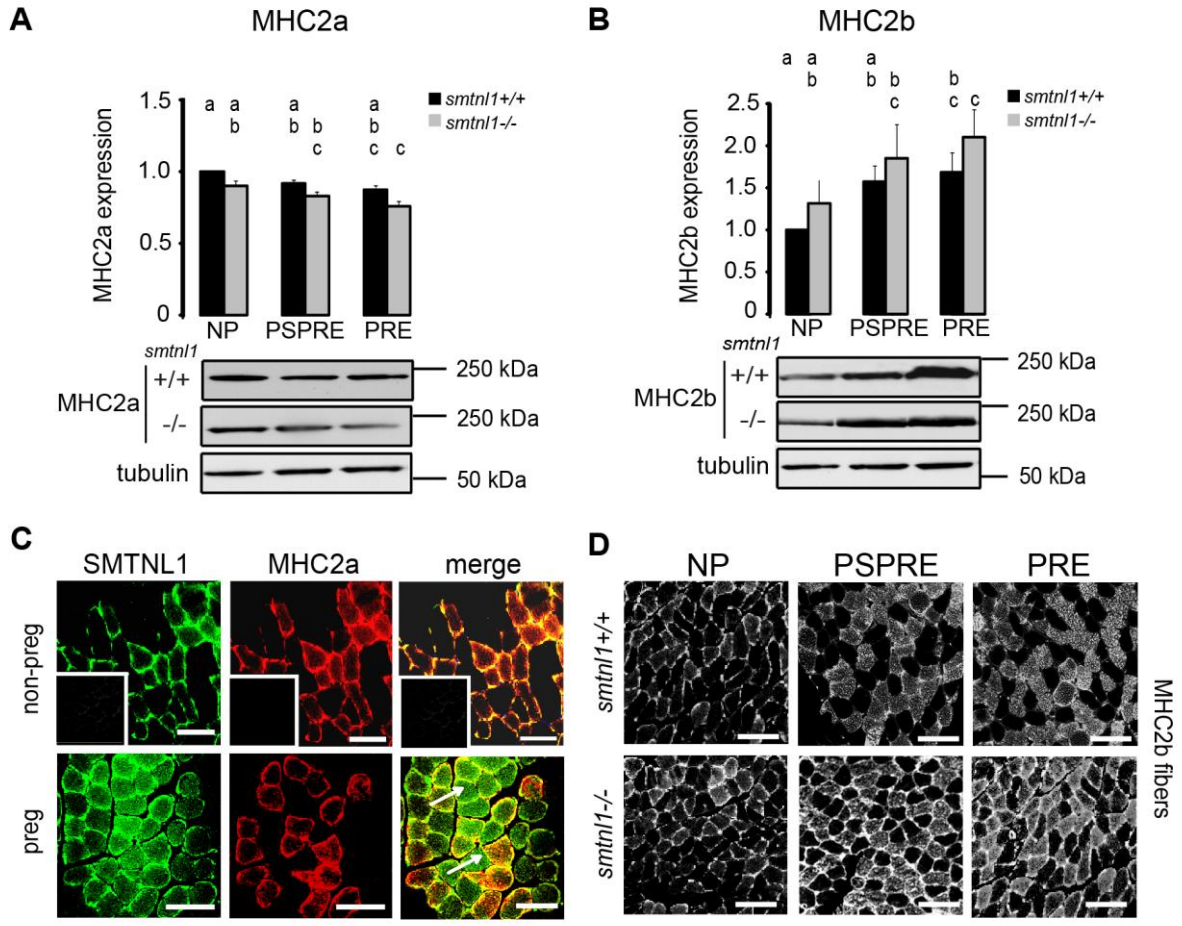

Figure 27. Pregnancy reduced MHC2a and induced MHC2b expression in skeletal muscle and these changes are enhanced by SMTNL1 deletion.

Protein expression level of MHC2a ***(A)*** *and MHC2b* ***(B)*** *in non-pregnant (NP), pregnant (PRE) and pseudopregnant (PSPRE) plantaris muscle by WB. n= 4-13/group, data presented as mean ± SEM, GLM with Tukey-test, different letters indicate significant differences, $p<0.05$.* ***(C)*** *Fiber typing by IHC and confocal microscopy of plantaris muscle. SMTNL1 (green) is expressed in type2a fibers (red) in control skeletal muscle. SMTNL1 expression shows localization in fibers different from type2a (arrows) in pregnancy. Inserts show secondary antibody controls. Scale bars: 20 μm.* ***(D)*** *Analysis of MHC2b expression (white) in plantaris muscle. Scale bar: 10 μm.*

Pregnancy or pseudo-pregnancy did not affect the expression of MHCI, the marker of oxidative slow type 1 fibers. The decrease of protein expression of type2a marker MHC2a was observed, while MHC2b increased by 20% indicating that fibers switched from oxidative to the more glycolytic phenotype in human pregnant skeletal muscle. The increased type2b content in pregnancy is accompanied by a 24% increase in glycogen content (Fig. 28B). These data suggest that pregnancy promotes the transformation of skeletal muscle fiber type

to a more glycolytic phenotype in mice and humans and that SMTNL1 may play a regulatory role in this process.

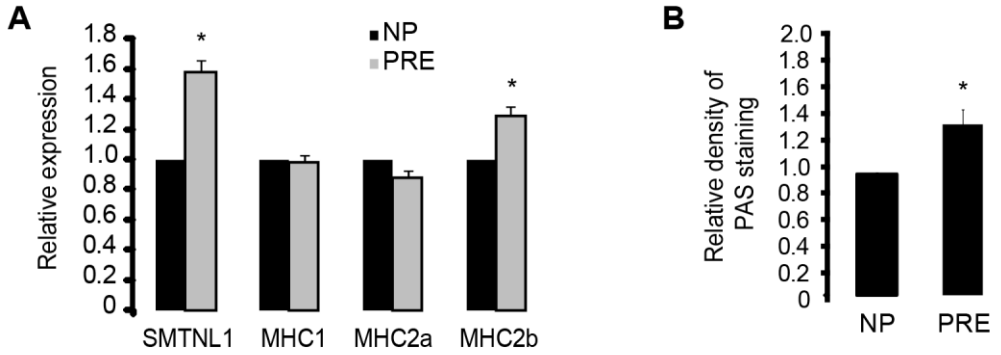

Figure 28. Expression of SMTNL1, MHC1/2a/2b and glycogen content of human skeletal muscle in pregnancy.
(A) *Immunohistochemical examination of protein expression level of SMTNL1, MHCI, MHC2a and MHC2b of human rectus abdominalis in pregnancy.* ***(B)*** *Quantitative periodic acid Schiff (PAS) staining for glycogen content of human rectus abdominalis sections. E and F, means + SEM (n = 4-5/group), t-test, *p<0.05.*

Table 11. Quantitative fiber counting of plantaris muscle of non-pregnant, pregnant and pseudopregnant (smtnl1+/+ and smtnl1-/-) mice. *Periodic acid Schiff (PAS), means ± SEM (n=14-15/group), t-test, $^{\#}p<0.1$, *p<0.05 and ** p < 0.001.*

	Non-pregnant		Pseudopregnant		Pregnant	
GENOTYPE	***smtnl1* +/+**	***smtnl1* -/-**	***smtnl1* +/+**	***smtnl1* -/-**	***smtnl1* +/+**	***smtnl1* -/-**
2a fiber type %	34.77±1.9	32.22±2.5	24.84±2.2 *	26.00±2.5 $^{\#}$	25.29±1.8 *	24.45±2.1 **
2b fiber type %	45.58±2.7	49.22±2.7	58.44±1.9	60.96±3.3 *	61.12±2.4 *	65.32±3.0 **
SMTNL1 positive fibers %	36.06±1.6	N/A	39.77±1.9	N/A	42.87±1.9 $^{\#}$	N/A
Relative PAS density	1.00±0.0	1.18±0.2	1.25±0.03	1.32±0.1 $^{\#}$	1.26±0.04 $^{\#}$	1.39±0.2 *

Further investigations in the same study completed at Duke University confirmed the relation between fiber type transformation and SMTNL1. Global gene expression analysis of plantaris muscle was carried out in four experimental groups: non-pregnant *smtnl1-/-*, pregnant WT and pregnant *smtnl1-/-* groups compared to non-pregnant WT (http://dx.doi.org/10.6084/m9.figshare.1273946). A total of 1384 genes were differentially expressed between the groups from which 195 genes were identified during the comparison of non-pregnant WT *versus* non-pregnant *smtnl1-/-*, and 1261 genes were differentially expressed when non-pregnant WT was compared to pregnant WT. Based on gene ontology analysis of differentially expressed genes, they are involved in cytoskeletal organization, calcium binding, regulation of growth, metabolic processes and steroid synthesis from the aspect of biological and molecular functions. Fifty percent of the genes altered by SMTNL1 deletion were related to transcriptional regulators and the remaining 50% included structural

molecules (23%) and enzyme regulators (15%). Pregnancy was found to be mainly related to glycolysis-glyconeogenesis, fatty acid synthesis, contractile proteins or signaling pathways involving steroid synthesis and nuclear hormone receptor signaling. SMTNL1 deletion caused mostly the up-regulation of signaling pathways of nuclear receptors and skeletal or smooth

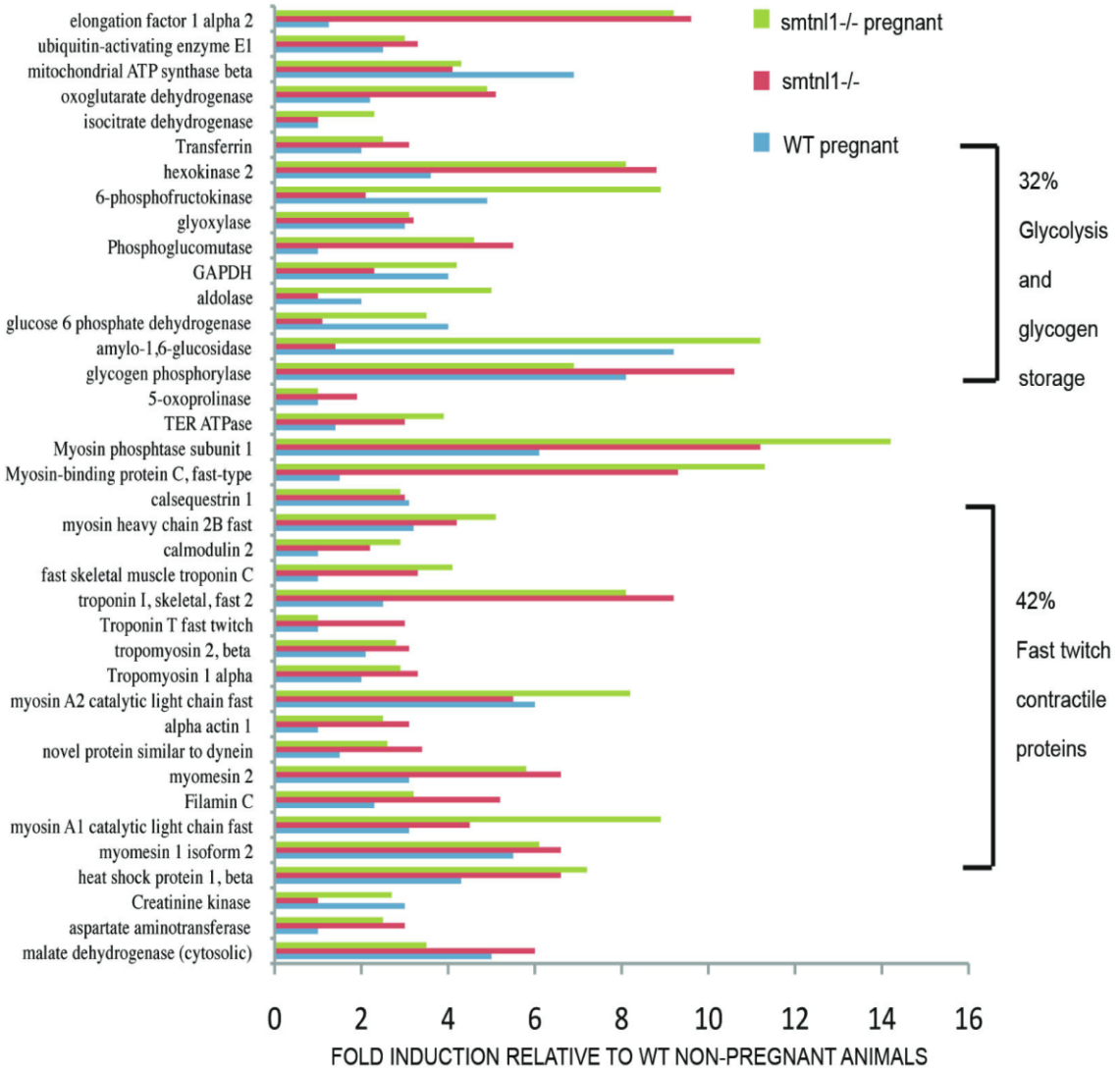

Figure 29. Proteomic analysis shows that pregnancy and SMTNL1 deletion induces expression of glycolytic enzymes and contractile proteins associated with Type2b fibers.
Plantaris muscle extracts were subjected to proteomic analysis prepared from smtnl1+/+ (WT), smtnl1+/+ pregnant (WP), smntl1-/- (KO) and smtnl1-/- pregnant (KOP) mice. The data show fold induction of proteins in WP, KO and KOP samples compared to WT.

muscle contraction. To support our findings at the protein expression level, multidimensional proteomic analysis of plantaris muscle extracts from the same four groups (non-pregnant WT, non-pregnant *smtnl1-/-*, pregnant WT and pregnant *smtnl1-/-*) were also carried out (Fig. 29) where pregnancy induced the expression of several glycolytic enzymes and contractile

proteins that are specifically associated with fast twitch type2b fibers *e.g.* enzymes of glycolysis or glycogen storage as well as MHC2b, fast twitch forms of troponins, fast twitch myosin light chains, and fast-type myosin-binding protein C, established markers of type2b fibers. Interestingly, the expression of MYPT1 was also increased upon the deletion of SMTNL1 in pregnancy supporting previous findings described in smooth muscle (Lontay 2010, JBC).

Proteomic data and the microarray analysis are well in line with the hypothesis that during pregnancy female mice adapt their skeletal muscle to a glycolytic phenotype. The finding that these pregnancy-induced adaptations are more emphasized in SMTNL1-deleted tissues, suggests that the protein may regulate this process.

DISCUSSION

Myosin phosphatase (MP) is a Ser/Thr specific protein phosphatase type 1 (PP1) enzyme and it is a well characterized regulator of muscle contractility and cytoskeleton-related cellular events through the dephosphorylation of the 20 kDa myosin light chain. MP is expressed in all types of muscle and in a wide variety of mammalian tissues with diverse cellular localization (Boudrez et al. 1999). MYPT1, the MP regulatory subunit was previously identified in the nucleus of hepatocytes and neuronal cells (Tran et al. 2004; Lontay et al. 2005; Wu et al. 2005), however, the possible role of MP in nuclear processes is still undetermined. In accordance with the nuclear localization of MYPT1, we confirmed colocalization of MYPT1 and the catalytic subunit PP1cδ forming MP holoenzyme in the nucleus of human hepatocellular carcinoma (HepG2) cells and remarkable PP1 activity was determined in HepG2 nuclear extracts. A number of MYPT1-binding proteins have been identified from nuclear fraction of HepG2 cells and we found the Thr^{80} residue in protein arginine methyltransferase 5 (PRMT5) as the target of RhoA-activated kinase (ROK)/MP and the phosphorylation/dephosphorylation of this site is shown to modulate the activity of PRMT5. The finding that ROK/MP enzyme pair effects on the same substrate is not a novel finding since numerous targets of ROK including myosin II, adducin and moesin are dephosphorylated at the ROK-specific phosphorylation site by MP (Hartshorne et al. 2004). Additionally, several regulatory pathways related to MP are driven by ROK since inhibitory phosphorylation of MYPT1 results in a decrease in MP activity and it is frequently regulated by ROK (Feng et al. 1999). While MYPT1 at Thr^{696} can be phosphorylated by numerous kinases, Thr^{850} is predominantly regulated by ROK (Muranyi et al. 2002). The interplay between MP and PRMT5 was also supported by protein-protein interaction analysis. First, the presence of PRMT5 in the MYPT1 nuclear interactome (Table 6) gave the opportunity for an interacting protein complex. Second, SPR-based *in vitro* binding assay identified a stable interaction between MYPT1 and PRMT5 and it was verified that PRMT5 binds to the N-terminal part of MYPT1 (Fig. 13).

Based on our results, counteraction of ROK/MP on the Thr^{80} phosphorylation site of PRMT5 regulates its methyltransferase activity both *in vitro* (Fig. 16) and *in vivo* (Fig. 19). PRMT5 protein includes multiple tyrosyl and seryl/threonyl residues that could be potentially targeted by phosphorylation. PRMT5 can be phosphorylated by a constitutively active janus kinase 2 mutant at the tyrosyl 304 and 307 residue resulting in the disruption of the interaction between MEP50 and PRMT5 and the inhibition of the activity of PRMT5 in patients with

myeloproliferative neoplasm (Liu et al. 2011). The ROK/MP regulated Thr^{80} residue and its surrounding peptide sequences are not part of the methyltransferase domain of PRMT5 and play no role in the formation of the heterooctameric structure of $PRMT5_4$:$MEP50_4$ based on the crystal structure of human PRMT5 (Antonysamy et al. 2012). $PRMT5^{T80}$ is located in a peptide sequence (GRDWNTLI/VV) well conserved among vertebrates but not in invertebrate orthologs. Furthermore, PRMT5 exhibits no sequence homology with PRMT1-4 enzymes (Krause et al. 2007) suggesting a selective regulatory function of its phosphorylation at Thr^{80}. The fact that phosphorylation of PRMT5 at Thr^{80} increases the activity of the enzyme without the recruitment of more MEP50 into the complex (Fig. 17) supports the hypothesis that this modification triggers changes either in the substrate- or in the S-adenosylmethionine methyl donor binding sites. Our results provide a yet unrecognized signalling mechanism which regulates PRMT5 activity directly by posttranslational modification.

Epigenetic regulation of gene transcription is one of the prominent functions of histone tail modifications. It is well established that PRMT5 has preference for the symmetrical dimethylation of H4R3, H2AR3 and H3R2/R8 *in vivo* shifting the balance to a suppressive mark (Migliori et al. 2012; Saha et al. 2016). Symmetrically dimethylated R3-motifs (the third Arg amino acid at the N-terminal sequence of histone proteins and their surrounding peptides) recruit the DNA methyltransferase DNMT3A to chromatin domains to suppress gene expression thus representing epigenetic silencing of gene expression (Pal et al. 2007). We provided several lines of evidence that silencing of MYPT1 results in a global change in gene expression through the activation of PRMT5 and by the indirect modulation of the "R3-motifs" of H2A and H4. Moreover, the general assumption that PRMT5 functions as a transcriptional co-repressor is not definite since symmetric-dimethyl-arginine-containing protein(s) can specifically associate with the IL-2 promoter after T-cell activation and increase gene expression (Richard et al. 2005). Our observation that cancer-related pathways are upregulated in hepatocellular carcinoma (HCC) upon MYPT1 silencing is the result of a higher expression and hyperactivation of PRMT5, which suppresses gene and protein expression of several tumor suppressors or increasing that of potential oncogenes. First, the tumor suppressor pRb expression was significantly decreased in siMYPT1 HepG2 cells suggesting the anti-tumor role of MYPT1 in HCC (Fig. 22). This is well in line with the findings that PRMT5 overexpression triggered the suppression of the transcription of the pRb in leukemia and in lymphoma cell (Wang et al. 2008). Second, *c*-Myc as a global transcriptional regulator can activate genes involved in cell proliferation and growth but it is

also able to repress genes involved in cell cycle and adhesion (Uribesalgo et al. 2012) raising the possibility of a yet-unexplored mechanism used by tumors to suppress differentiation and potentiate aggressiveness. *C*-Myc expression is significantly lower in HCC than in non-tumor tissues and is inversely proportional to the grade of differentiation (Yuen et al. 2001). We found that MYPT1 silencing resulted in a decrease in *c*-Myc protein expression suggesting again the tumorsuppressor effect of this MYPT1 subunit, and presumably MP itself, in HCC. Finally, we also found that tumor suppressor Rap1 was upregulated in siMYPT1 HepG2 cells (Fig. 22). Rap1 functions as a genome wide transcriptional regulator and a critical player in tumor malignancy. The fact that inhibition of Rap1 interfered with tumor development and induced higher apoptosis rates (Zha et al. 2014) also suggest that silencing of MYPT1 mimics the protein expression pattern of cancer cells and the tumor suppressor activity of MP.

The constant and unbalanced phosphorylation of MYPT1 at Thr^{850} suggested that it might be related to cancer formation (Wong et al. 2008). Based on the phosphorylation of $MYPT1^{T850}$ we confirmed that the activity of the MP decreased, the activity of PRMT5 phosphorylated at Thr^{80} increased and PRMT5-specific repressive R3-dimethylation increased in HCC and in other cancer cell lines suggesting the fundamental role of this pathway in tumorigenesis. Since both the stage and the grade of the tumors were directly related to the activity of this pathway, we hypothesized that this is an action governed by ROK. The downregulation of RhoA, an upstream activator of ROK (Yang et al. 2015) and the direct inhibition of ROK by Incarvine C and Y27632 decreased the phosphorylation of MYPT1 at Thr^{850} in lung cancer and HCC (Zhang et al. 2015), respectively, and the ROK-phosphorylated MYPT1 was localized not only in the cytoplasm but in the nucleus as well (Genda et al. 1999). Finally, PRMT5 was overexpressed and/or mutated in multiple tumor types including leukemia, lymphoma (Wang et al. 2008), lung (Gu et al. 2012), colorectal and breast cancer as well as in HCC and it resulted in an increased symmetrical dimethylation on H2A and H4 R3-motifs (Zhang et al. 2015). The prognosis of patients with HCC is associated with the expression level of PRMT5. The overexpression of PRMT5 increased the symmetric dimethylation of histone R3 motifs and we provided evidence that it is related to the enhanced phosphorylation level of PRMT5 at Thr^{80}.

Here we have provided new insights into the regulation of tumor suppressor pathways demonstrating that MP is a negative regulator of the PRMT5 oncoprotein. MP possesses a dual function in cancer-related pathways as it is not only a cytoskeletal regulator governing cell migration and metastasis but it also functions as a key regulator of gene expression and has anti-tumor features (Fig. 30). Taken together, the "MP/PRMT5/histoneR3" pathway plays

a critical role in tumorigenesis and cancer development, therefore the pharmacological interventions of this pathway by targeting MP may have important and promising clinical implications in therapeutics.

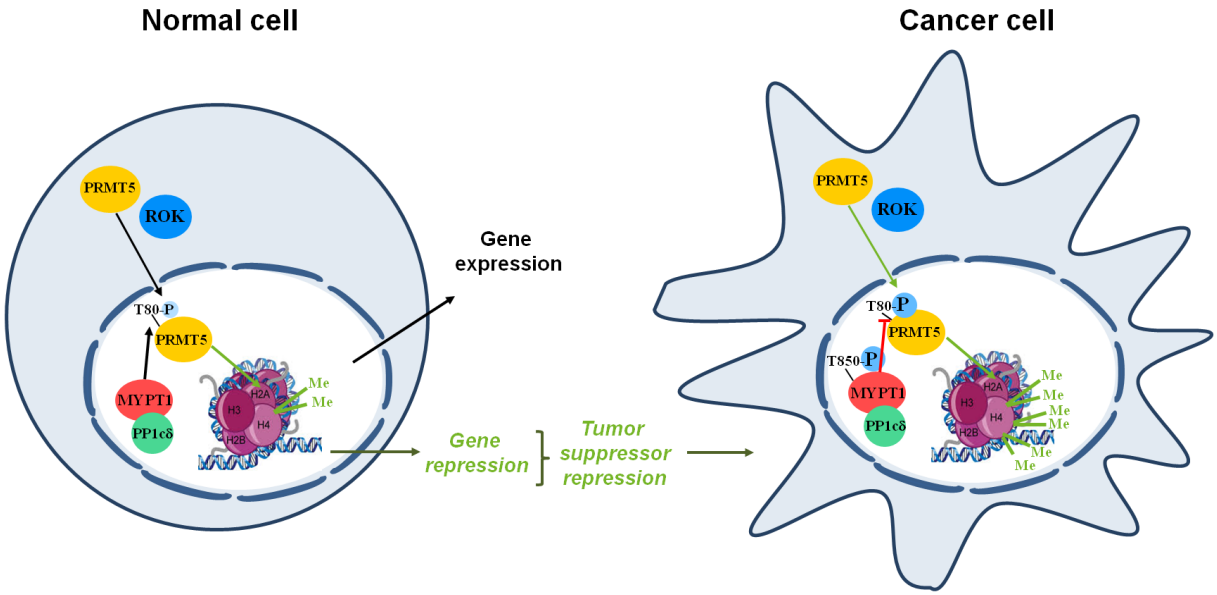

Figure 30. MP plays a tumor suppressor role and antagonizes ROK in HCC.
We hypothesize that MP and ROK are involved in gene expression. Under normal conditions MP modulates symmetrical dimethylation of histone core proteins in cell nucleus via dephosphorylation of PRMT5 at its activating phosphorylation site (Thr^{80}). In tumor cells inhibitory phosphorylation of MP on Thr^{850} is increased leading to higher phosphorylation level of PRMT5 at Thr^{80} by ROK. Activated PRMT5 provokes gene repression by raising symmetrical dimethylation of histone H2A/H4 Arg3 that triggers proto-oncogene activation and tumor formation.

One of the promising regulator of MP is the smoothelin-like 1 protein (SMTNL1) that was recently found to inhibit the activity of MP towards the phosphorylated 20 kDa myosin light chain of smooth muscle (Borman et al. 2009). SMTNL1 is expressed in smooth and skeletal muscle as well and is a regulator of vascular smooth muscle contractility and cardiovascular and skeletal muscle adaptation to exercise, development and pregnancy (Wooldridge et al. 2008; Lontay et al. 2010; Bodoor et al. 2011). According to initial assumptions, the molecular mechanism by which SMTNL1 alters MP activity appears to be the binding of SMTNL1 to myosin itself rather than to the phosphatase itself and modulates the ability of myosin to be dephosphorylated by MP. Wooldridge *et al.* found that SMTNL1 had no significant effect on MP activity when recombinant myosin light chains were used as a substrate but SMTNL1 could inhibit MP activity towards whole myosin *in vitro* (Wooldridge et al. 2008). The hypothesis is supported by the fact that radioactive-labeled ^{32}P-SMTNL1

was poorly dephosphorylated by PP1c catalytic subunit in the presence of MYPT1 suggesting that SMTNL1 is not a substrate for MP (Wooldridge et al. 2008; Borman et al. 2009). To answer the reverse question if SMTNL1 acts on MP we first wanted to clarify the direct interaction between MYPT1 and SMTNL1 based on binding assays by surface plasmon resonance (Fig. 13). Recombinant SMTNL1 was strongly bound to full-length, to N- or C-terminal truncated mutants of MYPT1 as well suggesting that different regions of MYPT1 are involved in the formation of the interaction with SMTNL1. Additionally, since calponin homologous (CH) domain deficient truncated SMTNL1 had no effect on MP activity (Borman et al. 2009), we can assume that the interaction between SMTNL1 and MYPT1 is accomplished by the involvement of different segments of the two proteins. Presumably N-terminal ankyrin repeat domains and C-terminal leucine zipper on MYPT1 and CH-domain of SMTNL1 could play a role in the formation of the complex. It is well in line with the previous findings that the N-terminal part of MYPT1, containing the ankyrin repeat domains serves as a platform for binding various interacting proteins of MP. Further investigations are needed to uncover the details of the binding.

Skeletal muscle shows plasticity, and is able to adapt its contractile phenotype in response to physiological stresses including exercise training, hormonal shifts, aging and pathological stress (Halayko et al. 2001). Skeletal muscle plasticity in endurance exercise training promotes the switching of skeletal muscle fiber content to a more oxidative phenotype characterized by an increase in the relative numbers of type I slow-twitch and type2a fast-twitch fibers, and a decrease in type2b fast-twitch glycolytic fibers (Booth et al. 1991; Fitts 2003). Pregnancy is also a physiological state that can promote major changes in smooth and skeletal muscle mainly mediated by the female sex steroid hormones estrogen and progesterone (Edwards 2005). SMTNL1 was found to be a regulator of adaptive responses in uterine smooth muscle during pregnancy. SMTNL1 selectively binds to progesterone receptor and not other steroid hormone receptors and co-regulates its transcriptional activity mediating gene expression in reproductive tissues (Bodoor et al. 2011). In non-pregnant state, SMTNL1 effects as a repressor of progesterone receptor function while during pregnancy increased expression of progesterone receptor and SMTNL1 and enhanced phosphorylation and nuclear translocation of SMTNL1 at Ser^{301} was observed which relieves the inhibitory effect of SMTNL1 towards progesterone receptor (Lontay et al. 2010). Based on proteomic, global gene array and fiber typing studies in WT and *smtnl1-/-* mice pregnancy induces switching of skeletal muscle to a glycolytic phenotype and this effect is mediated through SMTNL1. Fiber type switching means a change from type2a skeletal muscle fibers with increased free fatty

acid oxidation to the type2b skeletal muscle fibers with glycolytic phenotype because of the increased glucose content. We suggest that pregnancy-induced fiber switching to a more glycolytic phenotype is a coordinated physiological response resulting increased weight gain and generalized insulin resistance associated with normal pregnancy and infers the evolutionary advantage of enabling the mother to increase circulating glucose levels for proper foetal development as well as store fat more efficiently to meet the caloric demands of lactation.

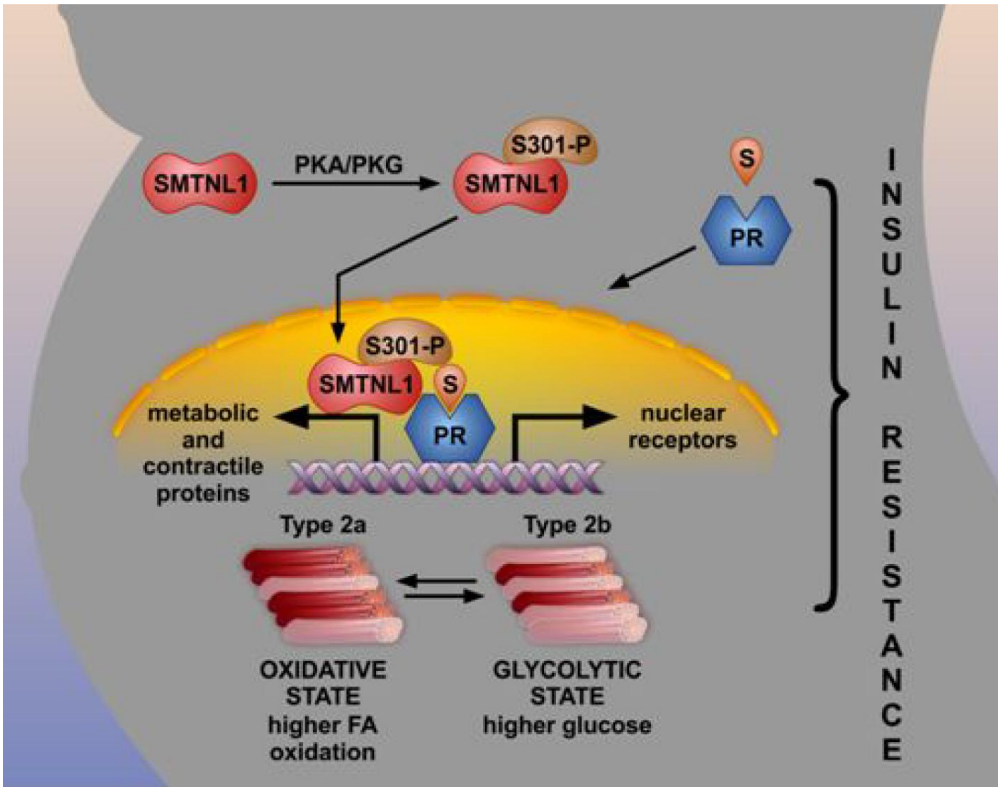

Figure 31. Model for the molecular mechanism by which SMTNL1 regulates skeletal muscle adaptations in response to pregnancy.

In response to elevated steroid hormone, progesterone (S) levels SMTNL1 and PR-B (PR) enter the nucleus. In the non-pregnant state SMTNL1 functions to repress PR-B activity however, during pregnancy this inhibition is relieved to promoting activation of skeletal muscle specific genes regulating the expression of metabolic and contractile proteins. This coordinated response adapts the mother's physiological state to support the weight gain originating from developing fetus. Switching to a glycolytic phenotype in skeletal muscle reduces the oxidative capacity of SKM promoting increased storage of fatty acid and inducing an insulin resistant state resulting in increased circulating glucose (Lontay et al. 2010).

SUMMARY

Myosin phosphatase (MP) holoenzyme is a protein phosphatase-1 type Ser/Thr specific enzyme consisting of a PP1cδ catalytic subunit, a myosin phosphatase target subunit-1 (MYPT1) and a 20 kDa subunit with unknown function. We identified the protein arginine methyltransferase 5 (PRMT5) enzyme of the methylosome complex as a novel interacting partner of MYPT1 in hepatocellular carcinoma cells. PRMT5 was found to be regulated by phosphorylation at Thr^{80} by RhoA-associated protein kinase and MP. Loss of MP function increased the level of the PRMT5-specific symmetric dimethylation on arginine residues of histone 2A/4, a repressing gene expression mark. It resulted in an overall change in the expression of genes affecting cellular processes like growth, proliferation and cell death, also affecting the expression of the retinoblastoma protein and *c*-Myc. Increased phosphorylation of PRMT5 at Thr^{80} and elevated symmetric dimethylation of H2A was described in human hepatocellular carcinoma and in other types of cancers in accordance with the increased phosphorylation of MYPT1 at inhibitory site Thr^{850}. Our results suggest a novel mechanism of tumorigenesis governed by ROK and MP via regulation of PRMT5 thereby modulating gene expression through histone arginine dimethylation.

MP activity can be regulated by the smoothelin-like 1 protein (SMTNL1) that is a regulator of vascular smooth muscle contractility and modulates cardiovascular and skeletal muscle adaptations (Wooldridge et al. 2008; Lontay et al. 2010). Under physiological conditions cytosolic SMTNL1 controls MP activity towards phosphorylated MLC20 causing changes in muscle contractility (Borman et al. 2009). Based on SPR binding assays, we verified binding of SMTNL1 to the regulatory subunit MYPT1 of MP suggesting direct protein-protein interaction between them.

During pregnancy, the metabolic properties of skeletal muscle are adapted to physiological challenges and increased expression of SMTNL1 was observed in uterine and vascular smooth muscle and sex-hormone related tissues. We found that pregnancy promotes fiber type changes from an oxidative to a glycolytic isoform in skeletal muscle regulated by SMTNL1, which alters the expression of transcriptional and enzyme regulators and structural molecules. We suggest that these events are natural adaptations of normal pregnancy and potentially infer evolutionary advantages to the mother by increasing her ability to store fat and her physical strength to carry the developing foetus.

ÖSSZEFOGLALÁS

A miozin foszfatáz (MP) holoenzim egy szerin/treonin specifikus protein foszfatáz, mely egy PP1cδ katalitikus, egy miozin foszfatáz szabályozó alegységből (MYPT1) és egy 20 kDa eddig ismeretlen funkciójú alegységből áll. Hepatocelluláris karcinóma sejtekben a MYPT1 új kölcsönhatójaként azonosítottuk a metiloszóma komplex egyik tagját, a protein arginin metiltranszferáz 5 (PRMT5) enzimet. A PRMT5 fehérje Thr^{80} oldallánca a MP és a RhoA-asszociált kináz (ROK) által katalizált foszforiláció révén szabályozódik. MYPT1 csendesítés hatására megemelkedett a PRMT5 által katalizált szimmetrikus dimetiláció a hiszton 2A és 4 fehérjék arginin oldalláncain, mely a celluláris folyamatokat befolyásoló gének expresszióját, mint pl. növekedés, proliferáció és sejthalál, valamint a retinoblasztóma és a *c*-Myc fehérjék kifejeződését is nagymértékben befolyásolta. A MYPT1 Thr^{850} gátló foszforilációs helyének emelkedett foszforilációjával összhangban a PRMT5 foszforilációja a Thr^{80} oldalláncon, valamint a H2A szimmetrikus dimetilációja is fokozódott humán májsejtes karcinóma és egyéb tumor típusok esetében. Eredményeink alapján a ROK és MP enzimpár a PRMT5 fehérjére gyakorolt hatásukon keresztül részt vesznek a hisztonok szimmetrikus dimetilációjának módosításában, ezáltal modulálva a génexpressziót és szabályozva a tumor képződés folyamatát.

A MP aktivitását szabályozó egyik fehérje a smoothelin-szerű 1 fehérje (SMTNL1), mely részt vesz a sima- és vázizomzat kontraktilitásának szabályozásában valamint azok fiziológiás stressz hatására történő adaptációjában (Wooldridge et al. 2008). Az SMTNL1 a sejtek citoplazmájában hatással van a MP aktivitására, ezáltal szabályozva az izom összehúzódás folyamatát (Borman et al. 2009). SPR kötődési kísérletekkel igazoltuk a két fehérje, azaz az SMTNL1 és a MP szabályozó alegysége, a MYPT1 között kialakuló közvetlen fehérje-fehérje kölcsönhatást.

A terhesség állapotával járó fiziológiai változásokra adott válaszként a vázizomzat metabolikus tulajdonságai megváltoznak és az SMTNL1 fokozott expressziója figyelhető meg a méh és a vérerek simaizomzatában valamint a nemi hormonokra érzékeny szövetekben. Vizsgálataink során vázizomrostokban a terhesség hatására bekövetkező oxidatívból glikolitikusabb állapotba történő izotípusváltást mutattunk ki. Feltételezéseink szerint ez a folyamat az SMTNL1 szabályozása alatt áll a különböző transzkripciós és enzim regulátorok és szerkezeti molekulák expressziójának módosításán keresztül. Feltételezhetően ez a folyamat egy a terhességre adott normál, az anya számára evolúciós előnyt jelentő, a magzat fejlődését és védelmét biztosító válasz.

REFERENCES

Aagaard, P. and J. L. Andersen (1998). "Correlation between contractile strength and myosin heavy chain isoform composition in human skeletal muscle." Med Sci Sports Exerc **30**(8): 1217-22.

Alessi, D., L. K. MacDougall, et al. (1992). "The control of protein phosphatase-1 by targetting subunits. The major myosin phosphatase in avian smooth muscle is a novel form of protein phosphatase-1." Eur J Biochem **210**(3): 1023-35.

Alfthan, K., L. Heiska, et al. (2004). "Cyclic AMP-dependent protein kinase phosphorylates merlin at serine 518 independently of p21-activated kinase and promotes merlin-ezrin heterodimerization." J Biol Chem **279**(18): 18559-66.

Allen, P. B., C. C. Ouimet, et al. (1997). "Spinophilin, a novel protein phosphatase 1 binding protein localized to dendritic spines." Proc Natl Acad Sci U S A **94**(18): 9956-61.

Alonso, A., J. Sasin, et al. (2004). "Protein tyrosine phosphatases in the human genome." Cell **117**(6): 699-711.

Amano, M., T. Kaneko, et al. (2003). "Identification of Tau and MAP2 as novel substrates of Rho-kinase and myosin phosphatase." J Neurochem **87**(3): 780-90.

Antonysamy, S., Z. Bonday, et al. (2012). "Crystal structure of the human PRMT5:MEP50 complex." Proceedings of the National Academy of Sciences of the United States of America **109**(44): 17960-17965.

Arimura, T., N. Suematsu, et al. (2001). "Identification, characterization, and functional analysis of heart-specific myosin light chain phosphatase small subunit." J Biol Chem **276**(9): 6073-82.

Baker, P. R., J. C. Trinidad, et al. (2011). "Modification Site Localization Scoring Integrated into a Search Engine." Molecular & Cellular Proteomics **10**(7).

Bannert, N., K. Vollhardt, et al. (2003). "PDZ Domain-mediated interaction of interleukin-16 precursor proteins with myosin phosphatase targeting subunits." J Biol Chem **278**(43): 42190-9.

Barford, D., Z. Jia, et al. (1995). "Protein tyrosine phosphatases take off." Nat Struct Biol **2**(12): 1043-53.

Barton, G. J. (1994). "Scop: structural classification of proteins." Trends Biochem Sci **19**(12): 554-5.

Bennett, V. and A. J. Baines (2001). "Spectrin and ankyrin-based pathways: Metazoan inventions for integrating cells into tissues." Physiological Reviews **81**(3): 1353-1392.

Biemann, K. (1990). "Appendix 5. Nomenclature for peptide fragment ions (positive ions)." Methods Enzymol **193**: 886-7.

Bodoor, K., B. Lontay, et al. (2011). "Smoothelin-like 1 Protein Is a Bifunctional Regulator of the Progesterone Receptor during Pregnancy." Journal of Biological Chemistry **286**(36): 31839-31851.

Bokoch, G. M. and C. J. Der (1993). "Emerging concepts in the Ras superfamily of GTP-binding proteins." FASEB J **7**(9): 750-9.

Bollen, M. (2001). "Combinatorial control of protein phosphatase-1." Trends Biochem Sci **26**(7): 426-31.

Bollen, M., S. M. Kee, et al. (1987). "Substrate specificity of phosphorylase kinase: effects of heparin and calcium." Arch Biochem Biophys **254**(2): 437-47.

Bollen, M., W. Peti, et al. (2010). "The extended PP1 toolkit: designed to create specificity." Trends in Biochemical Sciences **35**(8): 450-458.

Booth, F. W. and D. B. Thomason (1991). "Molecular and cellular adaptation of muscle in response to exercise: perspectives of various models." Physiol Rev **71**(2): 541-85.

Borman, M. A., T. A. Freed, et al. (2009). "The role of the calponin homology domain of smoothelin-like 1 (SMTNL1) in myosin phosphatase inhibition and smooth muscle contraction." Mol Cell Biochem **327**(1-2): 93-100.

Borman, M. A., J. A. MacDonald, et al. (2004). "Modulation of smooth muscle contractility by CHASM, a novel member of the smoothelin family of proteins." FEBS Lett **573**(1-3): 207-13.

Boudrez, A., K. Evens, et al. (1999). "Identification of MYPT1 and NIPP1 as subunits of protein phosphatase 1 in rat liver cytosol." FEBS Lett **455**(1-2): 175-8.

Brautigan, D. L. (2013). "Protein Ser/Thr phosphatases - the ugly ducklings of cell signalling." Febs Journal **280**(2): 324-345.

Broustas, C. G., N. Grammatikakis, et al. (2002). "Phosphorylation of the myosin-binding subunit of myosin phosphatase by Raf-1 and inhibition of phosphatase activity." J Biol Chem **277**(4): 3053-9.

Butler, T., J. Paul, et al. (2013). "Role of serine-threonine phosphoprotein phosphatases in smooth muscle contractility." American Journal of Physiology-Cell Physiology **304**(6): C485-C504.

Cao, W. S., S. N. Mattagajasingh, et al. (2002). "TIMAP, a novel CAAX box protein regulated by TGF-beta 1 and expressed in endothelial cells." American Journal of Physiology-Cell Physiology **283**(1): C327-C337.

Ceulemans, H. and M. Bollen (2004). "Functional diversity of protein phosphatase-1, a cellular economizer and reset button." Physiol Rev **84**(1): 1-39.

Chacko, S., M. A. Conti, et al. (1977). "Effect of phosphorylation of smooth muscle myosin on actin activation and Ca2+ regulation." Proc Natl Acad Sci U S A **74**(1): 129-33.

Chellappan, S. P., S. Hiebert, et al. (1991). "The E2F transcription factor is a cellular target for the RB protein." Cell **65**(6): 1053-61.

Chen, Y. H., M. X. Chen, et al. (1994). "Molecular cloning of cDNA encoding the 110 kDa and 21 kDa regulatory subunits of smooth muscle protein phosphatase 1M." FEBS Lett **356**(1): 51-5.

Chew, Y. P., M. Ellis, et al. (1998). "pRB phosphorylation mutants reveal role of pRB in regulating S phase completion by a mechanism independent of E2F." Oncogene **17**(17): 2177-86.

Choudhury, N., A. S. Khromov, et al. (2004). "Telokin mediates Ca2+-desensitization through activation of myosin phosphatase in phasic and tonic smooth muscle." Journal of Muscle Research and Cell Motility **25**(8): 657-665.

Choy, M. S., R. Page, et al. (2012). "Regulation of protein phosphatase 1 by intrinsically disordered proteins." Biochemical Society Transactions **40**: 969-974.

Cohen, P. (1990). "The Structure and Regulation of Protein Phosphatases." Advances in Second Messenger and Phosphoprotein Research **24**: 230-235.

Cohen, P., G. A. Nimmo, et al. (1977). "The substrate specificity and regulation of the protein phosphatases involved in the control of glycogen metabolism in mammalian skeletal muscle." Adv Enzyme Regul **16**: 97-119.

Cohen, P. T. (2002). "Protein phosphatase 1--targeted in many directions." J Cell Sci **115**(Pt 2): 241-56.

Cohen, P. T. W. (1997). "Novel protein serine/threonine phosphatases: Variety is the spice of life." Trends in Biochemical Sciences **22**(7): 245-251.

Connor, J. H., T. Kleeman, et al. (1999). "Importance of the beta12-beta13 loop in protein phosphatase-1 catalytic subunit for inhibition by toxins and mammalian protein inhibitors." J Biol Chem **274**(32): 22366-72.

Csortos, C., I. Czikora, et al. (2008). "TIMAP is a positive regulator of pulmonary endothelial barrier function." Am J Physiol Lung Cell Mol Physiol **295**(3): L440-50.

Deng, J. T., C. Sutherland, et al. (2002). "Phosphorylation of the myosin phosphatase inhibitors, CPI-17 and PHI-1, by integrin-linked kinase." Biochem J **367**(Pt 2): 517-24.

Dequiedt, F., H. Kasler, et al. (2003). "HDAC7, a thymus-specific class II histone deacetylase, regulates Nur77 transcription and TCR-mediated apoptosis." Immunity **18**(5): 687-98.

Dequiedt, F., J. Van Lint, et al. (2005). "Phosphorylation of histone deacetylase 7 by protein kinase D mediates T cell receptor-induced Nur77 expression and apoptosis." J Exp Med **201**(5): 793-804.

Dirksen, W. P., F. Vladic, et al. (2000). "A myosin phosphatase targeting subunit isoform transition defines a smooth muscle developmental phenotypic switch." Am J Physiol Cell Physiol **278**(3): C589-600.

Dubois, T., S. Howell, et al. (2003). "Novel in vitro and in vivo phosphorylation sites on protein phosphatase 1 inhibitor CPI-17." Biochem Biophys Res Commun **302**(2): 186-92.

Edwards, D. P. (2005). "Regulation of signal transduction pathways by estrogen and progesterone." Annu Rev Physiol **67**: 335-76.

Egloff, M. P., D. F. Johnson, et al. (1997). "Structural basis for the recognition of regulatory subunits by the catalytic subunit of protein phosphatase 1." EMBO J **16**(8): 1876-87.

Endo, S., X. Zhou, et al. (1996). "Multiple structural elements define the specificity of recombinant human inhibitor-1 as a protein phosphatase-1 inhibitor." Biochemistry **35**(16): 5220-8.

Erdodi, F., E. Kiss, et al. (2003). "Phosphorylation of protein phosphatase type-1 inhibitory proteins by integrin-linked kinase and cyclic nucleotide-dependent protein kinases." Biochem Biophys Res Commun **306**(2): 382-7.

Erdodi, F., B. Toth, et al. (1995). "Endothall thioanhydride inhibits protein phosphatases-1 and -2A in vivo." Am J Physiol **269**(5 Pt 1): C1176-84.

Eto, M., A. Karginov, et al. (1999). "A novel phosphoprotein inhibitor of protein type-1 phosphatase holoenzymes." Biochemistry **38**(51): 16952-7.

Eto, M., T. Kitazawa, et al. (2001). "Histamine-induced vasoconstriction involves phosphorylation of a specific inhibitor protein for myosin phosphatase by protein kinase C alpha and delta isoforms." J Biol Chem **276**(31): 29072-8.

Eto, M., T. Ohmori, et al. (1995). "A novel protein phosphatase-1 inhibitory protein potentiated by protein kinase C. Isolation from porcine aorta media and characterization." J Biochem **118**(6): 1104-7.

Eto, M., S. Senba, et al. (1997). "Molecular cloning of a novel phosphorylation-dependent inhibitory protein of protein phosphatase-1 (CPI17) in smooth muscle: its specific localization in smooth muscle." FEBS Lett **410**(2-3): 356-60.

Feng, J., M. Ito, et al. (1999). "Inhibitory phosphorylation site for Rho-associated kinase on smooth muscle myosin phosphatase." J Biol Chem **274**(52): 37385-90.

Feng, Y., J. X. Wang, et al. (2011). "Histone H4 Acetylation Differentially Modulates Arginine Methylation by an in Cis Mechanism." Journal of Biological Chemistry **286**(23): 20323-20334.

Fitts, R. H. (2003). "Effects of regular exercise training on skeletal muscle contractile function." Am J Phys Med Rehabil **82**(4): 320-31.

Fujioka, M., N. Takahashi, et al. (1998). "A new isoform of human myosin phosphatase targeting/regulatory subunit (MYPT2): cDNA cloning, tissue expression, and chromosomal mapping." Genomics **49**(1): 59-68.

Fukata, Y., K. Kimura, et al. (1998). "Association of the myosin-binding subunit of myosin phosphatase and moesin: dual regulation of moesin phosphorylation by Rho-associated kinase and myosin phosphatase." J Cell Biol **141**(2): 409-18.

Gallagher, P. J. and B. P. Herring (1991). "The carboxyl terminus of the smooth muscle myosin light chain kinase is expressed as an independent protein, telokin." J Biol Chem **266**(35): 23945-52.

Galvez-Santisteban, M., A. E. Rodriguez-Fraticelli, et al. (2012). "Synaptotagmin-like proteins control the formation of a single apical membrane domain in epithelial cells." Nature Cell Biology **14**(8): 838-U148.

Genda, T., M. Sakamoto, et al. (1999). "Cell motility mediated by Rho and Rho-associated protein kinase plays a critical role in intrahepatic metastasis of human hepatocellular carcinoma." Hepatology **30**(4): 1027-1036.

Gil, C., A. Falques, et al. (2011). "Protein kinase CK2 associates to lipid rafts and its pharmacological inhibition enhances neurotransmitter release." Febs Letters **585**(2): 414-420.

Gkountela, S., Z. W. Li, et al. (2014). "PRMT5 is Required for Human Embryonic Stem Cell Proliferation But Not Pluripotency." Stem Cell Reviews and Reports **10**(2): 230-239.

Gordon, E. A., T. C. Whisenant, et al. (2013). "Combining docking site and phosphosite predictions to find new substrates: Identification of smoothelin-like-2 (SMTNL2) as a c-Jun N-terminal kinase (JNK) substrate." Cellular Signalling **25**(12): 2518-2529.

Grassie, M. E., C. Sutherland, et al. (2012). "Cross-talk between Rho-associated Kinase and Cyclic Nucleotide-dependent Kinase Signaling Pathways in the Regulation of Smooth Muscle Myosin Light Chain Phosphatase." Journal of Biological Chemistry **287**(43): 36356-36369.

Gu, Z. P., S. Gao, et al. (2012). "Protein arginine methyltransferase 5 is essential for growth of lung cancer cells." Biochemical Journal **446**: 235-241.

Halayko, A. J. and J. Solway (2001). "Molecular mechanisms of phenotypic plasticity in smooth muscle cells." J Appl Physiol (1985) **90**(1): 358-68.

Hamaguchi, T., M. Ito, et al. (2000). "Phosphorylation of CPI-17, an inhibitor of myosin phosphatase, by protein kinase N." Biochem Biophys Res Commun **274**(3): 825-30.

Hartshorne, D. J., M. Ito, et al. (1998). "Myosin light chain phosphatase: subunit composition, interactions and regulation." Journal of Muscle Research and Cell Motility **19**(4): 325-341.

Hartshorne, D. J., M. Ito, et al. (2004). "Role of protein phosphatase type 1 in contractile functions: myosin phosphatase." J Biol Chem **279**(36): 37211-4.

Hemmings, H. C., Jr., P. Greengard, et al. (1984). "DARPP-32, a dopamine-regulated neuronal phosphoprotein, is a potent inhibitor of protein phosphatase-1." Nature **310**(5977): 503-5.

Hilfiker, S., F. Benfenati, et al. (2005). "Structural domains involved in the regulation of transmitter release by synapsins." J Neurosci **25**(10): 2658-69.

Hirano, K., M. Hirano, et al. (2004). "Regulation of myosin phosphorylation and myofilament Ca2+ sensitivity in vascular smooth muscle." J Smooth Muscle Res **40**(6): 219-36.

Hirano, K., M. Ito, et al. (1995). "Interaction of the ribosomal protein, L5, with protein phosphatase type 1." J Biol Chem **270**(34): 19786-90.

Hirano, K., B. C. Phan, et al. (1997). "Interactions of the subunits of smooth muscle myosin phosphatase." J Biol Chem **272**(6): 3683-8.

Horowitz, A., C. B. Menice, et al. (1996). "Mechanisms of smooth muscle contraction." Physiol Rev **76**(4): 967-1003.

Huang, F. L. and W. H. Glinsmann (1976). "Separation and characterization of two phosphorylase phosphatase inhibitors from rabbit skeletal muscle." Eur J Biochem **70**(2): 419-26.

Hunter, T. (1995). "Protein kinases and phosphatases: the yin and yang of protein phosphorylation and signaling." Cell **80**(2): 225-36.

Ichikawa, K., M. Ito, et al. (1996). "Phosphorylation of the large subunit of myosin phosphatase and inhibition of phosphatase activity." J Biol Chem **271**(9): 4733-40.

Ikebe, M. and D. J. Hartshorne (1985). "The role of myosin phosphorylation in the contraction-relaxation cycle of smooth muscle." Experientia **41**(8): 1006-10.

Ingebritsen, T. S. and P. Cohen (1983). "Protein phosphatases: properties and role in cellular regulation." Science **221**(4608): 331-8.

Ishida, H., M. A. Borman, et al. (2008). "Solution structure of the calponin homology (CH) domain from the smoothelin-like 1 protein: a unique apocalmodulin-binding mode and the possible role of the C-terminal type-2 CH-domain in smooth muscle relaxation." J Biol Chem **283**(29): 20569-78.

Ito, M., T. Nakano, et al. (2004). "Myosin phosphatase: structure, regulation and function." Mol Cell Biochem **259**(1-2): 197-209.

Jin, H., T. Sperka, et al. (2006). "Tumorigenic transformation by CPI-17 through inhibition of a merlin phosphatase." Nature **442**(7102): 576-9.

Johnson, D. F., G. Moorhead, et al. (1996). "Identification of protein-phosphatase-1-binding domains on the glycogen and myofibrillar targetting subunits." Eur J Biochem **239**(2): 317-25.

Johnson, S. A. and T. Hunter (2005). "Kinomics: methods for deciphering the kinome." Nature Methods **2**(1): 17-25.

Kao, H. Y., A. Verdel, et al. (2001). "Mechanism for nucleocytoplasmic shuttling of histone deacetylase 7." J Biol Chem **276**(50): 47496-507.

Khromov, A., N. Choudhury, et al. (2009). "Phosphorylation-dependent autoinhibition of myosin light chain phosphatase accounts for Ca2+ sensitization force of smooth muscle contraction." J Biol Chem **284**(32): 21569-79.

Khromov, A. S., K. Momotani, et al. (2012). "Molecular Mechanism of Telokin-mediated Disinhibition of Myosin Light Chain Phosphatase and cAMP/cGMP-induced Relaxation of Gastrointestinal Smooth Muscle." Journal of Biological Chemistry **287**(25): 20975-20985.

Khromov, A. S., H. Wang, et al. (2006). "Smooth muscle of telokin-deficient mice exhibits increased sensitivity to Ca2+ and decreased cGMP-induced relaxation." Proc Natl Acad Sci U S A **103**(7): 2440-5.

Kimura, K., Y. Fukata, et al. (1998). "Regulation of the association of adducin with actin filaments by Rho-associated kinase (Rho-kinase) and myosin phosphatase." J Biol Chem **273**(10): 5542-8.

Kimura, K., M. Ito, et al. (1996). "Regulation of myosin phosphatase by Rho and Rho-associated kinase (Rho-kinase)." Science **273**(5272): 245-8.

Kimura, K., A. Wakamatsu, et al. (2006). "Diversification of transcriptional modulation: large-scale identification and characterization of putative alternative promoters of human genes." Genome Res **16**(1): 55-65.

Kiss, A., B. Lontay, et al. (2008). "Myosin phosphatase interacts with and dephosphorylates the retinoblastoma protein in THP-1 leukemic cells: Its inhibition is involved in the attenuation of daunorubicin-induced cell death by calyculin-A." Cellular Signalling **20**(11): 2059-2070.

Kiss, E., A. Muranyi, et al. (2002). "Integrin-linked kinase phosphorylates the myosin phosphatase target subunit at the inhibitory site in platelet cytoskeleton." Biochem J **365**(Pt 1): 79-87.

Kissil, J. L., K. C. Johnson, et al. (2002). "Merlin phosphorylation by p21-activated kinase 2 and effects of phosphorylation on merlin localization." Journal of Biological Chemistry **277**(12): 10394-10399.

Koga, Y. and M. Ikebe (2008). "A novel regulatory mechanism of myosin light chain phosphorylation via binding of 14-3-3 to myosin phosphatase." Molecular Biology of the Cell **19**(3): 1062-1071.

Kornblau, S. M., M. Andreeff, et al. (1998). "Low and maximally phosphorylated levels of the retinoblastoma protein confer poor prognosis in newly diagnosed acute myelogenous leukemia: a prospective study." Clin Cancer Res **4**(8): 1955-63.

Koyama, M., M. Ito, et al. (2000). "Phosphorylation of CPI-17, an inhibitory phosphoprotein of smooth muscle myosin phosphatase, by Rho-kinase." FEBS Lett **475**(3): 197-200.

Kramer, J., A. M. Aguirre-Arteta, et al. (1999). "A novel isoform of the smooth muscle cell differentiation marker smoothelin." J Mol Med (Berl) **77**(2): 294-8.

Krause, C. D., Z. H. Yang, et al. (2007). "Protein arginine methyltransferases: evolution and assessment of their pharmacological and therapeutic potential." Pharmacol Ther **113**(1): 50-87.

Larsen, M. R., T. E. Thingholm, et al. (2005). "Highly selective enrichment of phosphorylated peptides from peptide mixtures using titanium dioxide microcolumns." Mol Cell Proteomics **4**(7): 873-86.

Lartey, J., J. Taggart, et al. "Altered Expression of Human Smooth Muscle Myosin Phosphatase Targeting (MYPT) Isovariants with Pregnancy and Labor." PLoS One **11**(10): e0164352.

Li, L., X. Zhang, et al. (2007). "[Effects of lactational exposure to soy isoflavones on steroid receptor expression in neonate rat ovaries]." Wei Sheng Yan Jiu **36**(5): 564-7.

Lieber, R. L. and J. Friden (2002). "Spasticity causes a fundamental rearrangement of muscle-joint interaction." Muscle Nerve **25**(2): 265-70.

Liu, F., X. Y. Zhao, et al. (2011). "JAK2V617F-Mediated Phosphorylation of PRMT5 Downregulates Its Methyltransferase Activity and Promotes Myeloproliferation." Cancer Cell **19**(2): 283-294.

Liu, Q. R., P. W. Zhang, et al. (2002). "KEPI, a PKC-dependent protein phosphatase 1 inhibitor regulated by morphine." J Biol Chem **277**(15): 13312-20.

Lontay, B., K. Bodoor, et al. (2010). "Smoothelin-like 1 Protein Regulates Myosin Phosphatase-targeting Subunit 1 Expression during Sexual Development and Pregnancy." Journal of Biological Chemistry **285**(38): 29357-29366.

Lontay, B., A. Kiss, et al. (2005). "Okadaic acid induces phosphorylation and translocation of myosin phosphatase target subunit 1 influencing myosin phosphorylation, stress fiber assembly and cell migration in HepG2 cells." Cell Signal **17**(10): 1265-75.

Lontay, B., B. Pal, et al. (2012). "Protein phosphatase-1M and Rho-kinase affect exocytosis from cortical synaptosomes and influence neurotransmission at a glutamatergic giant synapse of the rat auditory system." Journal of Neurochemistry **123**(1): 84-99.

Lontay, B., Z. Serfozo, et al. (2004). "Localization of myosin phosphatase target subunit 1 in rat brain and in primary cultures of neuronal cells." J Comp Neurol **478**(1): 72-87.

MacDonald, J. A., M. A. Borman, et al. (2001). "Identification of the endogenous smooth muscle myosin phosphatase-associated kinase." Proc Natl Acad Sci U S A **98**(5): 2419-24.

MacDonald, J. A., H. Ishida, et al. (2012). "Intrinsically Disordered N-Terminus of Calponin Homology-Associated Smooth Muscle Protein (CHASM) Interacts with the Calponin

Homology Domain to Enable Tropomyosin Binding." Biochemistry **51**(13): 2694-2705.
MacDonald, J. A., L. A. Walker, et al. (2000). "Phosphorylation of telokin by cyclic nucleotide kinases and the identification of in vivo phosphorylation sites in smooth muscle." Febs Letters **479**(3): 83-88.
MacMillan, L. B., M. A. Bass, et al. (1999). "Brain actin-associated protein phosphatase 1 holoenzymes containing spinophilin, neurabin, and selected catalytic subunit isoforms." J Biol Chem **274**(50): 35845-54.
Marciniak, R. A., D. B. Lombard, et al. (1998). "Nucleolar localization of the Werner syndrome protein in human cells." Proceedings of the National Academy of Sciences of the United States of America **95**(12): 6887-6892.
Mayford, M. and E. R. Kandel (1999). "Genetic approaches to memory storage." Trends Genet **15**(11): 463-70.
McBride, A. E., V. H. Weiss, et al. (2000). "Analysis of the yeast arginine methyltransferase Hmt1p/Rmt1p and its in vivo function. Cofactor binding and substrate interactions." J Biol Chem **275**(5): 3128-36.
McClatchey, A. I. and M. Giovannini (2005). "Membrane organization and tumorigenesis - the NF2 tumor suppressor, Merlin." Genes & Development **19**(19): 2265-2277.
McKinsey, T. A., C. L. Zhang, et al. (2001). "Control of muscle development by dueling HATs and HDACs." Curr Opin Genet Dev **11**(5): 497-504.
Mellacheruvu, D., Z. Wright, et al. (2013). "The CRAPome: a contaminant repository for affinity purification-mass spectrometry data." Nature Methods **10**(8): 730-+.
Migliori, V., J. Muller, et al. (2012). "Symmetric dimethylation of H3R2 is a newly identified histone mark that supports euchromatin maintenance." Nature Structural & Molecular Biology **19**(2): 136-144.
Moorhead, G., D. Johnson, et al. (1998). "The major myosin phosphatase in skeletal muscle is a complex between the beta-isoform of protein phosphatase 1 and the MYPT2 gene product." FEBS Lett **438**(3): 141-4.
Muranyi, A., D. Derkach, et al. (2005). "Phosphorylation of Thr695 and Thr850 on the myosin phosphatase target subunit: inhibitory effects and occurrence in A7r5 cells." FEBS Lett **579**(29): 6611-5.
Muranyi, A., J. A. MacDonald, et al. (2002). "Phosphorylation of the myosin phosphatase target subunit by integrin-linked kinase." Biochem J **366**(Pt 1): 211-6.
Muranyi, A., R. Zhang, et al. (2001). "Myotonic dystrophy protein kinase phosphorylates the myosin phosphatase targeting subunit and inhibits myosin phosphatase activity." FEBS Lett **493**(2-3): 80-4.
Murphree, A. L. and W. F. Benedict (1984). "Retinoblastoma: clues to human oncogenesis." Science **223**(4640): 1028-33.
Niiro, N. and M. Ikebe (2001). "Zipper-interacting protein kinase induces Ca(2+)-free smooth muscle contraction via myosin light chain phosphorylation." J Biol Chem **276**(31): 29567-74.
Okamoto, R., M. Ito, et al. (2005). "The targeted disruption of the MYPT1 gene results in embryonic lethality." Transgenic Res **14**(3): 337-40.
Ouimet, C. C., E. F. da Cruz e Silva, et al. (1995). "The alpha and gamma 1 isoforms of protein phosphatase 1 are highly and specifically concentrated in dendritic spines." Proc Natl Acad Sci U S A **92**(8): 3396-400.
Pal, S., R. A. Baiocchi, et al. (2007). "Low levels of miR-92b/96 induce PRMT5 translation and H3R8/H4R3 methylation in mantle cell lymphoma." Embo Journal **26**(15): 3558-3569.

Pankova, K., D. Rosel, et al. (2010). "The molecular mechanisms of transition between mesenchymal and amoeboid invasiveness in tumor cells." Cellular and Molecular Life Sciences **67**(1): 63-71.
Parra, M., H. Kasler, et al. (2005). "Protein kinase D1 phosphorylates HDAC7 and induces its nuclear export after T-cell receptor activation." J Biol Chem **280**(14): 13762-70.
Parra, M., T. Mahmoudi, et al. (2007). "Myosin phosphatase dephosphorylates HDAC7, controls its nucleocytoplasmic shuttling, and inhibits apoptosis in thymocytes." Genes Dev **21**(6): 638-43.
Patil, S. B. and K. N. Bitar (2006). "RhoA- and PKC-alpha-mediated phosphorylation of MYPT and its association with HSP27 in colonic smooth muscle cells." Am J Physiol Gastrointest Liver Physiol **290**(1): G83-95.
Payne, M. C., H. Y. Zhang, et al. (2006). "Myosin phosphatase isoform switching in vascular smooth muscle development." J Mol Cell Cardiol **40**(2): 274-82.
Pennisi, E. (2002). "Human genome project - Genome Institute wrestles mightily with its future." Science **298**(5599): 1694-1695.
Peter, J. B., R. J. Barnard, et al. (1972). "Metabolic profiles of three fiber types of skeletal muscle in guinea pigs and rabbits." Biochemistry **11**(14): 2627-33.
Phung, T. L., A. Roncone, et al. (1997). "Phosphoinositide 3-kinase activity is necessary for insulin-dependent inhibition of apolipoprotein B secretion by rat hepatocytes and localizes to the endoplasmic reticulum." Journal of Biological Chemistry **272**(49): 30693-30702.
Piekny, A. J., J. L. Johnson, et al. (2003). "The Caenorhabditis elegans nonmuscle myosin genes nmy-1 and nmy-2 function as redundant components of the let-502/Rho-binding kinase and mel-11/myosin phosphatase pathway during embryonic morphogenesis." Development **130**(23): 5695-704.
Pot, D. A. and J. E. Dixon (1992). "A thousand and two protein tyrosine phosphatases." Biochim Biophys Acta **1136**(1): 35-43.
Quensel, C., J. Kramer, et al. (2002). "Smoothelin contains a novel actin cytoskeleton localization sequence with similarity to troponin T." J Cell Biochem **85**(2): 403-9.
Ratz, P. H., K. M. Berg, et al. (2005). "Regulation of smooth muscle calcium sensitivity: KCl as a calcium-sensitizing stimulus." Am J Physiol Cell Physiol **288**(4): C769-83.
Rensen, S. S., V. L. Thijssen, et al. (2002). "Expression of the smoothelin gene is mediated by alternative promoters." Cardiovasc Res **55**(4): 850-63.
Richard, S., M. Morel, et al. (2005). "Arginine methylation regulates IL-2 gene expression: a role for protein arginine methyltransferase 5 (PRMT5)." Biochem J **388**(Pt 1): 379-86.
Riddick, N., K. Ohtani, et al. (2008). "Targeting by myosin phosphatase-RhoA interacting protein mediates RhoA/ROCK regulation of myosin phosphatase." J Cell Biochem **103**(4): 1158-70.
Rouleau, G. A., E. C. Twist, et al. (1993). "Analysis of the Nf2-Gene in Tumors Showing Loss of Heterozygosity on Chromosome-22." American Journal of Human Genetics **53**(3): 351-351.
Rubenstein, J. L., P. Greengard, et al. (1993). "Calcium-dependent serine phosphorylation of synaptophysin." Synapse **13**(2): 161-72.
Saha, K., G. Adhikary, et al. (2016). "MEP50/PRMT5 Reduces Gene Expression by Histone Arginine Methylation and this Is Reversed by PKC delta/p38 delta Signaling." Journal of Investigative Dermatology **136**(1): 214-224.
Schmidt, C. and H. Urlaub (2009). "iTRAQ-labeling of in-gel digested proteins for relative quantification." Methods Mol Biol **564**: 207-26.
Shadforth, I. P., T. P. Dunkley, et al. (2005). "i-Tracker: for quantitative proteomics using iTRAQ." BMC Genomics **6**: 145.

Shalaby, T. and M. A. Grotzer (2016). "MYC as Therapeutic Target for Embryonal Tumors: Potential and Challenges." Current Cancer Drug Targets **16**(1): 2-21.
Sheng, X. M., N. Bowen, et al. (2016). "GLI pathogenesis-related 1 functions as a tumor-suppressor in lung cancer." Molecular Cancer **15**.
Shevchenko, A., M. Wilm, et al. (1996). "Mass spectrometric sequencing of proteins from silver stained polyacrylamide gels." Analytical Chemistry **68**(5): 850-858.
Shi, Y. G. (2009). "Serine/Threonine Phosphatases: Mechanism through Structure." Cell **139**(3): 468-484.
Shimizu, H., M. Ito, et al. (1994). "Characterization of the myosin-binding subunit of smooth muscle myosin phosphatase." J Biol Chem **269**(48): 30407-11.
Shin, H. M., H. D. Je, et al. (2002). "Differential association and localization of myosin phosphatase subunits during agonist-induced signal transduction in smooth muscle." Circ Res **90**(5): 546-53.
Skinner, J. A. and A. R. Saltiel (2001). "Cloning and identification of MYPT3: a prenylatable myosin targetting subunit of protein phosphatase 1." Biochem J **356**(Pt 1): 257-67.
Sleno, L. and D. A. Volmer (2004). "Ion activation methods for tandem mass spectrometry." Journal of Mass Spectrometry **39**(10): 1091-1112.
Somlyo, A. P. and A. V. Somlyo (2003). "Ca2+ sensitivity of smooth muscle and nonmuscle myosin II: Modulated by G proteins, kinases, and myosin phosphatase." Physiological Reviews **83**(4): 1325-1358.
Steck, P. A., M. A. Pershouse, et al. (1997). "Identification of a candidate tumour suppressor gene, MMAC1, at chromosome 10q23.3 that is mutated in multiple advanced cancers." Nat Genet **15**(4): 356-62.
Strack, S., S. Kini, et al. (1999). "Differential cellular and subcellular localization of protein phosphatase 1 isoforms in brain." J Comp Neurol **413**(3): 373-84.
Strausberg, R. L., E. A. Feingold, et al. (2002). "Generation and initial analysis of more than 15,000 full-length human and mouse cDNA sequences." Proc Natl Acad Sci U S A **99**(26): 16899-903.
Sutherland, C. and M. P. Walsh (2012). "Myosin Regulatory Light Chain Diphosphorylation Slows Relaxation of Arterial Smooth Muscle." Journal of Biological Chemistry **287**(29): 24064-24076.
Takahashi, N., M. Ito, et al. (1997). "Localization of the gene coding for myosin phosphatase, target subunit 1 (MYPT1) to human chromosome 12q15-q21." Genomics **44**(1): 150-2.
Takizawa, N., Y. Koga, et al. (2002). "Phosphorylation of CPI17 and myosin binding subunit of type 1 protein phosphatase by p21-activated kinase." Biochem Biophys Res Commun **297**(4): 773-8.
Tan, I., C. H. Ng, et al. (2001). "Phosphorylation of a novel myosin binding subunit of protein phosphatase 1 reveals a conserved mechanism in the regulation of actin cytoskeleton." J Biol Chem **276**(24): 21209-16.
Terrak, M., F. Kerff, et al. (2004). "Structural basis of protein phosphatase 1 regulation." Nature **429**(6993): 780-4.
Terry-Lorenzo, R. T., M. Inoue, et al. (2000). "Neurofilament-L is a protein phosphatase-1-binding protein associated with neuronal plasma membrane and post-synaptic density." J Biol Chem **275**(4): 2439-46.
Toth, A., E. Kiss, et al. (2000). "Phosphorylation of MYPT1 by protein kinase C attenuates interaction with PP1 catalytic subunit and the 20 kDa light chain of myosin." FEBS Lett **484**(2): 113-7.
Totsukawa, G., Y. Yamakita, et al. (1999). "Activation of myosin phosphatase targeting subunit by mitosis-specific phosphorylation." J Cell Biol **144**(4): 735-44.

Tran, H. T., A. Ulke, et al. (2004). "Proteomic characterization of protein phosphatase complexes of the mammalian nucleus." Mol Cell Proteomics **3**(3): 257-65.
Trofatter, J. A., M. M. Maccollin, et al. (1993). "A Novel Moesin-Like, Ezrin-Like, Radixin-Like Gene Is a Candidate for the Neurofibromatosis-2 Tumor Suppressor." Cell **72**(5): 791-800.
Turner, S. R. and J. A. MacDonald (2014). "Novel Contributions of the Smoothelin- like 1 Protein in Vascular Smooth Muscle Contraction and its Potential Involvement in Myogenic Tone." Microcirculation **21**(3): 249-258.
Ulke-Lemee, A., H. Ishida, et al. (2014). "Two domains of the smoothelin-like 1 protein bind apo- and calcium-calmodulin independently." Biochimica Et Biophysica Acta-Proteins and Proteomics **1844**(9): 1580-1590.
Ulke-Lemee, A., S. R. Turner, et al. (2011). "Mapping and functional characterization of the murine Smoothelin-like 1 promoter." Bmc Molecular Biology **12**.
Uribesalgo, I., S. A. Benitah, et al. (2012). "From oncogene to tumor suppressor The dual role of Myc in leukemia." Cell Cycle **11**(9): 1757-1764.
van der Loop, F. T., G. Gabbiani, et al. (1997). "Differentiation of smooth muscle cells in human blood vessels as defined by smoothelin, a novel marker for the contractile phenotype." Arterioscler Thromb Vasc Biol **17**(4): 665-71.
van Eys, G. J., M. C. Voller, et al. (1997). "Smoothelin expression characteristics: development of a smooth muscle cell in vitro system and identification of a vascular variant." Cell Struct Funct **22**(1): 65-72.
van Heusden, G. P. (2009). "14-3-3 Proteins: insights from genome-wide studies in yeast." Genomics **94**(5): 287-93.
Velasco, G., C. Armstrong, et al. (2002). "Phosphorylation of the regulatory subunit of smooth muscle protein phosphatase 1M at Thr850 induces its dissociation from myosin." FEBS Lett **527**(1-3): 101-4.
Vetterkind, S., E. Lee, et al. (2010). "Par-4: A New Activator of Myosin Phosphatase." Molecular Biology of the Cell **21**(7): 1214-1224.
Vetterkind, S. and K. G. Morgan (2009). "The pro-apoptotic protein Par-4 facilitates vascular contractility by cytoskeletal targeting of ZIPK." J Cell Mol Med **13**(5): 887-95.
Wakula, P., M. Beullens, et al. (2003). "Degeneracy and function of the ubiquitous RVXF motif that mediates binding to protein phosphatase-1." J Biol Chem **278**(21): 18817-23.
Wang, L., S. Pal, et al. (2008). "Protein arginine methyltransferase 5 suppresses the transcription of the RB family of tumor suppressors in leukemia and lymphoma cells." Mol Cell Biol **28**(20): 6262-77.
Wehrens, X. H., B. Mies, et al. (1997). "Localization of smoothelin in avian smooth muscle and identification of a vascular-specific isoform." FEBS Lett **405**(3): 315-20.
Weiser, D. C., R. H. Row, et al. (2009). "Rho-regulated myosin phosphatase establishes the level of protrusive activity required for cell movements during zebrafish gastrulation." Development **136**(14): 2375-84.
Williams, K. R., H. C. Hemmings, Jr., et al. (1986). "DARPP-32, a dopamine- and cyclic AMP-regulated neuronal phosphoprotein. Primary structure and homology with protein phosphatase inhibitor-1." J Biol Chem **261**(4): 1890-903.
Witkiewicz, A. K. and E. S. Knudsen (2014). "Retinoblastoma tumor suppressor pathway in breast cancer: prognosis, precision medicine, and therapeutic interventions." Breast Cancer Research **16**(3).
Wong, C. C. L., C. M. Wong, et al. (2008). "Deleted in Liver Cancer 1 (DLC1) Negatively Regulates Rho/ROCK/MLC Pathway in Hepatocellular Carcinoma." PLoS One **3**(7).

Wooldridge, A. A., C. N. Fortner, et al. (2008). "Deletion of the protein kinase A/protein kinase G target SMTNL1 promotes an exercise-adapted phenotype in vascular smooth muscle." J Biol Chem **283**(17): 11850-9.

Wooldridge, A. A., J. A. MacDonald, et al. (2004). "Smooth muscle phosphatase is regulated in vivo by exclusion of phosphorylation of threonine 696 of MYPT1 by phosphorylation of Serine 695 in response to cyclic nucleotides." J Biol Chem **279**(33): 34496-504.

Wu, X., A. V. Somlyo, et al. (1996). "Cyclic GMP-dependent stimulation reverses G-protein-coupled inhibition of smooth muscle myosin light chain phosphate." Biochem Biophys Res Commun **220**(3): 658-63.

Wu, Y., A. Muranyi, et al. (2005). "Localization of myosin phosphatase target subunit and its mutants." J Muscle Res Cell Motil **26**(2-3): 123-34.

Xiao, G. H., A. Beeser, et al. (2002). "p21-activated kinase links Rac/Cdc42 signaling to merlin." Journal of Biological Chemistry **277**(2): 883-886.

Yamamoto, M., Y. Suzuki, et al. (1999). "Expressions of four major protein Ser/Thr phosphatases in human primary leukemic cells." Leukemia **13**(4): 595-600.

Yamashiro, S., Y. Yamakita, et al. (2008). "Myosin phosphatase-targeting subunit 1 regulates mitosis by antagonizing polo-like kinase 1." Dev Cell **14**(5): 787-97.

Yang, X. Y., F. S. Zheng, et al. (2015). "Loss of RhoA expression prevents proliferation and metastasis of SPCA1 lung cancer cells in vitro." Biomedicine & Pharmacotherapy **69**: 361-366.

Yuen, M. F., P. C. Wu, et al. (2001). "Expression of c-Myc, c-Fos, and c-Jun in hepatocellular carcinoma." Cancer **91**(1): 106-112.

Zagorska, A., M. Deak, et al. "New roles for the LKB1-NUAK pathway in controlling myosin phosphatase complexes and cell adhesion." Sci Signal **3**(115): ra25.

Zagorska, A., M. Deak, et al. (2010). "New Roles for the LKB1-NUAK Pathway in Controlling Myosin Phosphatase Complexes and Cell Adhesion." Science Signaling **3**(115).

Zha, Y., P. Gan, et al. (2014). "Downregulation of Rap1 promotes 5-fluorouracil-induced apoptosis in hepatocellular carcinoma cell line HepG2." Oncology Reports **31**(4): 1691-1698.

Zhang, B. L., S. H. Dong, et al. (2015). "Targeting protein arginine methyltransferase 5 inhibits colorectal cancer growth by decreasing arginine methylation of eIF4E and FGFR3." Oncotarget **6**(26): 22799-22811.

Zhang, J. G., D. D. Zhang, et al. (2015). "Incarvine C suppresses proliferation and vasculogenic mimicry of hepatocellular carcinoma cells via targeting ROCK inhibition." BMC Cancer **15**.

Zhang, Z., S. Zhao, et al. (1994). "Expression of recombinant inhibitor-2 in E. coli and its utilization for the affinity chromatography of protein phosphatase-1." Arch Biochem Biophys **308**(1): 37-41.

Zhang, Z. J., G. Bai, et al. (1993). "Expression and Characterization of Rat Protein Phosphatase-1-Alpha, Phosphatase-1-Gamma-1, Phosphatase-1-Gamma-2, and Phosphatase-1-Delta." Archives of Biochemistry and Biophysics **303**(2): 402-406.

Registry number: DEENK/53/2017.PL
Subject: PhD Publikációs Lista

Candidate: Adrienn Sipos
Neptun ID: I0DSCU
Doctoral School: Doctoral School of Molecular Medicine
MTMT ID: 10037471

List of publications related to the dissertation

1. **Sipos, A.**, Iván, J., Bécsi, B., Darula, Z., Tamás, I., Horváth, D., Medzihradszky-Fölkl, K., Erdődi, F., Lontay, B.: Myosin phosphatase and RhoA-activated kinase modulate arginine methylation by the regulation of protein arginine methyltransferase 5 in hepatocellular carcinoma cells.
Sci. Rep. 7 (40590), 1-15, 2017.
DOI: http://dx.doi.org/10.1038/srep40590
IF: 5.228 (2015)

2. Lontay, B., Bodoor, K., **Sipos, A.**, Weitzel, D. H., Loiselle, D., Safi, R., Zheng, D., Devente, J., Hickner, R. C., McDonnell, D. P., Ribar, T., Haystead, T. A. J.: Pregnancy and Smoothelin-like Protein 1 (SMTNL1) Deletion Promote the Switching of Skeletal Muscle to a Glycolytic Phenotype in Human and Mice.
J. Biol. Chem. 290 (29), 17985-17998, 2015.
DOI: http://dx.doi.org/10.1074/jbc.M115.658120
IF: 4.258

List of other publications

3. Dedinszki, D., **Sipos, A.**, Kiss, A., Bátori, R., Kónya, Z., Virág, L., Erdődi, F., Lontay, B.: Protein phosphatase-1 is involved in the maintenance of normal homeostasis and in UVA irradiation-induced pathological alterations in HaCaT cells and in mouse skin.
Biochim. Biophys. Acta-Mol. Basis Dis. 1852 (1), 22-33, 2015.
DOI: http://dx.doi.org/10.1016/j.bbadis.2014.11.005
IF: 5.158

Total IF of journals (all publications): 14,644
Total IF of journals (publications related to the dissertation): 9,486

The Candidate's publication data submitted to the iDEa Tudóstér have been validated by DEENK on the basis of Web of Science, Scopus and Journal Citation Report (Impact Factor) databases.

10 March, 2017

KEYWORDS

Arginine symmetrical dimethylation
Glycolytic fiber switch
Hepatocellular carcinoma
Myosin phosphatase (MP)
Pregnancy
Protein arginine methyltransferase 5 (PRMT5)
Protein phosphorylation
RhoA-associated protein kinase (ROK)
Smoothelin-like 1 protein (SMTNL1)
Tumorigenesis

TÁRGYSZAVAK

Arginin szimmetrikus dimetiláció
Glikolitikus izotípusváltás
Hepatocelluláris karcinóma
Miozin foszfatáz (MP)
Terhesség
Protein arginin metiltranszferáz 5 (PRMT5)
Fehérje foszforiláció
RhoA-asszociált protein kináz (ROK)
Smoothelin-szerű fehérje 1 (SMTNL1)
Tumorigenezis

ACKNOWLEDGEMENT

I am particularly grateful to my supervisor Dr. Beáta Lontay for guiding and supporting me and for all of the opportunities she has given me during the years of my Ph.D. education.

I would also like to thank Prof. László Virág and Prof. Pál Gergely, our current and previous heads of the Department of Medical Chemistry for give all of the opportunities for my work.

I sincerely thank Prof. Ferenc Erdődi for his professional contribution to my work.

I appreciate to Andrea Docsa, Ágota Kelemenné and Ági Némethné for their excellent technical contribution and to Éva Neiszné for her excellent help.

Many thanks to all members of our laboratory for sharing work and everyday life and that we supported each other: Dr. Judit Iván, Dr. Andrea Kiss, Evelin Major, Emese Tóth, Dániel Horváth, István Tamás, Dr. Bálint Bécsi, Zoltán Kónya and Dr. Dénes Nagy.

Special thanks to Dr. Péter Bay for giving me the scientific basics and for his personal and friendly support.

Many thanks to my best friends Dr. Petra Lakatos, Csilla Szűcs-Somogyi, Dr. Judit Iván, Dr. Éva Kerekes, Dr. Edit Mikó for their invaluable personal contribution and for all of the pleasant experiences. I would also like to thank Dr. Margit Péter, Katalin Petrényi, Dr. Katalin Kovács, Zsuzsi Valkó, Dr. Dóra Dedinszki, Dr. Csaba Hegedűs and Tamás Fodor for their friendship and for the time we spent together.

I sincerely and gratefully thank Márton Szitás for everything.

Many special thanks to my loving Family for supporting and encouraging me and for their inexhaustible patience.

I acknowledge the microarray analysis to Szilárd Póliska (UD Genomed, Debrecen, Hungary), the help of Beatrix Dienes in confocal microscopy, Bálint Bécsi for SPR analysis and Zsuzsanna Darula for LC-MS/MS analysis.

This work was supported by BMC Korea Research Fund, PD OTKA 104878, OTKA 109249, TÁMOP-4.2.2.A-11/1/KONV-2012-0025 projects and Mecenatúra (DE-OEC Mec-5/2011). The doctoral training program was supported by TÁMOP-4.2.2/B-10/1-2010-0024 and TÁMOP-4.2.2B-15/1/KONV-2015-0001 projects.

APPENDIX

The thesis is based on the following publications: